

EFFECTS OF RADIATION EXPOSURE ON LUNG CARCINOGENESIS

APPROVED BY SUPERVISORY COMMITTEE

Jerry W. Shay, Ph.D.
Professor of Cell Biology

David A. Boothman, Ph.D.
Professor Simmons Cancer Center

John D. Minna, M.D.
Professor of Internal Medicine

Michael D. Story, Ph.D.
Associate professor of Radiation
Oncology

DEDICATION

Dedicated to my lovely wife Nikki for all of her love and support.

EFFECTS OF RADIATION EXPOSURE ON LUNG CARCINOGENESIS

by

OLIVER DELGADO

DISSERTATION

Presented to the Faculty of the Graduate School of Biomedical Sciences

The University of Texas Southwestern Medical Center at Dallas

In Partial Fulfillment of the Requirements

For the Degree of

DOCTOR OF PHILOSOPHY

The University of Texas Southwestern Medical Center at Dallas

Dallas, Texas

December, 2009

Copyright

by

OLIVER DELGADO, 2009

All Rights Reserved

ACKNOWLEDGEMENTS

I would like to acknowledge and thank first and foremost my mentors, Jerry Shay and Woody Wright. The complementarity of your distinctive thoughts and approaches provided me with an unparalleled environment to learn and mature as a young scientist.

I would like to thank my thesis committee: Dr. David Boothman, Dr. John Minna, and Dr. Michael Story for their comments and support throughout the years. In addition, thank you to Dr. James Richardson who taught me to see the order within an H&E section.

Thanks to all the current and former Shay/Wright lab members that have made my time in the lab both enjoyable and challenging. In particular, I would like to thank David Minna, Suzie Hight, Kimberly Batten, Erin Kitten, Phil Smiraldo, Andres Roig, Richard MacDonnell, Gail Marian, and Aadil Kaisani for their help and/or advice with one or all of my projects.

Thank you to the entire UTSW NSCOR team; especially to those that ventured with me to the deep reaches of space (I mean Brookhaven National Laboratory).

I would like to give a special thank you to my wife, Nikki. Without your love, patience, and support throughout these years I would have been lost.

Last but definitely not least, I would like to acknowledge and thank my parents, Armando and Minervina Delgado. Everything I am and have achieved is due to you.

EFFECTS OF RADIATION EXPOSURE ON LUNG CARCINOGENESIS

OLIVER DELGADO, Ph.D.

The University of Texas Southwestern Medical Center at Dallas, 2009

JERRY W. SHAY, Ph.D.

Lung cancer is one of the most prevalent forms of cancer in both men and women with over 1.3 million annual related deaths worldwide. Analysis of several human populations exposed to radiation reveals that the lung is remarkably susceptible to the carcinogenic effects of radiation exposure. The considerable lung surface area and slow rate of epithelial turnover may have causal roles in this vulnerability. This may be due to the increased probability

that a progenitor cell of the lung, which is proposed to be the cancer-initiating cell, may acquire multiple carcinogenic alterations from radiation exposure. Currently, the lung is believed to have several facultative progenitor cells, situated throughout the lung epithelium, that are regionally restricted in their regenerative capacity. Normal human bronchial epithelial cells (HBECs), immortalized through the expression of Cdk4 and hTERT, provide a sustainable cell reagent for the evaluation of the radiation effects *in vitro*. These HBECs retain a novel multipotent capacity *in vitro* (capable of differentiating into both central and peripheral lung cell types) and thus may represent an unrestricted progenitor of the adult lung that resembles an embryonic progenitor. Studies to determine whether the differentiation state influences radiation exposure effects, such as DNA damage and repair, are ongoing. As cellular responses change upon the acquisition of oncogenic mutations, the effects of fractionated or acute radiation exposure on lung carcinogenesis *in vivo* were determined utilizing the transgenic LA1 K-ras mouse model of lung cancer compared to wildtype littermates. Radiation-induced carcinogenesis is a major concern not only for cancer patients being treated with therapeutic radiation but also for astronauts on long-term space missions. X-ray radiation did not affect the incidence or progression of lung carcinogenesis in this mouse model of lung cancer. High-energy ^{56}Fe - particle irradiation (a type of radiation present in deep space), however, significantly increased the incidence of invasive carcinoma when administered as a

fractionated dose but not as a single acute dose. These results demonstrate that pre-initiated lesions may be more susceptible to malignant transformation upon exposure to radiation. Thus, radiation may have an impact on both lung cancer initiation and progression.

TABLE OF CONTENTS

TITLE	i
DEDICATION	ii
TITLE PAGE	iii
COPYRIGHT	iv
ACKNOWLEDGEMENTS	v
ABSTRACT	vi
TABLE OF CONTENTS	ix
PRIOR PUBLICATIONS	xiii
LIST OF FIGURES	xiv
LIST OF TABLES	xvii
LIST OF APPENDICES	xviii
LIST OF ABBREVIATIONS	xix
CHAPTER ONE: INTRODUCTION	1
1.1. Basic Lung Biology	1
1.2. Lung Development	10
1.3. Stem Cells of the Lung: Homeostasis and Repair	16
1.4. Lung Cancer, Mouse Models of Lung Cancer, and Lung Cancer Stem Cells	35
1.5. Radiation and Lung Cancer	46

CHAPTER TWO: MULTIPOTENCY OF IMMORTALIZED HUMAN	
BRONCHIAL EPITHELIAL CELLS	53
2.1. Introduction.....	53
2.2. Results.....	59
2.2.1. <i>In Vitro Analysis of HBEC3 KT Potency</i>	59
2.2.2. <i>Transcriptional Analysis of HBEC3 KT Cell Line</i>	64
2.2.3. <i>Development of a 3D Differentiation Model Using the HBEC3 KT</i> <i>Cell Line</i>	68
2.3. Discussion	72
2.4. Materials and Methods.....	79
CHAPTER THREE: CHARACTERIZATION OF <i>IN VITRO</i> TRANSFORMED	
HBEC3 KT POPULATION AND CLONES ISOLATED IN SERUM AND	
SERUM-FREE.....	84
3.1. Introduction.....	84
3.2. Results.....	89
3.2.1. <i>Analysis of 3D Differentiation Capacity of in vitro Transformed</i> <i>HBEC3 KT Cells</i>	89
3.2.2. <i>Characterization of in vitro Transformed HBEC3 KT Clones</i> <i>Isolated in Presence or Absence of Serum</i>	90

3.2.3. <i>Evaluation of Tumorigenicity of in vitro Transformed HBEC3 KT Clones Isolated in Serum</i>	97
3.3. Discussion	98
3.4. Materials and Methods	102
CHAPTER FOUR: INVASIVE CANCER INDUCED BY RADIATION IN LA1 K-RAS MOUSE MODEL OF LUNG CANCER.....	106
4.1. Introduction.....	106
4.2. Results.....	111
4.2.1. <i>Effect of Acute or Fractionated Doses of 1.0 Gy X-Rays of ⁵⁶Fe- Particles on Wildtype and LA1 KRAS Mice</i>	111
4.2.2. <i>Genomic Analysis of Pulmonary Radiation Response to Irradiation</i>	120
4.2.3. <i>Determination of Relative Biological Effect of ⁵⁶Fe- Particle Compared to X-ray Irradiation</i>	122
4.2.4. <i>Determination of Relative Biological Effect of Fractionating ⁵⁶Fe- Particle Irradiation</i>	124
4.3. Discussion	125
4.4. Materials and Methods.....	131
CHAPTER FIVE: DISCUSSION AND FUTURE DIRECTIONS.....	135

APPENDICES	141
BIBLIOGRAPHY.....	175
VITAE.....	189

PRIOR PUBLICATIONS

- Roig, A. I., Eskiocak, U., Hight, S. K., Kim, S. B., **Delgado, O.**, Souza, R. F., Spechler, S. J., Wright, W. E., and Shay, J. W. Immortalized epithelial cells derived from human colon biopsies express stem cell markers and differentiate *in vitro*. *Gastroenterology*, In press
- Scherer, S. E.,..., **Delgado, O.**..., and Gibbs, R. A. The finished DNA sequence of human chromosome 12. (2006) *Nature* **440**(7082), 346-351
- Muzny, D. M.,..., **Delgado, O.**..., and Gibbs, R. A. The DNA sequence, annotation and analysis of human chromosome 3. (2006) *Nature* **440**(7088), 1194-1198
- Ross, M. T.,..., **Delgado, O.**..., and Bentley, D. R. The DNA sequence of the human X chromosome. (2005) *Nature* **434**(7031), 325-337
- Gibbs, R. A.,..., **Delgado, O.**..., and Collins, F. (2004) Genome sequence of the Brown Norway rat yields insights into mammalian evolution. *Nature* **428**(6982), 493-521
- Dederich, D. A., Okwuonu, G., Garner, T., Denn, A., Sutton, A., Escotto, M., Martindale, A., **Delgado, O.**, Muzny, D. M., Gibbs, R. A., and Metzker, M. L. Glass bead purification of plasmid template DNA for high throughput sequencing of mammalian genomes. (2002) *Nucleic Acids Res* **30**(7), e32

LIST OF FIGURES

Figure 1-1 Plasticized human lungs.....	2
Figure 1-2 Basic lung architecture.....	4
Figure 1-3 Representative cell types of central and peripheral airways.....	6
Figure 1-4 Phases of lung development.....	12
Figure 1-5 Models of stem cell hierarchy for high and low turnover tissues.	18
Figure 1-6 Cell renewal hierarchy of the adult lung.....	29
Figure 1-7 Direct versus indirect actions of radiation.	48
Figure 2-1 HBEC3 KT cells simultaneously express markers of several lung epithelial cells.	61
Figure 2-2 Marker expression in HBEC3 KTs is independent of proliferative status.	63
Figure 2-3 TTF-1 expression and localization changes with proliferative status in HBEC3 KT cell line.....	65
Figure 2-4 Transcriptional profile indicates HBEC3 KT cells resemble embryonic progenitor cells of murine lung.....	67
Figure 2-5 Multipotent progenitor maintenance genes and pathways up-regulated in HBEC3 KT cells coincident with marker expression.	69
Figure 2-6 HBEC3 KT cells cultured in 3D environment of reconstituted basement membrane form cyst-like structures when co-cultured with IMR90 fetal lung fibroblasts.....	70

Figure 2-7 Multipotent progenitor maintenance genes and pathways down-regulated in HBEC3 KT cyst-like structures.	71
Figure 2-8 Features suggestive of pneumocyte differentiation in HBEC3 KT cyst-like structures.	73
Figure 2-9 Tubule formation and potential branching morphogenesis induced in HBEC3 KT cells cultured on reconstituted basement membrane.	74
Figure 3-1 <i>In vitro</i> transformed HBEC3 KT cells form dysregulated 3D structures when cultured in reconstituted basement membrane.	88
Figure 3-2 Isolation of <i>in vitro</i> transformed HBEC3 KT clones in presence of serum enhances formation of dysregulated 3D structural phenotype.	92
Figure 3-3 Serum exposure selects for cells that resist influence of serum and is independent of c-Myc expression levels.	95
Figure 3-4 Serum exposure either directly or indirectly effects exogenous factors in <i>in vitro</i> transformed HBEC3 KT clones isolated in presence of serum.	96
Figure 4-1 Characteristics of LA1 KRAS mouse model of lung cancer.	110
Figure 4-2 Irradiation scheme.	112
Figure 4-3 1.0 Gy dose of ⁵⁶ Fe particle irradiation significantly decreases lifespan of LA1 K-ras mice.	113
Figure 4-4 Radiation exposure does not affect tumor incidence in LA1 KRAS and wildtype mice.	115
Figure 4-5 Histological features of invasive adenocarcinomas.	116

Figure 4-6 Incidence of several non-lung related factors detrimental to murine health.....	119
Figure 4-7 Whole lung microarray analysis one year post-irradiation.	121
Figure 4-8 Irradiation with a fractionated 3.0 Gy dose of X-rays significantly affects survival and health of LA1 KRAS and wildtype littermate mice.	123
Figure 4-9 Fractionation of 1.0 Gy dose of ⁵⁶ Fe- particles into ten 0.1 Gy doses impacts survival of LA1 KRAS and wildtype littermate mice identically to acute and five 0.2 Gy fractionated regimen.	126
Figure 4-10 Current survival of LA1 KRAS and wildtype littermate mice irradiated with either an acute dose of 0.1 Gy or 0.2 Gy ⁵⁶ Fe- particles.	128

LIST OF TABLES

Table 1.1 Markers of lung epithelial cells.	22
Table 1.2 Five year survival rates per lung cancer histological stage.	36
Table 4.1 Lifetime carcinoma incidence in unirradiated and LA1 KRAS mice irradiated with either an acute or fractionated 1.0 Gy dose of X-ray or ⁵⁶ Fe-particles.	117
Table 4.2 Carcinoma incidence in unirradiated and LA1 KRAS mice irradiated with either an acute or fractionated 1.0 Gy dose of X-ray or ⁵⁶ Fe- particles adjusted for survival.....	118
Table 4.3 Lifetime and survival adjusted carcinoma incidence in LA1 KRAS mice irradiated with either a fractionated 2.0 Gy or 3.0 Gy dose of X-rays compared to a fractionated 1.0 Gy dose of ⁵⁶ Fe- particles.....	125
Table 4.4 Lifetime and survival adjusted carcinoma incidence in LA1 KRAS mice irradiated with five or ten 0.1 Gy doses of ⁵⁶ Fe- particles compared to a five 0.2 Gy doses of ⁵⁶ Fe- particles.....	127

LIST OF APPENDICES

Appendix A. Genes with significant expression changes in quiescent versus proliferating HBEC3 KT cells.	141
Appendix B. Maintenance gene and pathway gene list for taqman® assay with corresponding identifiers	145
Appendix C. 1671 differentially expressed in LA1 KRAS mice compared to unirradiated controls one year after fractionated 1.0 Gy dose of ⁵⁶ Fe- particle irradiation.	146
Appendix D. Enriched annotation terms from genes significantly changed in LA1 KRAS mouse lungs one year after fractionated 1.0 Gy dose of ⁵⁶ Fe- particle irradiation.	154
Appendix E. Enriched annotation terms related to inflammation from genes significantly changed in LA1 KRAS mouse lungs one year after fractionated 1.0 Gy dose of ⁵⁶ Fe- particle irradiation.	170

LIST OF ABBREVIATIONS

ALDH	Aldehyde Dehydrogenase
AQP5	Aquaporin-5
BADJ	Bronchioalveolar Duct Junction
BASC	Bronchioalveolar Stem Cell
BPE	Bovine Pituitary Extract
BrdU	Bromodeoxyuridine
BSA	Bovine Serum Albumin
CCSP/CC10	Clara Cell Specific Protein
CDK4	Cyclin Dependent Kinase 4
CGRP	Calcitonin Gene Related Peptide
Clara ^V	Variant Clara Cell
CSC	Cancer Stem Cell
CyP450	Cytochrome P450
DAVID	Database for Annotation, Visualization, and Integrated Discovery
DEL	Deletion Mutation in Exon 19 of EGFR
DNA	Deoxyribonucleic Acid
DOX	Doxycycline
DSB	Double-Strand Break
EGF	Epidermal Growth Factor
EGFR	Epidermal Growth Factor Receptor

EMT	Epithelial-to-Mesenchymal Transition
EPHA4	Ephrin Type-A Receptor 4 Precursor
ERR	Excess Relative Risk
ETS	Environmental Tobacco Smoke
ETV5	ETS Translocation Variant 5
FDR	False Discovery Rate
⁵⁶ Fe-	Iron Atom
FGF10	Fibroblast Growth Factor 10
FGFR3	Fibroblast Growth Factor 3
FOXA2	Forkhead Box Protein A2
FOXJ1	Forkhead Box Protein J1
FOXO3	Forkhead Box Protein O3
FZD1	Frizzled 1
G	Guanine
GCR	Galactic Cosmic Rays
GSA	Goat Serum Albumin
GSK3-β	Glycogen Synthase Kinase 3 - Beta
[³ H]-TdR	Tritiated Thymidine
HBEC	Human Bronchial Epithelial Cell
HBEC3	Human Bronchial Epithelial Cell Line 3
HER1	Human Epidermal Growth Factor Receptor 1

HER2	Human Epidermal Growth Factor Receptor 2
HZE	High Atomic Number and Energy
ID2	Inhibitor of DNA Binding 2
IF	Immunofluorescence
IHH	Indian Hedgehog
K5	Keratin 5
K14	Keratin 14
L858R	Missense Mutation in Exon 21 of EGFR
LET	Linear Energy Transfer
LSS	Life Span Study
MUC5AC	Mucin 5 Subtype AC
NASA	National Aeronautics and Space Administration
NBF	Neutral Buffered Formalin
NCRP	National Council on Radiation Protection and Measurement
NEB	Neuroepithelial Body
NO ₂	Nitrogen Dioxide
NSCLC	Non-Small-Cell Lung Cancer
NSCOR	NASA Specialized Center of Research
NSRL	NASA Space Radiation Laboratory
O ₃	Ozone
PFA	Paraformaldehyde

PTCH1	Patched 1
PTCH2	Patched 2
PNEC	Pulmonary Neuroendocrine Cell
PRP9.5	Protein Gene Product 9.5
Q-PCR	Quantitative Reverse Transcription Polymerase Chain Reaction
RB	Retinoblastoma
RNA	Ribonucleic Acid
RT-PCR	Reverse Transcription Polymerase Chain Reaction
SCC	Squamous Cell Carcinoma
SCLC	Small-Cell Lung Cancer
SHH	Sonic Hedgehog
SOX2	Sex determining region Y- box 2
SOX9	Sex determining region Y- box 9
SP-C	Surfactant Protein C
SPE	Solar Particle Event
SPF	Specific Pathogen Free
SPRY	Sprouty
SSB	Single-Strand Break
T	hTERT
T	Thymine
T1 α	Podoplanin Precursor

T790M	Secondary Mutation in Exon 20 of EGFR
TA	Transit-Amplifying
TGF- β	Transforming Growth Factor Beta
TTF1	Thyroid Transcription Factor 1
TK	Tyrosine Kinase
TKI	Tyrosine Kinase Inhibitor
UTSW	University of Texas Southwestern Medical Center at Dallas
vCE	Variant CCSP-expressing
Z	Atomic Number

CHAPTER ONE.

Introduction

1.1. Basic Lung Biology.

The lung is a complex organ whose primary function is to mediate the essential process of gas exchange, termed respiration, between the bloodstream of an animal and the surrounding atmosphere (Cardoso and Lu, 2006; Guyton and Hall, 2006). Both ventilation of the lung tissue and the subsequent respiration are facilitated by the physical architecture and cellular composition of the lung. After passing through the upper respiratory tract, comprised of the nasal passages, pharynx, and larynx, air crosses into the lung tissue, or lower respiratory tract. Airflow inside the lung is conducted through a continuous network of branched tubules that taper gradually with each bifurcation (Figures 1.1 and 1.2). Each of these tubules terminates in a septated saccular structure where respiration occurs (Figure 1.2) (Netter, 2006). Gradual changes in the epithelial lining along the proximal-distal axis of this airway contribute vital, though functionally distinct, roles to this respiratory process (Figure 1.3) (Crystal et al., 2008).

The proximal end of the lung originates at the larynx, or the most distal end of the upper respiratory tract, and is formed by an unbranched tube termed the trachea. Surrounding the trachea a series of cartilaginous C-shaped rings maintain

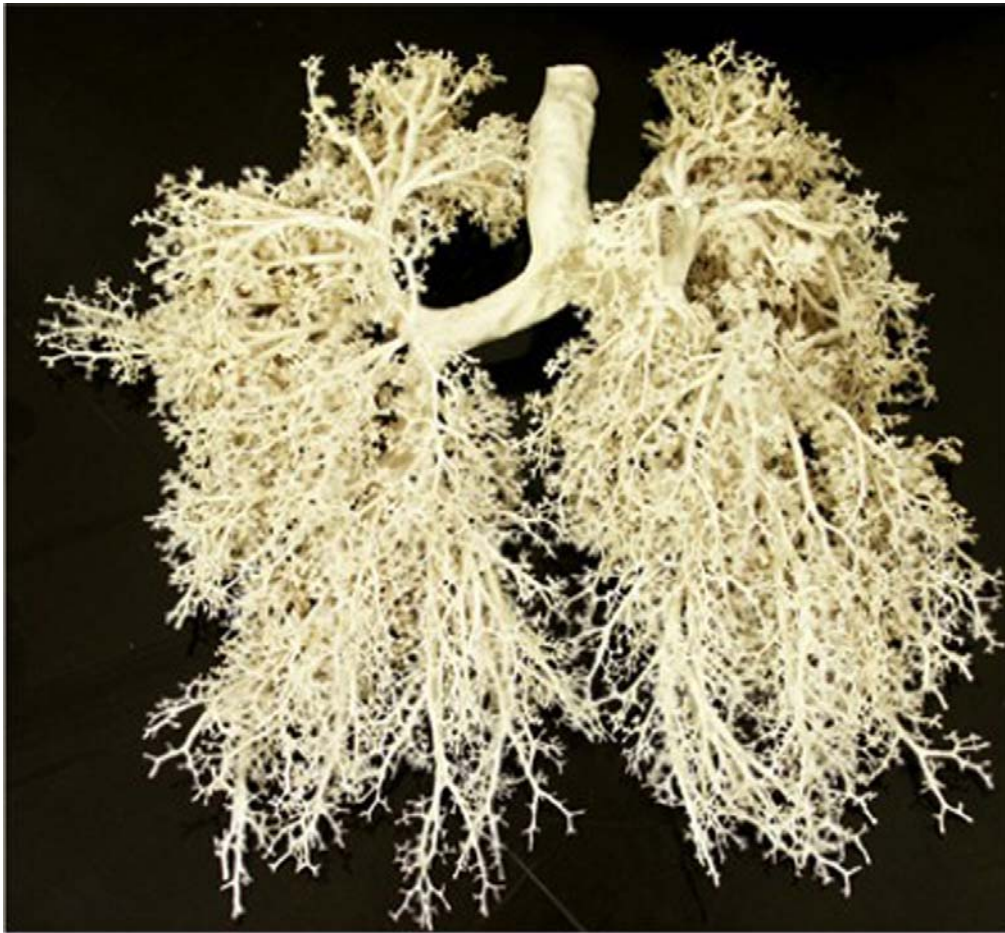


Figure 1.1. Plasticized human lungs demonstrates branched network of tubules.

(Jonathan Natiuk. Lungs. July 6, 2003. <http://www.sxc.hu/photo/33787>)

the structural integrity of the tube thus permitting an unobstructed airflow through this “windpipe” (Figure 1.2). Posterior to these C-shaped rings is a layer of smooth muscle that functions to modulate airflow rate when needed (Netter, 2006). Epithelial cells lining the trachea, referred to as the respiratory epithelium, consist of predominantly three distinct cell types whose combined function is to condition the inhaled air and filter out particulates and potentially infectious agents. Goblet cells serve to secrete a colloid called mucus that coats the trachea in order to entrap any foreign matter and assists in humidifying the inspired air. Ciliated pseudostratified columnar cells, which project motile cilia from their apical surface, then propel the secreted mucus layer cranially towards the upper respiratory tract with a continuous beating motion of their cilia. The function of the third cell type, the basal cell, will be discussed in a succeeding section (Figure 1.3 A) (Crystal et al., 2008).

At the carina, a cartilaginous ridge located approximately at the level of the 5th thoracic vertebra, the trachea bifurcates into two primary bronchi. These bronchi are similar to the trachea in cellular composition and function, but contain fewer cartilaginous rings and have a smaller diameter (Figure 1.2) (Netter, 2006). Pulmonary neuroendocrine cells (PNECs), that are present as single cells sporadically throughout the entire adult lung epithelia, are also concentrated in clusters called neuroepithelial bodies (NEBs) that are situated around this

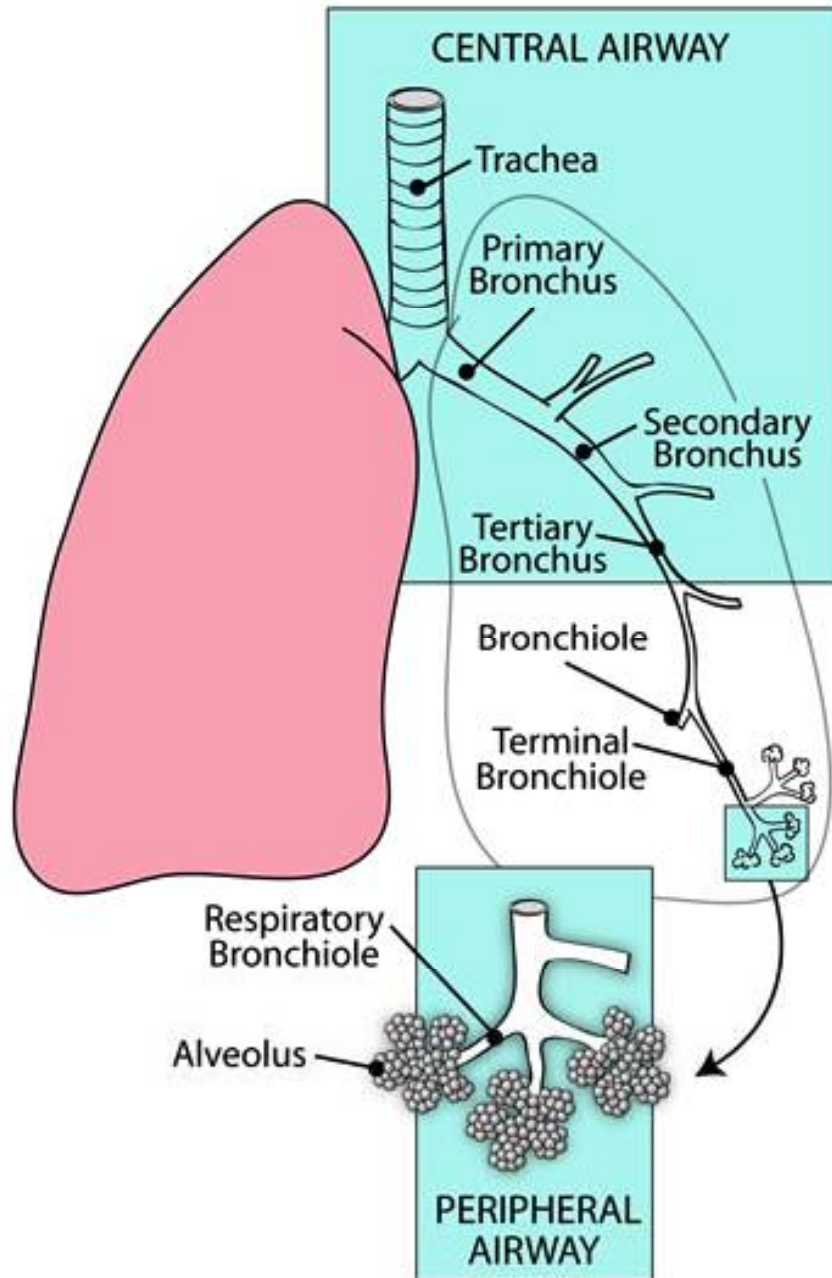


Figure 1.2. Basic Lung Architecture.

The lung is comprised of a continuous branched tubule tract that terminates in multiple septated saccular structures. Central airways function to cleanse and humidify inspired air. Peripheral airways function to facilitate gas exchange between the environment and the bloodstream.

bifurcation and, more frequently, at subsequent branch points (Figure 1.3 A). The function of these PNEC cells is to assist in regulating the pulmonary response to stimuli such as hypoxia, but the precise molecular mechanisms involved are not known. It has also been suggested that the PNEC cells may play an actual role in the bifurcation process during lung development.

Each primary bronchus further subdivides into several secondary, or lobar, bronchi. The number of lobar branches varies between the left and right primary bronchus in humans and among other respiratory mammals (Netter, 2006). This differential branching of two primary bronchi into several lobar bronchi specifies the number of lobes per side of the lung (Figure 1.2). It is within the lobar bronchi that the progressive changes in the epithelial lining first become apparent.

Goblet cell density declines in these airways in comparison to the primary bronchi and trachea, while another cell type, the simple ciliated columnar cell, begins to emerge alongside the ciliated pseudostratified columnar epithelial cells. Changes in the tissue surrounding these lobar bronchi are also visible at this stage. The abundance and size of the cartilaginous rings decreases to that of sparse cartilaginous plates and more smooth muscle is found encapsulating the bronchi. These alterations enhance mucus clearance thus preventing a substantial mucus layer from penetrating deeper into the lung tissue where the transformation of

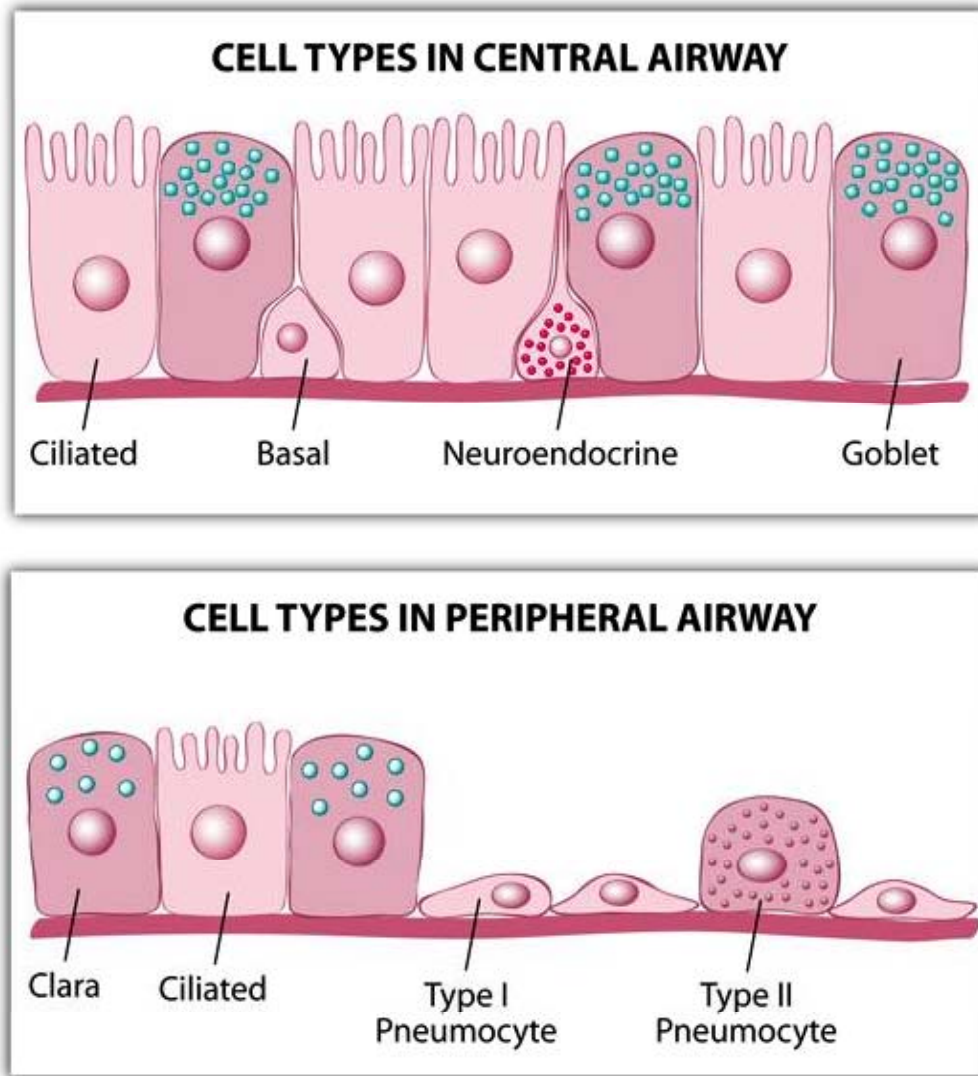


Figure 1.3. Representative cell types of central and peripheral airways. (A) Central airways predominantly consist of columnar ciliated, secretory goblet, and basal cells. Neuroendocrine cells are also present sporadically. (B) Tubules of peripheral airways consist of secretory Clara cells with some cuboidal ciliated cells. Secretory Type II pneumocytes make up the majority of the cells in the alveoli while the flattened Type I pneumocytes take up the majority of the surface area.

large, structurally reinforced, conductive airways into the small, minimally supported, respiratory airways is completed.

Subsequent branching of each of the lobar bronchi into the tertiary, or segmental, bronchi extend this transition, as these are the last of the large airways whose patency is maintained with sporadic cartilage plates (Figure 1.2) (Netter, 2006). Almost indistinguishable from the lobar bronchi, the lining of the segmental bronchi consists of both ciliated pseudostratified columnar and simple ciliated columnar cells. Predominantly, the segmental bronchi are unique due to the isolation of each bronchus into a distinct bronchopulmonary segment that is separated by a layer of connective tissue (Netter, 2006). Each isolated segment is capable of functioning completely independent of one another.

Primary bronchioles, formed by the subdivision of segmental bronchi, are notable as these are the first airways that do not contain any cartilaginous support (Figure 1.2). Elastic fibers connected to the surrounding tissue supplant cartilage plates in this respect. Smooth muscle circumventing the primary bronchioles is, however, comparable to the more proximal tubes (Netter, 2006). The epithelium of the primary bronchioles gradually transforms from being comprised of mainly simple ciliated columnar cells at the proximal end to simple ciliated cuboidal cells at the distal end. Another cell type, the Clara cell, which is a dome-shaped cell

that has protective and detoxifying roles, is also present for the first time within the epithelial lining of the primary bronchioles (Figure 1.3 B). Degradation of mucus produced in the large airways and secretion of a surfactant protein that reduces surface tension in the bronchioles are some of the protective roles attributed to Clara cells.

Each primary bronchiole tube further divides into two or more smaller bronchioles called terminal bronchioles (Figure 1.2) (Netter, 2006). Clara cells make up the majority of the epithelial lining of the terminal bronchioles along with few ciliated cuboidal cells (Figure 1.3 B). It is at this point along the tubular tract of the lung that the conducting airways are considered to end in the progressive transition from conducting to respiratory airways.

The first phase that is regarded to as the respiratory airways begins with the emergence of several respiratory bronchioles from each terminal bronchiole (Figure 1.2). Decidedly, the most striking feature of the respiratory bronchiole is a discontinuous epithelial layer. This discontinuity is due to air pockets situated between the simple cuboidal cells throughout the proximal lining of these bronchioles. Some ciliated cuboidal cells are present in the respiratory bronchioles, but only towards the most proximal end.

The principle mediators of respiration, however, are the septated saccular structures, termed alveoli, in which this continuous branched network ends. Specifically, these sacs are located at the distal end of short passages called alveolar ducts that branch from the respiratory bronchioles (Figure 1.2) (Netter, 2006). There are between two to eleven alveolar ducts for every respiratory bronchiole. Each alveolar duct is lined with simple cuboidal cells and knobs of smooth muscle that allow for constriction of these ducts. An atrium at the end of each duct, from which five or six alveolar sacs emanate, completes the tubule structure of the lung tissue.

Alveoli are unique in architecture and cellular composition compared to the rest of the lung. While the framework of a tubular network befits the function of conducting and conditioning the air, the saccular architecture of the alveoli facilitates the actual process of gas exchange. This provides the maximal surface area accessible for gas exchange to occur between the atmosphere and the bloodstream. As with the cells of the tubular network, the epithelial lining also contributes to the function of the alveoli.

There are three cell types that are found within the alveolar sacs. Type I pneumocytes are squamous cells that cover over ninety-five percent of the alveolar wall and lie in close apposition to the endothelial cells that carry the

bloodstream. Gas exchange occurs directly through these cells and is enhanced by their flattened morphology (Figure 1.3 B). The most abundant pneumocytes, however, are the cuboidal Type II pneumocytes that are interspersed among the Type I pneumocytes, but make up only five percent of the lining due to their morphology (Figure 1.3 B). One of the functions of the Type II pneumocytes is to secrete several surfactant proteins that reduce the surface tension within the alveolar sacs. Another ascribed function of the Type II cells will be described below. The alveolar macrophages, the third cell type, are not attached to the alveolar wall and serve to engulf particles and infectious agents that have penetrated the alveoli.

Overall, the lung is well suited for regulating the respiratory process. Physical changes along its tract accommodate the bidirectional passage of air while gradually expanding the surface area available for potential gas exchange. Cells lining the airways also adjust along the lung tract to meet the required task of conditioning air in order to facilitate gas exchange and minimize any potentially adverse effects of the interaction with the environment.

1.2. Lung Development.

Lung development is a dynamic process that involves the interaction between cells from multiple lineages and their environment culminating in the

intricate tissue described in the preceding section. Insight into this developmental process has been provided largely through studies in model organisms owing to the conserved nature the lung. The entire process spans across the embryonic, fetal, and post partum periods of development. Five discrete stages that are based on the structural features present at a given moment have been defined to describe all of lung development (Figure 1.4) (Maeda et al., 2007).

The first of these stages is the embryonic stage in which the prospective lung emerges from the primitive foregut and proceeds to establish the trachea and major bronchial tubes (Figure 1.4). There is a slight difference between human and rodent lung development at this early stage. Human lung development begins with the formation of the laryngotracheal groove on the ventral side of foregut endoderm. This groove will eventually deepen and fuse forming the pharynx and trachea. The emergent lung appears from the caudal end of this groove. In rodents, however, the lungs directly bud from the ventral aspect of the foregut with the tracheal primordium arising anterior to these buds (Maeda et al., 2007).

Fibroblast growth factors, particularly Fibroblast growth factor 10 (FGF10), secreted from the neighboring splanchnic mesenchyme induces the

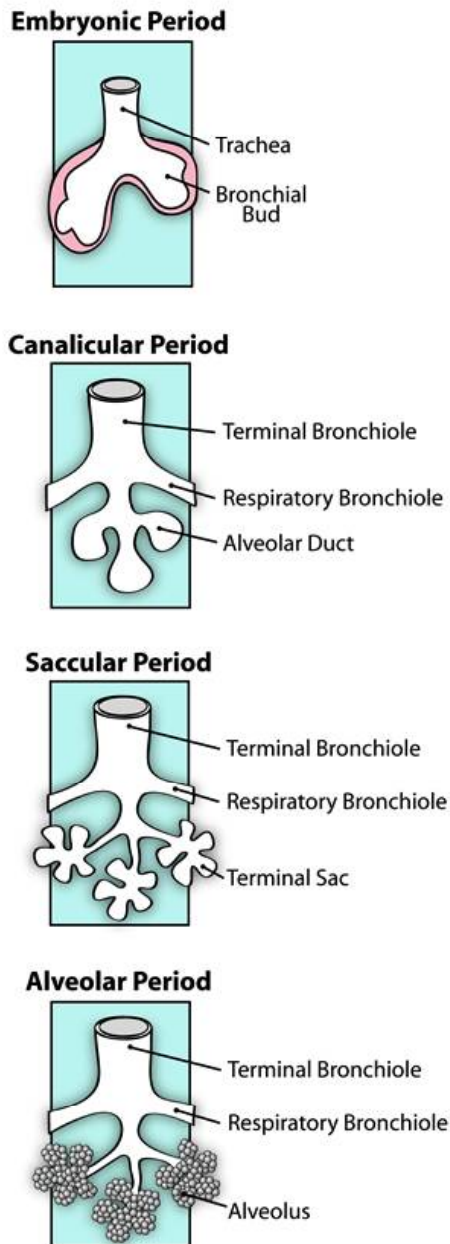


Figure 1.4. Phases of lung development.

Lung development proceeds through five discrete stages. In the embryonic stage, lung buds emerge from primitive foregut and bifurcates to form what will become primary bronchi. The majority of the lung is formed and differentiation begins during the pseudoglandular stage (not shown) and the canalicular stages. Saccular structures that will become alveoli emerge during the saccular stage. These structures become septated and differentiate in the alveolar stage post-partum.

budding of the lung primordium in both humans and rodents (Bellusci et al., 1997b; Min et al., 1998; Sekine et al., 1999; Serls et al., 2005). Overlapping expression of the transcription factors Forkhead box protein A2 (FOXA2) and Thyroid transcription factor 1 (TTF1) demarcate the region from which budding will occur (Besnard et al., 2004; Lazzaro et al., 1991). Chemotaxis and proliferation of the emergent cells towards the FGF10 signal continues until both autocrine and paracrine signaling abrogate both the response to and production of FGF10, respectively. Upregulation of Sprouty (Spry) within the advancing lung cells in response FGF stimulation has been shown to oppose further growth factor activation (Mailleux et al., 2001; Tefft et al., 1999). Down-regulation of FGF10 production has been shown to involve both the Sonic hedgehog (SHH) and Transforming growth factor beta (TGF- β) signaling pathways (Bellusci et al., 1997a; Cardoso and Lu, 2006).

Elimination of the inductive FGF10 signal provided by the adjacent mesenchyme temporarily arrests the growth and migration of the expanding lung primordium. The nascent bud is then reactivated by the onset of FGF10 secretion from mesenchymal cells surrounding the suppressed region (Cardoso and Lu, 2006; Maeda et al., 2007). The spatial position of these mesenchymal cells, and the restriction of further activation of the lung bud apex, results in the stimulation of two lateral buds to emerge from the region abutting this apex thus forming the

first bifurcation (Metzger and Krasnow, 1999). As with the primary lung bud, these lateral buds will proliferate and migrate towards their respective FGF10 gradient until the reciprocal suppression described above recurs (Affolter et al., 2003). It is these lateral buds that form the two primary bronchi of the mature lung. Throughout the remaining embryonic stages, this reiterative branching process establishes what will become the lobar and segmental bronchi.

Lung development progresses in the pseudoglandular stage, which is the second of the lung development stages and when the lung resembles an endocrine gland (Maeda et al., 2007). In this phase, the branching process proceeds to form the primary and terminal bronchiole tubules. The linings of the existing proximal airways begin to differentiate into the ciliated and goblet cells present in the mature lung. Smooth muscle cells that encapsulate the larger airways likewise begin to differentiate from the mesenchymal cells that were suppressed by reception of SHH ligand secreted from the advancing lung (Cardoso and Lu, 2006; Maeda et al., 2007). This differentiation process is dependent on the activation of the SHH pathway within these mesenchymal cells (Pepicelli et al., 1998; Weaver et al., 2003). Cartilage around the larger airways and Type II cells in the most distal terminal bronchioles are also observed for the first time during the pseudoglandular stage.

Formation of the respiratory bronchioles and alveolar ducts takes place in the third developmental stage, the canalicular stage (Figure 1.4) (Maeda et al., 2007). The lumens of the established airways dilate throughout this phase while their lining continues to differentiate in a proximal to distal direction. Endothelial cells, which will form the vasculature that carries the bloodstream, also differentiate from the surrounding mesenchyme and begin to position themselves in close proximity to the developing respiratory airways (Stenmark and Abman, 2005). Type I cells in the alveolar ducts are also apparent towards the end of the canalicular stage. Although the lung is not completely formed, the process of respiration can occur by the end of the canalicular stage.

During the saccular, or fourth developmental stage, the sacs that will become the alveoli are formed from the alveolar ducts (Figure 1.4) (Maeda et al., 2007). These sacs are lined by both Type II and Type I pneumocytes however the septa between the vasculature and sacs remains thick impairing gas exchange. At the end of this phase, which ends at birth, all of the airways are established and terminate in a number of saccular structures that contain protrusions and are capable of sustaining life at birth.

The final stage of lung development is the alveolar stage and involves the maturation of the alveoli and vasculature encircling the alveoli (Maeda et al.,

2007). Enlargement of each protrusion from the saccular structures and further septation of the surrounding mesenchyma commences this maturation process (Figure 1.4). Surfactant protein secretion from the Type II pneumocytes increases and more Type I cells differentiate through this period. Vasculature surrounding the alveoli becomes more complex and positioned in even closer apposition to the Type I pneumocytes in order to facilitate gas exchange. The alveolar stage persists for years post partum (Burri, 2006).

Ultimately, lung development consists of recurrent waves of budding, growth, and branching of endodermally derived cells orchestrated by the constant interplay between these cells and the mesenchyma into which they have grown. Differentiation of these endodermal cells into the many distinct cell types that line the adult lung and the surrounding mesenchymal cells into those enveloping the adult lung is additionally influenced by this crosstalk. This evolving process of producing and adapting to environmental changes spans all of in utero and post partum development.

1.3. Stem Cells of the Adult Lung: Homeostasis and Repair.

The adult lung is continuously exposed to deleterious agents and requires an efficient mechanism of repair in order to maintain its integrity and functional capacity throughout a lifetime. As with the study of lung development, insight

into how this is achieved has been primarily through research utilizing model organisms. These studies demonstrate that the turnover of the epithelial lining of the adult lung is a slow process. In the mouse, this period of complete epithelial turnover may persist for approximately one hundred days (Rawlins and Hogan, 2006, 2008).

The classical model of homeostasis and repair, which is utilized by most tissues such as skin, blood, and colon, relies on multipotent stem cells that are capable of reconstituting all of the cell types of that tissue (Wagers and Weissman, 2004; Weissman et al., 2001). These tissue stem cells, which are sometimes referred to as progenitor cells, are situated at specific locations within the tissue termed niches. Cells and matrix components in the vicinity of the niche concurrently assist in the regulation of these tissue stem cells (Lunyak and Rosenfeld, 2008; Weissman et al., 2001; Yin and Li, 2006). Under normal conditions, tissue stem cells proliferate infrequently and are believed to be capable of extended self-renewal through symmetric and asymmetric divisions (Figure 1.5 A). Symmetric division produces two daughter cells that are identical to the parental cell and predominately occurs during tissue development. In contrast, asymmetric division produces only one daughter cell that is identical to the parental and a second cell, called a transit-amplifying (TA) cell, that is

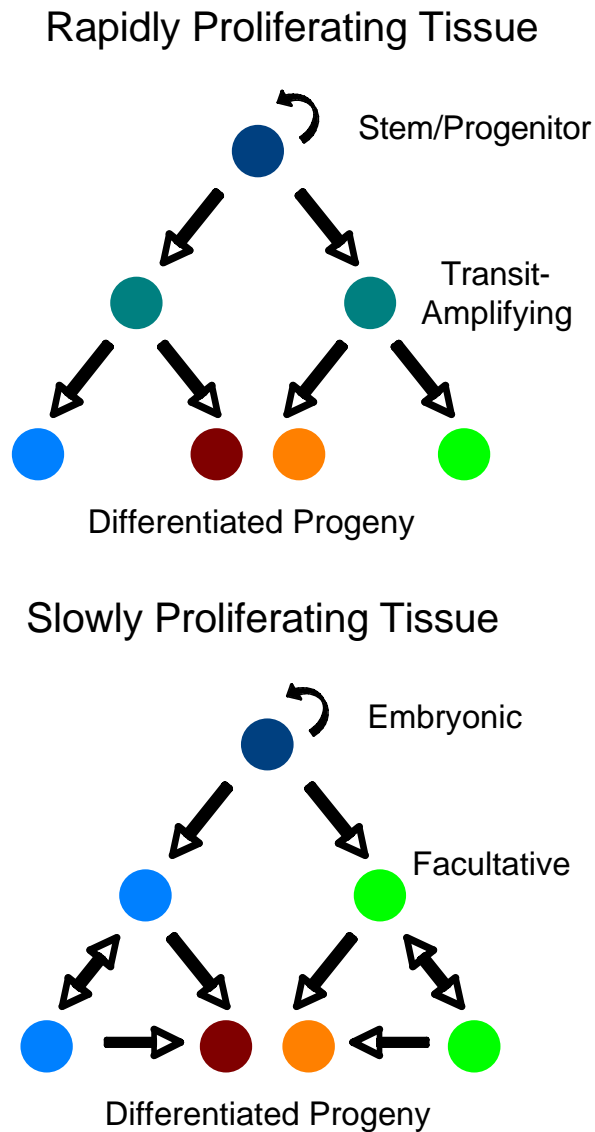


Figure 1.5. Models of stem cell hierarchy for high and low turnover tissues.

(A) Rapidly proliferating tissues are regenerated by the classical stem cell model. Undifferentiated stem cells lie upstream of all other cell types in this model. These cells infrequently proliferate, can self-renew, and give rise to similarly undifferentiated progeny termed transit-amplifying cells. Transit-amplifying cells rapidly proliferate and can give rise to some or all of the tissue cell types. (B) Slowly proliferating tissues develop from embryonic stem cells, which do not exist in adult tissue. Instead, quiescent cells that have a differentiated function in the adult tissue regenerate the tissue when needed. These cells can differentiate into some or all of the cells of the tissue.

designated to differentiate into one or more of the cell types of that particular tissue. TA cells are similar to the tissue stem cells in that they retain a multipotent capacity, but they have a higher rate of proliferation and their self-renewal is limited (Figure 1.5 A) (Weissman et al., 2001). In certain tissues, such as blood, the TA cells are restricted in the number of cell types into which they may differentiate and are termed oligopotent (Bellantuono, 2004). This lineage restriction thus establishes a hierarchy based on potency within these tissues and provides a method for subdividing the pools from which each lineage may be replenished and increasing the accessibility to a regenerative cell at any given moment.

For tissues that have high turnover rates and require constant and rapid cellular replenishment, the utility of this stem cell organization is immediately apparent. Tissue homeostasis throughout a lifespan requires immediate access to viable stem cells. In order to maintain a large enough pool of tissue stem cells that are competent to sustain the health of an organ, many rounds of division are required of each stem cell. With each round of division the viability of any proliferating tissue stem cell decreases. This loss of viability could be through the introduction of a damaging mutation into the genome of the stem cell or by the induction of the permanent cell cycle arrest, termed replicative senescence, caused by telomere attrition (Bodnar et al., 1998). Through the stringent regulation of a

tissue stem cell, the potential for any loss of viability within this regenerative pool is minimized. The utilization of a rapidly expanding TA cell pool therefore satisfies the demanding requirements imposed by lifetime tissue maintenance through the use of an expendable surrogate for the tissue stem cell.

The study of tissue stem cells has been influenced dramatically by methods that permit the detection and evaluation of these cells *in vivo*. Label retention experiments in which analogs of the nucleoside thymidine such as tritiated thymidine ($[^3\text{H}]\text{-TdR}$) or bromodeoxyuridine (BrdU) are incorporated into the genomic deoxyribonucleic acid (DNA) of actively dividing cells are common assays for detection of these stem cells. Continuous administration of either $[^3\text{H}]\text{-TdR}$ or BrdU to a mouse for an extended period of time, called a pulse, allows for incorporation the respective analog into the actively proliferating cells of the animal. Cells that incorporate the analog during the pulse phase are designated as “labeled” as may be detected by various means.

After the pulse phase, the animal and any analog that has been successfully incorporated into cells is monitored for a period of time, termed a chase. As cell division occurs during the chase period, the label is gradually lost. The incorporated analog is then serially diluted from the genome of the TA cells with each division until there is no longer any analog available for further

incorporation. A tissue stem cell, on the other hand, is capable of retaining more of its label due to the infrequent rate of cell division thus providing a method to locate any potential tissue stem cell niches and the resident tissue stem cells that are mostly quiescent.

In order to determine which cell type within the assayed tissue has retained the administered label, histological features and protein expression are evaluated for those that are unique to either particular cell types of that tissue or of those that have been defined for known stem cells from other tissues. The use of this assay in the lung tissue is thus possible because each of the lung epithelial cell types described previously has a distinctive histological feature and/or a unique protein “marker”. Each cell type of the lung with its corresponding identifiers is listed in Table 1.1.

Cell Type	Markers
Basal	p63, Keratin 5 (K5), K14
Goblet	Mucin 5 subtype AC (MUC5AC)
Ciliated	Forkhead box protein J1 (FOXJ1), apical acetylated tubulin
PNEC	Calcitonin gene related peptide (CGRP), Protein gene product 9.5 (PGP9.5)
Clara	TTF1, CC10, SP-A, SP-D, CypP450 family members
Clara ^v	TTF1, CC10
Type II Pneumocyte	TTF1, CC10, SP-A, SP-C, SP-D
Type I Pneumocyte	Aquaporin-5 (AQP5), Podoplanin precursor (T1 α)

Table 1.1. Markers of lung epithelial cells.

Several studies have attempted to determine whether a putative stem cell resides within the adult lung by using the label retention assay in mice (Rawlins and Hogan, 2006). However, due to the slow turnover of the epithelial lining of the lung tissue, the loss of any incorporated label would occur only after an extensive chase period making the discovery of a true label-retaining cell difficult. Early studies, focusing entirely on the trachea and bronchi, thus exploited the fact that the incorporation of any pulsed label would only occur in the actively dividing cells and then this label would be transmitted to their progeny. This would allow for a rudimentary stem cell hierarchy to be established within these regions. The basal cell, designated as such due to their localization to the basal layer of the pseudostratified epithelia, was consistently found to be the most

upstream cell type in this hierarchal organization (Donnelly et al., 1982). An “indeterminate” secretory cell type that has minimal secretory granules in later studies was determined to be a Clara cell and was placed immediately downstream of the basal cells (Evans et al., 1978; Evans et al., 1986). These studies also demonstrated that the last cell in this hierarchal stratification, which does not proliferate and is not capable of differentiating into any other cell type, is the ciliated cell. Recently studies have provided substantiating evidence for this stratification in addition to demonstrating that the ciliated cell is capable of undergoing morphological changes that assists in protecting the respiratory tract after an acute injury (Lawson et al., 2002; Park et al., 2006; Rawlins et al., 2007).

In order to circumvent the limitations imposed by the slow epithelial turnover rate in the lung, more recent studies have relied on the repair of the lung tissue in response to injury in conjunction with the label retention assay. This application of an injury model has provided a novel method to evaluate the tissue stem cell hierarchy and its relation to the regeneration of the lung epithelium. The only caveat with this application being that the cellular turnover observed could be somewhat different than that which occurs during normal tissue homeostasis.

Injury of the lung epithelia may be accomplished through the application of a variety of toxic agents that in some cases are only deleterious to specific cell

types. Ciliated cells, for example, are the only cells that are ablated by oxidant gases such as nitrogen dioxide (NO₂) or ozone (O₃) (Evans et al., 1976a, b; Schwartz et al., 1976). A short pulse of [³H]-TdR immediately after the ablation of the ciliated cells with NO₂ in mice revealed that a non-ciliated columnar serous cell, which was shown to be a Clara cell, is the primary cell stimulated to proliferate in response to this damage and is capable of differentiating into both ciliated cells and Clara cells (Barth and Muller, 1999; Evans et al., 1986). These reparative murine Clara cells have also shown to lose their secretory granules, a feature associated with a more differentiated Clara cell, upon being induced to divide (Evans et al., 1978; Liu et al., 1994). This led to the distinction of these dividing Clara cells from their quiescent differentiated counterparts. Interestingly, goblet cells were also shown to respond equivalently in this repair process supporting that these cells may also have a progenitor-like capacity (Evans et al., 1986).

Another selective toxic agent that has been used extensively in these types of injury models is the aromatic hydrocarbon naphthalene, which selectively kills Clara cells. The basis for this selectivity is the expression of the cytochrome P450 (CYP450) mono-oxygenases within Clara cells. These proteins function to metabolize many different endogenous and exogenous compounds and this provides the Clara cells with their detoxifying ability (Guengerich, 2002).

Paradoxically, it is also this detoxifying ability that destines the Clara cell to be killed by naphthalene. The metabolism of naphthalene by the CyP450 family members expressed in Clara cells produces epoxides that are toxic and it is these epoxides that kill the cells (Buckpitt et al., 1992).

Studies that have utilized the naphthalene induced injury model to evaluate the regenerative properties of the lung specifically targeted a lung cell type that repeatedly has been shown to have a progenitor cell capacity. Upon the ablation of the Clara cells in the trachea and bronchi, the resident basal cells that previously were shown to potentially function as progenitor cells completely regenerated the entire epithelia including the Clara cells (Borthwick et al., 2001). Lineage labeling experiments, in which the expression of an exogenous construct that is driven by the Keratin 14 (K14) promoter permanently marks only basal cells and their descendents, has provided supporting evidence for these results (Hong et al., 2004a, b). However, even though in the lung K14 is considered to be a basal cell specific marker, the expression of K14 has been detected in proliferating cells that are not basal cells during the reparative process in the trachea (Liu et al., 1994).

In addition to providing corroborating evidence for the existence of potential tissue stem cells in the trachea and bronchi, the use of naphthalene has

permitted the study of stem cells and repair in the distal tubules that contain many more Clara cells and no basal cells. These studies, which originally did not apply the label retention assay, have led to the identification of a non-ciliated cell type that resides immediately adjacent to the NEB clusters at tubule bifurcations and that expresses the Clara cell marker, Clara cell secretory protein (CCSP or CC10) (Hong et al., 2001; Reynolds et al., 2000a; Stripp et al., 1995). The distinguishing feature of these cells compared to Clara cells is that these cells do not express the CYP450 family members and are thus resistance to the naphthalene treatment. These cells have been termed variant Clara (Clara^V) cells or variant CCSP-expressing (vCE) cells (Hong et al., 2001; Reynolds et al., 2000a). After naphthalene-induced damage, the Clara^V cells rapidly proliferate and differentiate into all of the regional epithelial cells except for PNECs, which also are stimulated to divide after naphthalene treatment, and basal cells (Reynolds et al., 2000a; Reynolds et al., 2000b). Subsequent research has elucidated that the PNEC cell lineage is unique in their regenerative properties. PNECs are capable of self-renewal, but they cannot differentiate into any other cell type of the lung (Hong et al., 2001; Ito et al., 2003).

Further examination of the distal bronchiole tubules utilizing this method revealed another niche in which the Clara^V cells were present and also responded to the naphthalene-induced damage. These Clara^V cells are localized at the

bronchioalveolar duct junction (BADJ) and are also capable of regenerating all the regional epithelial cell types (Giangreco et al., 2002). The lack of NEBs or PNECs in the vicinity of this niche demonstrates that the BADJ Clara^V cells and their regulation are completely independent from the influence of NEBs suggesting that they may be somewhat different from the Clara^V cells that are adjacent to NEBs.

A recent independent study has expanded upon, and at the same time somewhat complicated, the understanding of the regenerative cells that reside within the BADJ niche. In this study, the cells located at the BADJ were demonstrated to not only be both positive for the Clara cell marker CC10 as previously described, but also positive for the Type II pneumocyte marker Surfactant protein C (SP-C) (Kim et al., 2005). These cells were also shown to be naphthalene resistant and rapidly proliferated in response to the naphthalene-induced damage. Label retention experiments provide some evidence that the Clara^V cells are derived from the “double positive” cells in the BADJ niche. To further investigate the characteristics and potential of these “double positive” cells in the peripheral airways, another cell-specific toxic agent was employed. With this injury model the Type I pneumocytes in the alveoli are selectively ablated by treatment with the antibiotic bleomycin (Aso et al., 1976). Previous studies utilizing this or other injury models demonstrated that the Type II pneumocytes

are capable of differentiating into the Type I pneumocyte cell type suggesting that Type II pneumocytes, which can self-renew, may function as progenitor cells that can regenerate the alveoli (Adamson and Bowden, 1974; Aso et al., 1976; Evans et al., 1975). “Double positive” cells were resistant to bleomycin treatment and induced to proliferated in response to this damage, but the potential ability of these cells to regenerate the alveolus by differentiating into the Type I alveolar cell type was through the use of an *in vitro* assay. Even still, these results led to the designation of these “double positive” cells as bronchioalveolar stem cells (BASCs) that maintain both the bronchiole tubules and the alveoli (Kim et al., 2005).

When taken altogether, the results described above, combined with the slow turnover rate of the lung epithelium, have revealed several inconsistencies that prevent their integration into the classic stem cell model that relies on a single adult lung tissue stem cell. Dependent on the assay utilized or the regions being investigated, it appears that multiple cell types are competent to regenerate both themselves and other cells types of the lung (Figure 1.6). One of these cell types, the basal cell, was shown to be competent to regenerate all of the cell types of the lung except for the PNECs and the Type II and Type I pneumocytes of the alveoli. However, the basal cell is only present in the trachea and bronchi, which

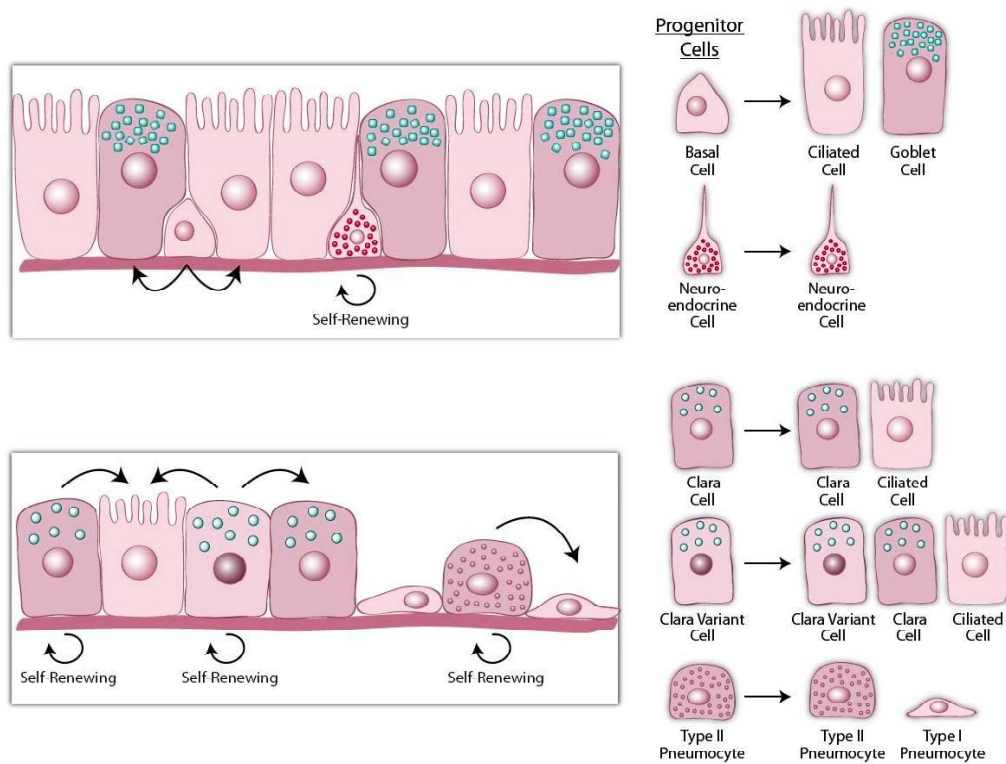


Figure 1.6. Cell renewal hierarchy of the adult lung.

(A) In the central airways, basal cells are capable of self-renewal and differentiation into ciliated and goblet cells (in mice, basal cells may additionally differentiate into Clara cells). (B) In the peripheral airways, Clara cells and Clara^V can self-renew and differentiate into ciliated cells. Clara^V cells can also differentiate into Clara cells. Type II pneumocytes in the alveolus self-renew and differentiate into Type I pneumocytes.

precludes its potential as a global stem cell of the lung (Figure 1.6) (Borthwick et al., 2001; Rock et al., 2009).

The Clara cell, which is capable of both self-renewal and differentiating into the ciliated and goblet cell types, is another regenerative cell type in the lung (Figure 1.6). There has been no direct evidence, although, that these cells are capable of becoming basal cells and, as with the basal cells, they cannot differentiate into PNECs or the Type II and Type I pneumocytes. The criteria that a tissue stem cell should be a rare cell is also not met with the Clara cell type since Clara cells are frequently found throughout the lung and that frequency increases along the length of the lung in a proximal-distal direction. Clara^V cells, on the other hand, satisfy more of the established criteria for tissue stem cells in that they are a relatively rare cell type that resides in well-defined niches, are resistant to various forms of damage, and they retain the same regenerative capabilities as Clara cells (Figure 1.6). Lack of any direct evidence that these cells are capable of becoming basal cells again prohibits the designation of these cells as the tissue stem cell of the lung.

The isolation and characterization of the BASCs from the BADJ introduced an intriguing stem cell candidate due to their ascribed ability to potentially regenerate both the bronchiole tubes and the alveoli (Kim et al., 2005).

This regenerative capacity and what role if any that these BASCs play in either homeostasis or injury repair, however, have been critically scrutinized and called into question by recent studies that utilized novel mouse aggregation chimera and lineage tracing studies (Giangreco et al., 2009; Rawlins et al., 2009; Rock et al., 2009).

These studies also independently demonstrated that there does not appear to be a single stem cell of the lung. Rather the current model suggests that the lung is divided into compartments and each compartment contains its own progenitor cell. The trachea and bronchi comprise the most proximal of these compartments and the basal cell is the resident stem cell of this region (Figure 1.6) (Borthwick et al., 2001; Rock et al., 2009). Clara^V cells in the bronchiole tubes have been labeled as the stem cells of this second central compartment (Figure 1.6) (Hong et al., 2001; Rawlins et al., 2009; Reynolds et al., 2000a; Reynolds et al., 2000b). Finally, the lack of any evidence that, aside from the Type II pneumocyte, there is not another cell which has a self-renewal capability and can regenerate the cells of the alveoli led to the designation of the Type II cells as the stem cells of the third and most distal compartment (Adamson and Bowden, 1974; Aso et al., 1976; Evans et al., 1975). PNECs are still considered to be an independent lung cell type that after becoming specified only maintains itself (Figure 1.6) (Ito et al., 2003).

Another intriguing result that can be drawn from the recent aggregation chimera and lineage tracing studies is that, in the context of stem cell biology, the interpretation of any resultant from utilizing an injury model should be distinguished from what occurs during tissue homeostasis. When combined with the results from the studies described above, the classical stem cell model does not appear applicable to the lung tissue. Instead, an alternate model that has emerged from the examination of several other tissues that have slow turnover rates with injury models is more befitting (Figure 1.5 B). The fundamental difference between this model and the classic model of a stem cell hierarchy is with the TA cell population.

In the classical stem cell model, a rare undifferentiated stem cell divides infrequently to give rise to an actively dividing TA population that remains relatively undifferentiated (Figure 1.5 A). Exposure to various stimuli then induces the TA cell to differentiate into one or more of the cell types of that particular tissue. This is irrespective of whether the tissue is in repair or undergoing steady state maintenance. The TA population in a tissue that has a slow turnover rate such as the pancreas, liver, and lung, on the other hand, is made up predominantly of a pool of cells that are quiescent during homeostasis and only actively divide in response to injury (Alison et al., 2004; Dor et al.,

2004). While quiescent, these TA cells function as one of the differentiated cells of the tissue and can make up a considerable amount of the tissue. It is due to this functional duality that these cells have been termed “facultative” stem cells (Figure 1.5 B).

Application of this alternate stem cell model to the lung tissue restructures the current thinking on how this tissue is maintained. The concept that the lung is segregated into distinct compartments based on their mode of regeneration remains intact in this model. Primarily, this is because there is no *in vivo* evidence that any cell residing outside of the alveolus has the capacity to regenerate Type II or Type I pneumocytes. For the most proximal compartment consisting of the trachea and the bronchi, the basal retains the designation of the resident stem cell. Clara^V cells and Type II pneumocytes are considered to be the stem cells for the bronchioles and alveoli respectively. Clara cells would function as a facultative TA cell population in this model.

When comparing the three cell types that could be deemed stem cells in this model, the basal cell is the only cell type that is close to meeting the criteria of a being a typical tissue stem cell. All three of these cell types possess the primary criteria of a stem cell in that they self-renew and can regenerate other cell types of the lung. Each has also been shown to be resistant to various toxic agents

or injuries and proliferate infrequently during steady state maintenance. However, only the basal cell and Clara^V cells reside in distinct niches that may play a role in regulating their behavior. Of these two cell types, the basal cell is the only cell that does not become induced to divide in response to injury and do not have any known differentiated function or morphology. The Clara^V cells and Type II pneumocytes are more analogous to facultative stem cells in respect to their differentiation status. Hence, the basal cells could be considered the true lung tissue stem except that, as noted above, they have not been shown to be able to differentiate into Type II or Type I pneumocytes.

In summary, the lung has evolved a robust strategy in order to maintain and repair itself and contend with the constant onslaught of noxious agents to which it is exposed. The integration of several different mechanisms is fundamental to this strategy. First and foremost is the segregation of the lung tissue into compartments along the proximodistal axis. Each compartment contains a different stem cell that enables prompt regeneration when needed. Interestingly, the lung may also be classified into these same compartments based on their functional contribution to the respiratory process. Another important component utilized by the lung to enhance its repair is the facultative TA cell population of Clara cells. The presence of these dual-natured cells throughout the lung tubules, which are poised to respond immediately to damage, permits

expedient regeneration without the excessive proliferation of any single cell.

Altogether, the maintenance and repair strategy utilized by the lung is well suited to keep such a vital organ healthy throughout a lifetime.

1.4. Lung Cancer, Mouse Models of Lung Cancer, and Lung Cancer Stem Cells.

Even though the lung tissue is fortified by a remarkable regeneration strategy, the exposure of the lung to a constant barrage of deleterious insults inevitably succeeds in undermining the vitality of the tissue. Of the potential lung disorders that may arise from the contribution of environmental factors and genetic susceptibilities, lung cancer is one of the most prevalent and devastating. In 2009, it is estimated that there will be approximately 220,000 new lung cancer cases diagnosed and 159,000 deaths attributed to lung cancer in the United States alone making it the most common cause of cancer and cancer related deaths in both men and women. Five-year survival rates are entirely dependent on the tumor stage, or the extent the tumor has progressed, at the time of diagnosis and onset of treatment (Table 1.2) (ACS, 2009). Research into the etiology of lung cancer in order to improve early detection and enhance prognosis has revealed many of the molecular alterations that predispose an individual to the onset of some form of lung cancer.

Lung cancer, which arises from the epithelial lining of the respiratory tract, is divided into two main types based on their histopathology. Non-small-cell lung cancer (NSCLC) is the most prevalent of these groups making up about 85% of all lung cancer cases. The other group, small-cell lung cancer (SCLC), encompasses the remaining 15% of lung cancer cases and, as will be discussed

Stage	5-year Survival Rate
I	56%
II	34%
III	10%
IV	2%

Table 1.2. Five year survival rates per lung cancer histological stage.
(Adapted from 2009, American Cancer Society)

below, may be considered an entirely unique form of lung cancer due to its neuroendocrine origin. NSCLCs, on the other hand, shelter a wide spectrum of tumor types that permits further subdivision of this category into three different subtypes. These subtypes, which are again based on their distinct histopathology, are squamous cell carcinoma (SCC), large cell carcinoma, and adenocarcinoma.

The influences of exposure to tobacco smoke, whether directly or indirectly, on the incidence of lung cancer are well known and are associated with all forms of the disease. This correlation with the exposure to tobacco smoke and

lung cancer incidence, however, varies with the specific tumor type. Both SCLC and SCC are the two most common tumor types that are found in smokers. While adenocarcinoma is another tumor type that is commonly found in smokers, it is the most common type of cancer that is found in patients that have never smoked. These distinctions can be made due to the stringent classification of patients in relation to their level of exposure. Patients that have only been exposed to environmental tobacco smoke (ETS) or smoked less than 100 cigarettes are considered to be “never smokers”. Anyone that has had an exposure level above having smoked 100 cigarettes is deemed a “smoker” and are then sub-classified dependent on whether they have quit smoking within the preceding twelve months. The utility of classification method is obvious when one considers the fact that smokers have a 10 to 20-fold higher risk of developing lung cancer when compared to never smokers.

As with most cancers, the progression of lung cancer is a multi-step process that involves the alteration of several genes that regulate factors such as cell growth, death, and differentiation. These genes are termed tumor suppressors or oncogenes dependent on whether or not they inhibit or promote cancer progression respectively. The loss of a tumor suppressor or the activation of an oncogene may suffice to either to predispose or initiate a lesion. However, the combination is generally mutually required for a tumor to progress.

While there is some specificity as to which genes are disrupted among the lung cancer subtypes, the mechanisms behind these changes are relatively universal. Genetic alterations such as DNA mutations and chromosomal amplifications or deletions are some of the major players that are associated with the incidence of lung cancer. Epigenetic changes that alter the accessibility to chromatin or DNA sequences are also common. The mutation of one or more key residues in the DNA of a critical gene can confer an advantage to a cell at any stage of cancer progression. A number of genes have been found mutated in some or all of the various types of lung cancer. This includes the most commonly mutated tumor suppressor gene in cancer, p53.

The *p53* gene protein product is a transcription factor that has been widely studied due to its role in either the instigation of a cell cycle arrest or the induction of cell death, termed apoptosis, in response to cellular damage or stress. Most of the mutations in *p53* (70% - 80%) are missense mutations that occur within its DNA binding domain and are found in approximately 50% of NSCLCs and 90% of SCLCs, respectively. These mutations inactivate p53 by preventing it from binding to DNA thus abolishing its transcriptional ability and permitting the continued proliferation and/or survival of aberrant cells. The transversion of the nucleotide base guanine (G) for thymine (T) is one such missense mutation and

may be caused by the carcinogens present in tobacco smoke. As such, *p53* is found to be mutated more often in smokers compared to never smokers.

Nonsense mutations that create a truncated protein or deletion of the 17p13 chromosomal region in which the *p53* gene is located are other, less frequent, mechanisms that functionally silence the *p53* tumor suppressor and have also been found in lung cancer.

As mentioned above, the tumor promoting effect observed when *p53* is inactivated is a feature associated with the loss of the negative regulation imposed by the protein product of a tumor suppressor gene. The acquisition of this promoting effect is somewhat facilitated by the fact that these tumor suppressor genes are not completely independent in the regulation of any given function. They are often part of a linear pathway comprised of several upstream or downstream genes, which allows for a more stringent regulation of the pathway and the resultant cellular function. Alteration of any one of these pathway genes would then deregulate the pathway and elicit the same response.

One such regulatory pathway that is commonly altered in many forms of cancer, including lung cancer, is the p16-Cyclin D1-Cyclin dependent kinase 4 (CDK4)-Retinoblastoma (RB) pathway. In the absence of a growth stimulus, RB binds to the E2F1, E2F2, and E2F3 transcription factors that are essential for the

transition from the G1 phase of the cell cycle to the S phase. With RB bound, these E2F family members are prevented from binding to DNA and transcribing their target genes and therefore the cell cycle is blocked at the G1/S transition. The presence of a growth stimulus, however, induces the complex of Cyclin D1 and CDK4 to form, which activates the kinase activity of CDK4. RB is then phosphorylated multiple times by the Cyclin D1-CDK4 complex causing the release the E2F family members and the G1/S transition to occur. If the growth stimulus is present concurrently with some form of damage or stress, the cell cycle inhibitor p16 disrupts the Cyclin D1-CDK4 complex and prevents the cell cycle from proceeding.

Alterations in both p16 and RB have been found in the different types of lung cancer, but, as with p53, there are some disparities between tumor types. Loss of p16 is more common in NSCLCs compared to SCLCs. Inversely, RB is lost in approximately 90% of SCLC and only 15% - 30% of NSCLCs. It is extremely rare for both genes products to be altered in any one type of lung cancer. This latter characteristic is common for all tumor suppressor genes or oncogenes that are part of a multi-component linear pathway that regulates a function critical for tumor progression.

Some of the most pervasive proto-oncogenes that become altered in lung cancer fit into this criterion, as they are components of the same growth stimulatory pathway. It should be noted that term proto-oncogene refers to a normal gene that becomes an oncogene upon its overexpression or mutation. The human epidermal growth factor receptor 1 (HER1 or more commonly, EGFR) is a proto-oncogene and the most upstream component of one such growth pathway. EGFR is a transmembrane tyrosine kinase (TK) receptor that initiates a growth-signaling cascade through the binding an extracellular growth signal. This induces the homo- and heterodimerization of EGFR with itself or one of the other three EGFR family members, respectively. Once dimerization occurs, the intercellular TK domains on apposing receptors phosphorylate the other receptor initiating the intercellular signaling cascade. In addition to the proliferative signal that the activation of this cascade produces, it also suppresses apoptosis and promotes the process of new blood vessel formation called angiogenesis.

Overexpression of any one of these receptors would permit promiscuous interactions between receptors and inappropriate activation of the growth pathway. EGFR has been found to be overexpressed in approximately 70% of NSCLCs and one of its family members, human epidermal growth factor 2 (HER2), has been found in roughly 30%. Another mechanism that prematurely activates this pathway through the alteration of EGFR is the mutation of the TK

domain. These mutations have been found in approximately 24% of NSCLCs and are caused by a deletion, insertion, or missense mutation in one of the first four exons of the TK domain. Two mutations in particular, an in-frame deletion in exon 19 (DEL) and a missense mutation in exon 21 (L858R), make up over 80% of all of the oncogenic mutations of *EGFR* found in lung cancer. Patients that have an *EGFR* mutation fall into relatively specific categories. These patients are more often female, which are commonly of East Asian decent, considered never smokers, and have adenocarcinoma and not squamous cell carcinoma. An important characteristic of these tumors is that, regardless of which mutation is present, they are responsive to one of the FDA approved TK inhibitors (TKIs). More recently, another secondary mutation in exon 20 of the TK domain (T790M) has been found in patients with an *EGFR* mutation that either did not respond to a TKI or relapsed after treatment. This mutation alters the binding kinetics of the TKIs thus diminishing their effectiveness.

Transgenic mouse models in which any one of the above mutant EGFRs can be induced specifically within the lung tissue have been developed to study the role of EGFR mutation in lung carcinogenesis (Politi et al., 2006). These mutant EGFRs may be induced by the administration of doxycycline (DOX) in either the animal chow or water. Upon induction of either the DEL or L858R mutant EGFRs, lesions emerge within the lung and mimic lung cancer

progression in humans. Progression of these lesions to malignancy in these models, however, is not common reiterating the necessity of acquiring multiple alterations in the carcinogenic process. If DOX is removed or a TKI is administered in the presence of DOX, these tumors regress and this regression is dependent on the length of induction. Long-term induction results in some tumors that do not regress, which demonstrates the presence of at least one additional alteration in these lesions. In contrast, tumors that develop from the expression of the T790M EGFR mutant are insensitive to TKIs.

Downstream of EGFR is a member of the plasma membrane associated G-protein RAS family that mediates the signaling related to activation of EGFR and several other receptors. There are three members of this family, HRAS, KRAS, and NRAS, and mutations in each family member are found in various types of cancer. Oncogenic mutations of the KRAS family member, however, predominate in lung cancer making up 90% of the mutated RAS found. Several mutations have been found in the *KRAS* gene that result in an activated form of KRAS and uncouples pathway activation from any dependence on an upstream growth factor or receptor. These *KRAS* mutations are present in 10% - 15% of all NSCLCs and approximately 20% - 30% of lung adenocarcinomas. They are not present in SCLCs. As with *p53*, there is also a strong correlation with *KRAS*

mutations and smoking as 90% of patients contain a G to T transversion in exon 12 that may be due to the carcinogens present in tobacco smoke.

As with the mutation of EGFR, the significance of oncogenic *KRAS* mutations in lung carcinogenesis has been demonstrated through the creation of various transgenic mouse models that express an oncogenic *KRAS* in the lung (Fisher et al., 2001; Jackson et al., 2001; Johnson et al., 2001). In each model, irrespective of the method in which the oncogenic *KRAS* is expressed, lesions develop in the lung once the mutant *KRAS* is expressed. These lesions also do not commonly progress to malignancy even if expressed in the absence of p53 (Johnson et al., 2001). The resistance of initiated tumors to malignant transformation validates the utility of transgenic mouse models in the study of lung cancer as the requisite acquisition of multiple mutations is conserved.

Another family of genes found to be altered in lung cancer is the *MYC* family of transcription factors. There are three members of this family, *MYC*, *MYCN*, and *MYCL*, and have roles in many different cellular processes including cell proliferation and apoptosis (Adhikary and Eilers, 2005). The most common form of alteration found in lung cancer is amplification of one of the *MYC* genes and are found in 18% of SCLCs and 8% of NSCLCs. This frequency is somewhat higher in cultured SCLC and NSCLC cell lines (31% and 20%,

respectively) (Richardson and Johnson, 1993; Sato et al., 2007). There is some specificity of which family member is amplified in each type of lung cancer. Amplification of all three family members has been found in SCLCs, but only the *MYC* gene is frequently amplified in NSCLCs (Sato et al., 2007).

When all of these alterations are considered together, the complexity of the lung carcinogenesis is readily apparent. However, whether the acquisition of several of these alterations is sufficient to transform any lung cell type and how the resultant tumor is maintained is not currently well understood. One hypothesis steadily garnering support in many different cancer types is that of the cancer stem cell (CSC). This concept proposes that within each tumor resides a cancer stem cell that is capable of self-renewal and producing all the diverse cells of within each tumor. CSCs do not have to be tissue stem cells that have acquired the requisite alterations although they would have similar properties and active signaling pathways (Visvader and Lindeman, 2008). Evidence for the cancer stem cell has been found in several different cancers such as that from blood, breast, and brain (Al-Hajj et al., 2003; Lapidot et al., 1994; Singh et al., 2004). Recently, the same criteria have been utilized to identify a putative lung cancer stem cell within lung tumor samples (Eramo et al., 2008). Further analysis is required to determine the precise role of the putative lung cancer stem cell in lung

carcinogenesis and whether there is an universal lung cancer stem cell capable of generating all of the lung cancer subtypes.

1.5. Radiation and Lung Cancer.

Many hazardous agents have been described as having the potential to induce lung cancer by inflicting damage upon the lung tissue. Of these, radiation exposure is one of the best documented. Analysis of the cancer incidence in different populations previously exposed to radiation, including atomic bomb survivors, uranium miners, and radiotherapy patients, has provided a foundation for the association of radiation exposure and carcinogenesis (Denman et al., 2003; Little, 2009; Preston et al., 2007; Suit et al., 2007). Of note are the appreciable dependencies of the carcinogenic risk on the tissue type and the total dose of radiation exposure. While the incidence of cancer in most tissues increases with moderate and high doses of radiation, several tissues, such as the lung, have also been shown to be remarkably susceptible to low doses of radiation (Little, 2009; Ron, 2003; Suit et al., 2007; Tubiana, 2009). A recent report on Life Span Study (LSS) cohort of Hiroshima and Nagasaki atomic bomb survivors calculates that the excess relative risk (ERR) of cancer per Gy of radiation for all solid tumors is 0.47. Lung cancer is the second most common cancer in the LSS cohort, representing 10% of all the solid tumor cases in this cohort, and thus has a higher ERR per Gy; 0.81 (Little, 2009; Preston et al., 2007). One factor which may

confound the ERR calculation for lung cancer and produce this elevated result is an additive or synergistic effect between radiation and smoking (Pierce et al., 2003).

In order to elucidate how radiation exposure may translate into this increased carcinogenic risk, an understanding of how radiation impacts biological material is required. Radiation is defined as energy that is emitted from a source and exists in two distinct forms, electromagnetic and particulate. The exposure of biological material to radiation becomes dangerous when this energy is sufficient to displace electrons from atoms within or in the immediate vicinity of the exposed material. This process is termed ionization and is damaging due to its ability to break chemical bonds. Any radiation capable of inducing an ionization event is defined as ionizing radiation (Hall and Giaccia, 2006).

The primary target for ionizing radiation, which results in a biological effect, is the DNA within the exposed material. There are two general methods of action, direct and indirect, in which an ionization event may lead to DNA damage. Distinction between the two methods depends on whether the radiation directly ionizes the target atoms or ionizes an intermediary molecule, such as water, which in turn proceeds to ionize the target atoms (Figure 1.7). The method of action utilized by radiation depends on the energy transferred per unit length of track

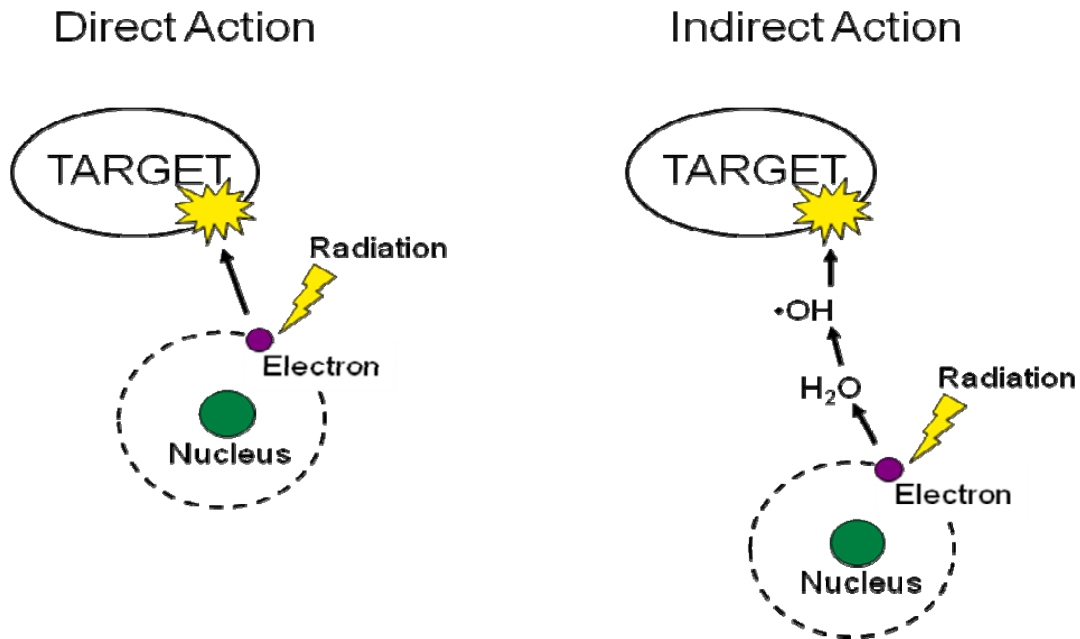


Figure 1.7. Direct versus indirect actions of radiation.

(A) Direct action. Secondary electron ejected due to absorption of radiation energy directly interacts with and ionizes target molecule. (B) Indirect action. Ejected secondary electron interacts with and ionizes other molecules, commonly water, which results in a free radical ($\bullet\text{OH}$) that proceeds to interact with and ionize target molecule. (Adapted and modified from (Hall and Giaccia, 2006))

defined as the linear energy transfer (LET). Electromagnetic radiation, such as gamma (γ) or X-rays, has low LET values and ionizes their target atoms predominantly through indirect action. Particulate radiation, on the other hand, has a wide range of LET values and is capable of both indirect and direct action. More specifically, particles with low LET values ionize their targets via indirect action while particles with high LET values principally, but not exclusively, ionize their targets through direct action (Hall and Giaccia, 2006).

Another critical feature for the induction of a biological effect is the how the deposited energy is spatial distributed within the exposed material. Electromagnetic radiation, which is made up of “waves” of photons, impacts matter in a uniform fashion. Since electromagnetic radiation indirectly ionizes their target atoms and deposits less energy per unit track, each ionization event is sparsely localized throughout the exposed material. Particulate radiation, however, impacts matter in a non-uniform fashion centered along the track of each interacting particle. The direct action of ionization and higher amounts of energy deposited per unit track results in a dense cluster of ionization events along each particle path through the exposed material (Hall and Giaccia, 2006). These differences in the spatial distribution of ionization events translate into appreciable differences in the resultant DNA damage.

There are several types of damage to DNA that can result from the disruption of its chemical bonds by ionizing radiation. The most common is the formation of a break in a single strand of the backbone of the DNA. These breaks are easily repaired and generally do not produce a biological effect. However, if a second break coincidentally occurs in the backbone of the opposite strand and is near the first break, then a double-strand break (DSB) may occur and the DNA is fractured in two. This is a rare event with low LET radiation exposure. DSBs are considered to be the foremost form of radiation-induced damage that causes a detrimental biological effect. Repair of a DSB is less efficient than the repair of a single-strand break (SSB) and is at times inaccurate. This inaccuracy in repair is one method in which an alteration that leads to a biological effect may be introduced (Wyman and Kanaar, 2006).

Another manner in which the induction of a DSB may lead to a biological effect is when two or more DSBs occur concurrently within the same cell. Inappropriate rejoining of the fractured DNA may result in one of a number of chromosomal aberrations. Some of these aberrations are not tolerable and lead to cell death. Other aberrations, such as deletions, inversions, and translocations, are not lethal and the genetic dysregulation that emerges has been shown to be potentially carcinogenic (Hall and Giaccia, 2006; Sachs et al., 2000).

While the induction of DSBs in the backbone of DNA is considered the predominant cause of radiation-induced biological effects, damage to the nucleotide bases of DNA by radiation exposure may also elicit the same response. The oxidation or the complete losses of one or more nucleotide bases are two of the methods in which radiation exposure leads to base damage (Hall and Giaccia, 2006; Pouget et al., 2002). As with the repair of a DSB, inefficient or incorrect repair of these lesions may introduce the necessary modification for cellular dysregulation. Further, clustering of DNA damage, which may include a combination of SSBs, DSBs, and base damage within one or two helical turns of DNA, are known to be more effective in eliciting a biological effect (Hall and Giaccia, 2006; Shikazono et al., 2009).

Regardless of the mechanism behind a specific biological effect, each effect can be classified based on whether the severity of the effect is directly related to the radiation dose. Effects that worsen as the radiation dose increases are termed deterministic because the dose determines the extent of the effect. Inversely, effects whose severity is independent of the dose received are termed stochastic due to the random nature of the end result. Based on these criteria, radiation-induced carcinogenesis is defined as a stochastic effect because the risk of cancer increases with dose but the grade of cancer does not (Hall and Giaccia,

2006). Therefore, the type of the exposed biological material may significantly influence the radiation effect.

Altogether, there is a clear association between radiation and carcinogenesis. The random alteration of DNA molecules from the deposition of energy by radiation presents a definite challenge for any cell. Different cell types may respond differently to this insult and therefore lead to the disparate risks of cancer across tissue types. Further investigation into the general and tissue specific cellular response to radiation is required translate the epidemiological data into a global model for assessing the carcinogenic risk from radiation.

CHAPTER TWO.

Multipotency of Immortalized Human Bronchial Epithelial Cells

2.1. Introduction.

The lung is a complex and vital organ that mediates gas exchange between the bloodstream of the organism and its environment. Continuous exposure of the lung to deleterious agents warrants an efficient mechanism of repair in order to maintain its integrity and functional capacity throughout a lifetime. Studies on lung development and regeneration of the mature lung tissue utilizing model organisms have provided valuable insights into lung homeostasis and maintenance. These studies have also demonstrated that the adult lung does not adhere to the classic stem cell model established for tissues that have high turnover rates such as the blood and colon (Figure 1.5 A) (Wagers and Weissman, 2004). Instead, the lung appears to conform to an alternate model established in tissues with slow turnover rates and in which a tissue stem cell has not been reported (Alison et al., 2004; Dor et al., 2004; Giangreco et al., 2009). In this model, quiescent cells throughout the tissue that function as differentiated cells retain the capacity to divide and differentiate in other cell types of that tissue. These cells have been termed facultative stem cells due to their versatile nature (Figure 1.5 B) (Rawlins and Hogan, 2006).

Analysis of the epithelial lining of the pulmonary tract by various methods has identified Clara cells, Clara^V cells, and Type II pneumocytes as potential facultative stem cells of the lung (Figure 1.6) (Evans et al., 1975; Evans et al., 1978; Giangreco et al., 2002; Hong et al., 2001; Randell, 2006; Reynolds et al., 2000a). In the adult lung, under normal conditions, these cells meet the criteria of a facultative stem cell in that they are quiescent and have a differentiated phenotype. When the lung epithelium is damaged, these cells are induced to proliferate and then regenerate into specific cells types within their vicinity of the lung. Clara^V cells have demonstrated the highest degree of reparative potential in that they are able to self renew and differentiate into Clara cells, goblet cells, and ciliated cells (Hong et al., 2001; Randell, 2006; Rawlins et al., 2009; Reynolds et al., 2000a; Reynolds et al., 2000b). The regenerative potential of Clara cells is somewhat limited in comparison to Clara^V cells because, while Clara cells can self renew and differentiate into goblet and ciliated cells, there is no evidence that they can become Clara^V cells (Evans et al., 1978; Evans et al., 1986; Rawlins et al., 2009). Type II pneumocytes are unique such that these are the only alveolar cells that have been shown to have any regenerative capacity. They are also the only cell type for which there is evidence to support a role in alveolar regeneration (Figure 1.6) (Evans et al., 1975; Pitt and Ortiz, 2004; Rawlins and Hogan, 2006). Collectively, the restricted regeneration potential observed with each of these cells suggests they have retained an oligopotent capacity and not the

multipotent capacity attributed to a tissue stem cell (Wagers and Weissman, 2004; Weissman et al., 2001).

The limited differentiation capacity of these cells and rapid response to damage has led to the suggestion that the facultative stem cells may be analogous to the TA cells of the classic stem cell model (Snyder et al., 2009). Thus, the possibility of a tissue stem cell, or progenitor cell, for the lung remains debatable. Only one cell in the lung epithelium, the basal cell, has been characterized to have features that would permit it to be loosely interpreted as a lung tissue stem cell. This designation is primarily due to the lack of any differentiated morphology or function attributed to the basal cell (Figures 1.3 A and 1.6). As for the regenerative capacity, however, the basal cells only have an oligopotent capacity since there is no evidence that these cells may become Clara^V cells or any of the alveolar pneumocytes. It should be noted, however, that much of the details concerning lung homeostasis and repair have been elicited from the use of model organisms such as the mouse, which may not directly recapitulate what occurs in humans. There are subtle differences between the lungs of each species. Demonstrating one such inherent difference between the human lung and the murine lung is that the existence of the Clara^V cell has only been shown in mice and there is no evidence that these cells exist in humans.

A persuasive model proposed for the lung that integrates all of the characteristics described above is that only during lung development is there a lung tissue stem cell, deemed the embryonic progenitor cell, with the potential to differentiate into all cell types of the lung. It is believed that during the development, the epithelial stem cells of the lung become restricted in their potency and therefore the adult lung does not contain a multipotent stem cell. Once a cell becomes restricted, it then would be oligopotent and capable of regenerating cells only within its own region (Figure 1.5 B). This region could then be considered a distinct compartment of the lung. The regional localization and restricted regenerative capacity of each purported facultative stem cell of the lung along the proximodistal axis of the pulmonary tract supports this concept.

The lung has been characterized as being subdivided into compartments based on their functional contribution to the respiratory process (Figure 1.2). Interestingly, these subdivisions appear to coincide with the different facultative stem cell compartments. The most proximal compartment is comprised of the trachea and bronchi and primarily functions to cleanse and humidify the inspired air. This central compartment is maintained by the basal cell in humans, but in mice the Clara cell and Clara^V cell may contribute to its regeneration when needed (Figure 1.6 A). Distal to the bronchi is the peripheral compartment that is made up by the bronchiole tubes, which mainly function to conduct the air.

Furthest is the alveolar sac in which air is exchanged (Figure 1.6 B). In humans, it has been suggested that there may exist an atypical basal cell that resides within the bronchiole tubes and repairs these tubules, but there is no direct evidence for this. The evidence in mice, on the other hand, for both the Clara cells and Clara^V retaining the capacity of regenerating the bronchiole tubes, and are thus the facultative stem cells of the bronchiole tubes, is extensive (Barth and Muller, 1999; Evans et al., 1978; Evans et al., 1986; Giangreco et al., 2009; Giangreco et al., 2002; Hong et al., 2001; Rawlins et al., 2009; Reynolds et al., 2000a). The existence of the Clara^V cell in humans remains unclear, as is whether or not the Clara cells perform a similar reparative function in humans. The alveolar sacs into which the pulmonary tract terminates and gas exchange physically occurs constitute the terminus of the peripheral compartment. Only the Type II pneumocyte have the capacity *in vivo* to proliferate and regenerate cells of the alveoli (Figure 1.6 B) (Evans et al., 1975; Rawlins and Hogan, 2006). Altogether, current understanding of lung homeostasis and repair bolsters the argument that the lung does not have any multipotent tissue stem cells.

Acceptance of this model for lung homeostasis and repair, however, has been hindered by the lack of experimental approaches for the human lung. Until recently, there have been few reports of the successful culture of normal human lung epithelial cells. This changed in 2004 when a method for the long-term

culture of normal human bronchial epithelial cells (HBECs) through the expression of *Cdk4* (K) and *hTERT* (T) was reported (Ramirez et al., 2004). The HBECs provide a sustainable cell reagent suitable for the evaluation of lung biology *in vitro* (Ramirez et al., 2004). Previous work from our lab demonstrated that the immortalized HBEC cell line number 3 (HBEC3 KT) retains nuclear expression of the basal cell marker p63 when cultured in a 2-dimensional (2D) monolayer. It was also shown that, when cultured atop a fibroblast-embedded collagen matrix, or a 3-dimensional (3D) environment, and then exposed to an air-liquid interface, these cells are capable of differentiating into the representative ciliated and goblet cells of the pulmonary tract from which they are derived (Vaughan et al., 2006). These results suggest that the HBEC3 KT cells are akin to basal cells under the culture conditions studied to date. The possibility that these cells are indeed similar to basal cells may be attributed to the fact that, if the basal cells retain the highest level of potency in the bronchi, then they would be the most competent cells to emerge and sustain in culture from a lung tissue explant. However, it is important to note that the characterization of these cells has been limited so far, and that what may be characterized *in vitro* without the normal stromal cell microenvironment may be quite different depending on the *in vitro* conditions provided.

Currently, it is unknown how the facultative stem cells of the lung are regulated. In certain systems, epigenetic changes permanently alter the transcriptional program of a stem cell or differentiating cell (Kohyama et al., 2008; Lunyak and Rosenfeld, 2008). The environment in which a cell resides such as the stem cell niche has also been shown to impact the potential of a cell (Kohyama et al., 2008; Yin and Li, 2006). Comparison of the different lung compartments in which each facultative stem cell resides suggests that the restricted potency is at least somewhat imparted by their environment. Since these restrictions would be eliminated or at least loosened by placing cells in culture, then the true potential of any facultative or stem cell may be assessed. The similarities of the HBEC3 KT cells with the basal cells of the lung make these cells an ideal reagent for this analysis. Our analysis demonstrates that the HBEC3 KT cell line retains a multipotent capacity *in vitro*, and supports the concept that the local microenvironment and stem niche may influence the compartmental restriction *in vivo*.

2.2. Results.

***In Vitro* Analysis of HBEC 3KT Potency.**

Previous studies have established that the HBEC3 KT cell line resembles the basal cell of the lung and retains a similar oligopotent capacity. However, the

potential of these cells to differentiate into other cell types of the lung, including the Clara cell, has not been examined. We proceeded to assess the *in vitro* differentiation potential of the HBEC3 KT cells through immunofluorescence (IF) analysis of established protein markers for multiple cells types of the lung. In order to establish a baseline expression profile for the HBEC3 KT cells, these cells were cultured in differentiation media as a confluent 2D monolayer for 2 days and then analyzed for the various markers. Surprisingly, under these conditions the HBEC3 KT cells were simultaneously positive for markers of several different lung epithelial cells including basal cells, Clara cells, and Type II pneumocytes (Figure 2.1 A-G). When cultured for five days under identical conditions, some heterogeneity in expression was observed (Figure 2.1 H-N). The basal cell marker, p63 (Daniely et al., 2004), which was detected in the nuclei of all HBEC3 KT cells at two days, was only observed in 50% of these cells after five days (Figure 2.1 A and H). Expression of CC10, a marker for Clara cells and which has limited expression in Type II pneumocytes (Coppens et al., 2007; Rawlins et al., 2009), also changed from uniform expression levels within the population at two days to increased levels in approximately 20% of the HBEC3 KT cells after five days of culture (Figure C and J). None of the other markers tested demonstrated changes in expression between timepoints (Figure 2.1 B, D-G, I, and K-N).

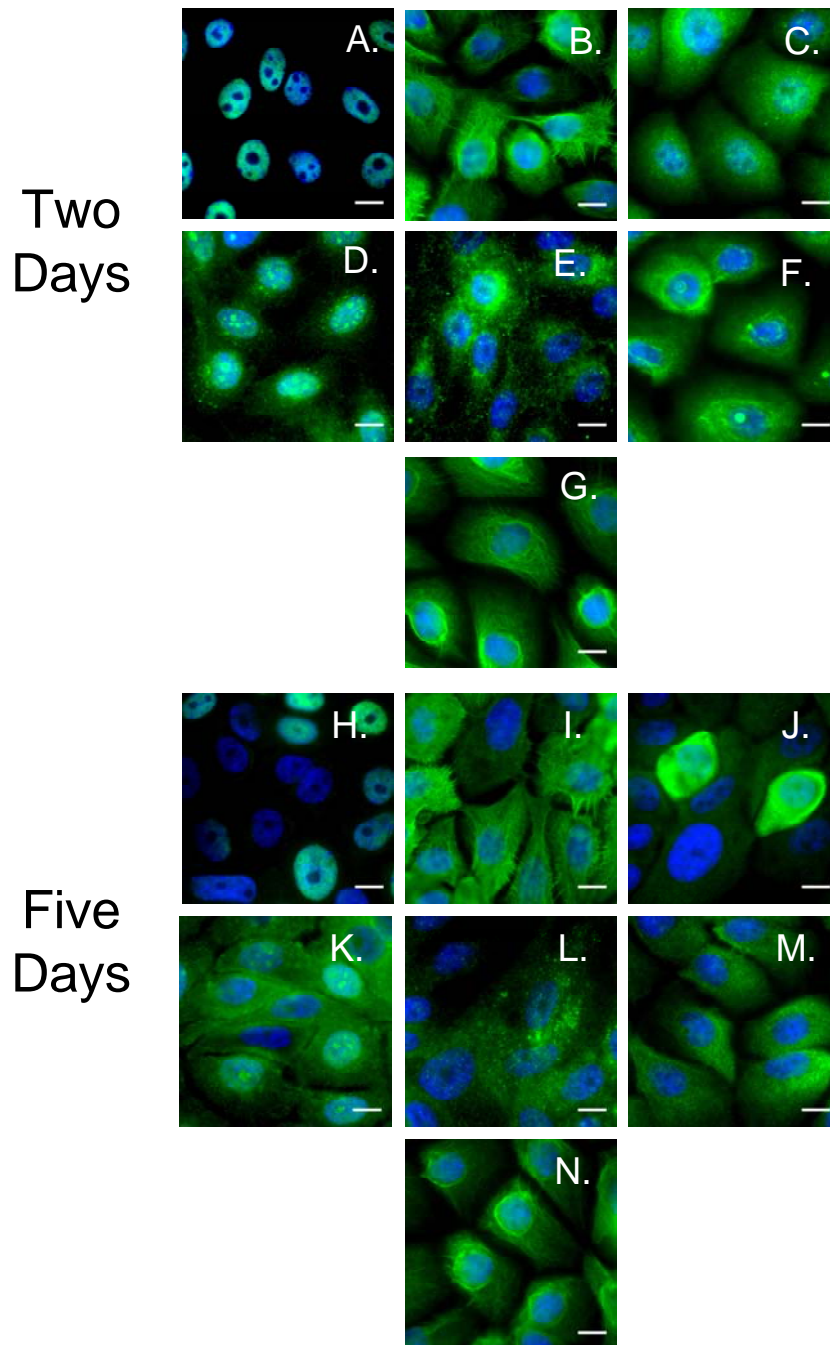


Figure 2.1 HBEC3 KT cells simultaneously express markers of several lung epithelial cells.

(A-G) HBEC3 KT marker expression two days after plating. (A., p63; B., K14; C., CC10; D., SP-C; E., SP-A; F., SP-D; G., K19). (H-N) HBEC3 KT marker expression five days after plating (H., p63; I., K14; J., CC10; K., SP-C; L., SP-A; M., SP-D; N., K19). (Scale bar equal 10 μ m.)

Since expression of each of the above markers is generally considered to be indicative of terminal differentiation, we proceeded to examine whether the expression of these markers varied under proliferative conditions. Analysis of Ki-67 expression by IF two days after plating demonstrated that approximately 95% of the HBEC3 KT cells are actively proliferating when seeded at sub-confluence compared to only 40% when plated at confluence (Figures 2.2 A and B). By day five, the proliferative index fell for both low and high density (48% and 11%, respectively) (Figures 2.2 A and B). Irrespective of the proliferative state, all assessed markers, p63, K14, K19, CC10, SP-A, SP-C, and SP-D are expressed in the HBEC3 KT cells (Figure 2.2 C - I). However, there are distinct morphological differences in the cytoplasmic proteins compared to the predominantly quiescent population. These markers appear homogeneous throughout the cytoplasm as should be expected in an actively dividing cell (Figure 2.2 C - I).

Expression of each of the peripheral lung cell markers detected (SP-A, SP-C, SP-D, and CC10) have all been shown be dependent on the transcription factor TTF-1 (Bohinski et al., 1994). Therefore, we sought to determine whether TTF-1 is expressed in the HBEC3 KT cell line under the previously described

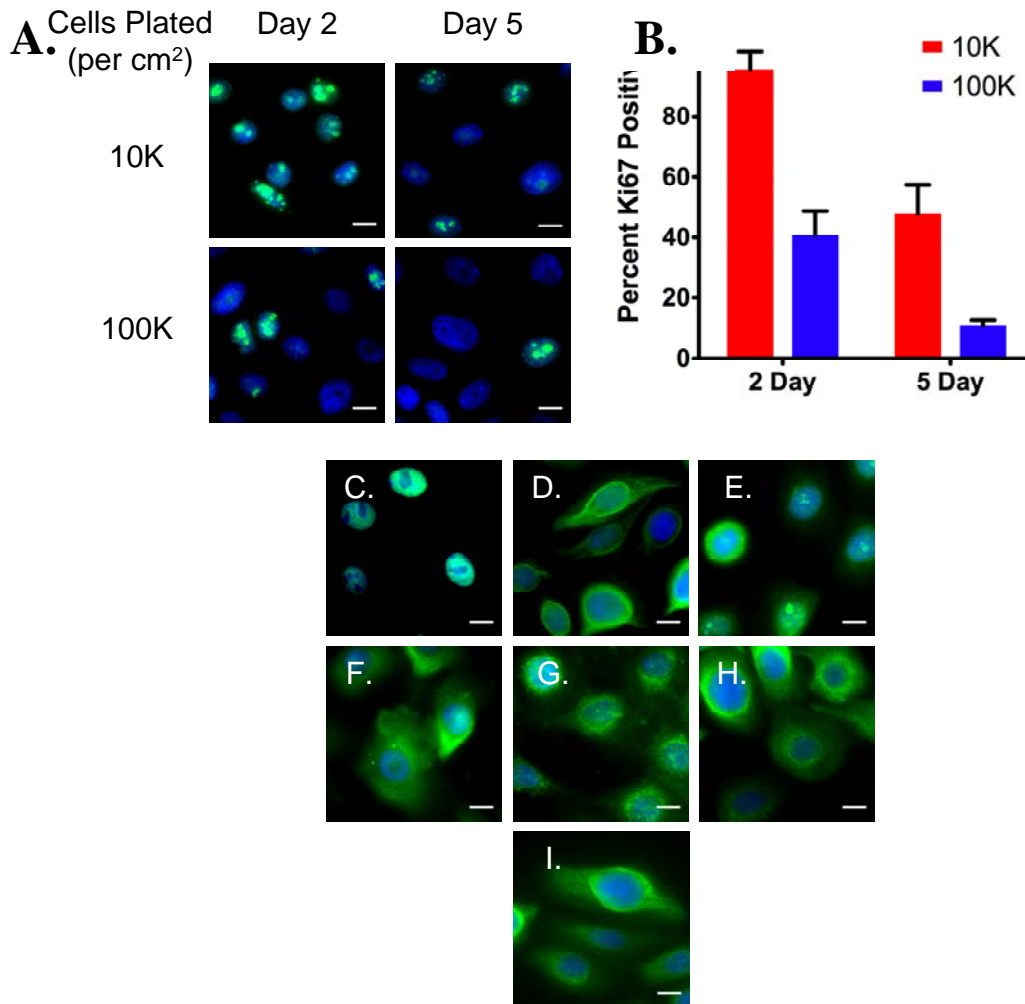


Figure 2.2. Marker expression in HBEC3 KT is independent of proliferative status.

(A) Immunofluorescence staining of Ki67 in HBEC3 KT cells two or five days after being plated at low (10K) or high (100K) density demonstrates proliferation status under each condition. (B) Quantitation of percent Ki67 positive nuclei per condition in (A). (C-I) Marker analysis of HBEC3 KT cells when proliferation index is highest (two days after seeding at low density) indicates that marker expression is not dependent on proliferative status. (C) p63 (D) K14 (E) SP-C (F) CC10 (G) SP-A (H) SP-D (I) K19 (scale bar equals 10 μ m)

culture conditions. When cultured at low density, TTF-1 is expressed in the HBEC3 KT cell line and its localization appears to change over time (Figure 2.3 A). Two days after plating all of HBEC3 KT cells have TTF-1 localized in the exclusively in the cytoplasm. By five days, the number of TTF-1 positive HBEC3 KT cells dropped to roughly 50% of the population and was detected only in the nucleus of these cells suggestive that TTF-1 is transcriptionally active in the HBEC3 KT cells (Figure 2.3 A). Interestingly, if the HBEC3 KT cells are plated at confluence TTF-1 is not detectable in any HBEC3 KT cells neither at two days or five days (Figure 2.3 A and B).

Transcriptional Analysis of HBEC3 KT Cell Line.

Although the adult lung has been characterized as only having regionally restricted oligopotent progenitor cells, during lung branching morphogenesis there are multipotent embryonic progenitor cells that are capable of differentiating into every epithelial cell type of the respiratory tract. These embryonic progenitor cells have been described to remain at the actively proliferative distal tips of the emerging lung, have a distinct expression profile, and express markers of multiple cell types of the lung (Liu and Hogan, 2002; Ringvoll et al., 2008; Wuenschell et al., 1996). To determine whether the HBEC3 KT cells resemble an embryonic progenitor, we performed microarray analysis on proliferating and quiescent HBEC3 KT cells five days after plating. Comparison between these two

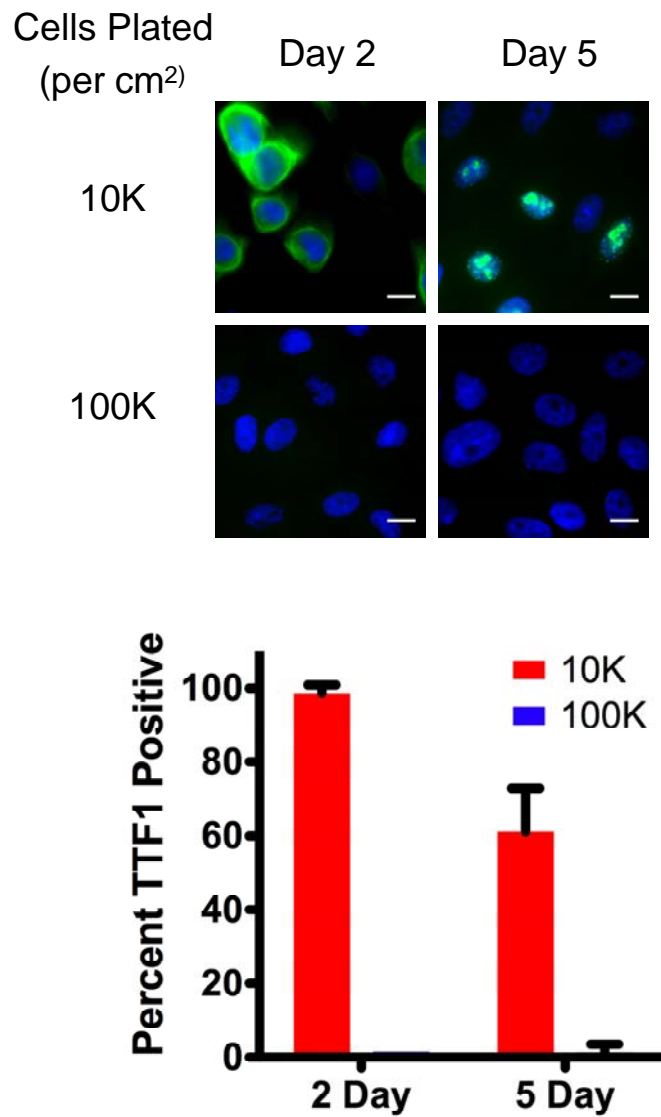


Figure 2.3. TTF-1 expression and localization changes with proliferative status in HBEC3 KT cell line.

(A) TTF1 (green) is expressed and localized to cytoplasm two days after plating HBEC3 KT cells at low density (10K). After five days of growth, approximately 60% of HBEC3 KT cells expressed TTF1 localized in nucleus. TTF1 is not detected when plated at high density (100K) (scale bars equal 10 μ m). (B) Quantitation of total TTF1 positive cells seeded in each condition described in (A) (error bars are SEM).

conditions indicated that 323 genes were differentially expressed by at least 2-fold difference and at a 1.0% false discovery rate (FDR) (Figure 2.4 A and Appendix A). Among these genes are several that have been ascribed to embryonic progenitor cells of the lung. Notably, two of the most critical genes, Sex determining region Y- box 9 (SOX9) and ETS translocation variant 5 (ETV5), and the endodermal marker FOXA2 are significantly down-regulated upon the induction of quiescence in the HBEC3 KT cells (Figure 2.4 B and Appendix A). SOX9 expression was confirmed through immunofluorescence staining (Figure 2.4 C). Another gene characterized to be important in the embryonic progenitor cells, Inhibitor of DNA binding 2 (ID2), however, is significantly up-regulated under these conditions (Figure 2.4 B and Appendix A). Other interesting genes that are significantly up-regulated in quiescent HBEC3 KT cells include SP-D, Forkhead box protein O3 (FOXO3), Ephrin type-A receptor 4 precursor (EPHA4), several aldehyde dehydrogenase (ALDH) genes, and multiple CyP450 genes, keratin genes, mucin genes. Fibroblast growth factor 3 (FGFR3), which has been shown to play a role in alveolar development is also up-regulated (Appendix A).

To further define stem-like properties in the HBEC3 KT cells, Q-PCR analysis of genes and pathways known to be important in multipotent stem cells was performed from RNA extracted under proliferative and quiescent conditions.

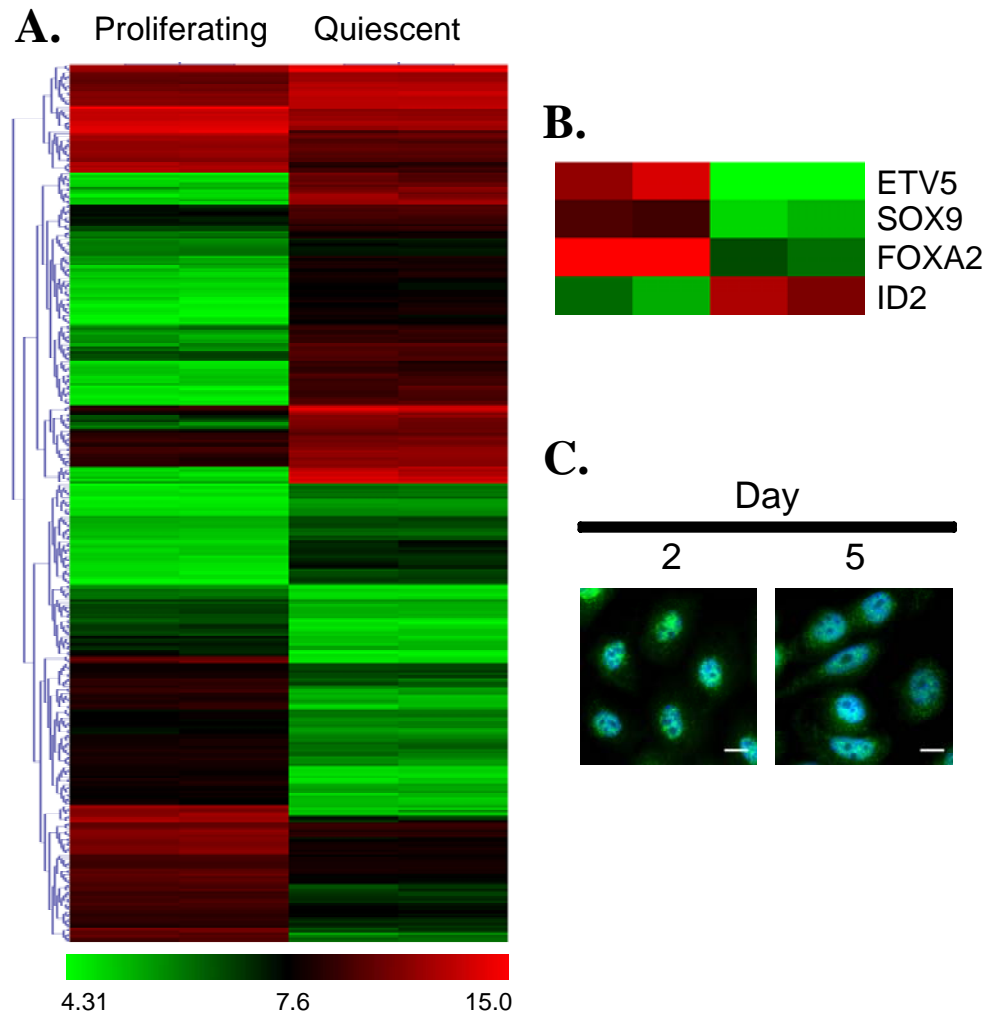


Figure 2.4. Transcriptional profile indicates HBEC3 KT cells resemble embryonic progenitor cells of murine lung.

(A) Gene expression profile of quiescent versus proliferating HBEC3 KT cells (scale log₂ normalized). (B) Expression profile of genes characterized as having critical roles in lung development and embryonic progenitor cells. (C) Immunofluorescence staining of SOX9 in quiescent HBEC3 KT cells (scale bar equals 10 μ m).

Many of these genes, such as Nanog, Sex determining region Y- box 2 (SOX2), Frizzled 1 (FZD1), β -catenin, Notch 1, Notch 2, Notch 3, Indian hedgehog (IHH), Patched 1 (PTCH1), and Patched 2 (PTCH2), are up-regulated when the HBEC3 KT cells are quiescent (Figures 2.5 A – D). By immunofluorescence, expression of Octamer-binding transcription factor 4 (OCT4) was not detected in either condition, while Polycomb complex protein BMI-1 (BMI-1) was detected in both conditions (Figures 2.5 E - H).

Development of a 3D Differentiation Model Using the HBEC3 KT Cell Line.

A previous differentiation model demonstrated that the HBEC3 KT cell line retains an oligopotent capacity to differentiate into both ciliated and goblet cells. In order to evaluate whether the novel expression profile discovered enables the HBEC3 KT cells to differentiate into other cell lineages, a 3D culture model utilized for other tissues such as the breast was modified for use with the HBEC3 KT cells (Figure 2.6 A) (Lee et al., 2007). HBEC3 KT cells within reconstituted basement membrane (Matrigel™) do not proliferate without the co-culture with IMR90 fetal lung fibroblasts (Figures 2.6 B and C). Upon IMR90 stimulation, HBEC3 KT cells develop into regular sphere-like structures with strong adherens junctions after five days of growth (Figures 2.6 B – E). Q-PCR analysis of the multipotent progenitor genes and pathways previously analyzed in the HBEC3 KT cells are down-regulated after five days of culture (Figure 2.7 A -

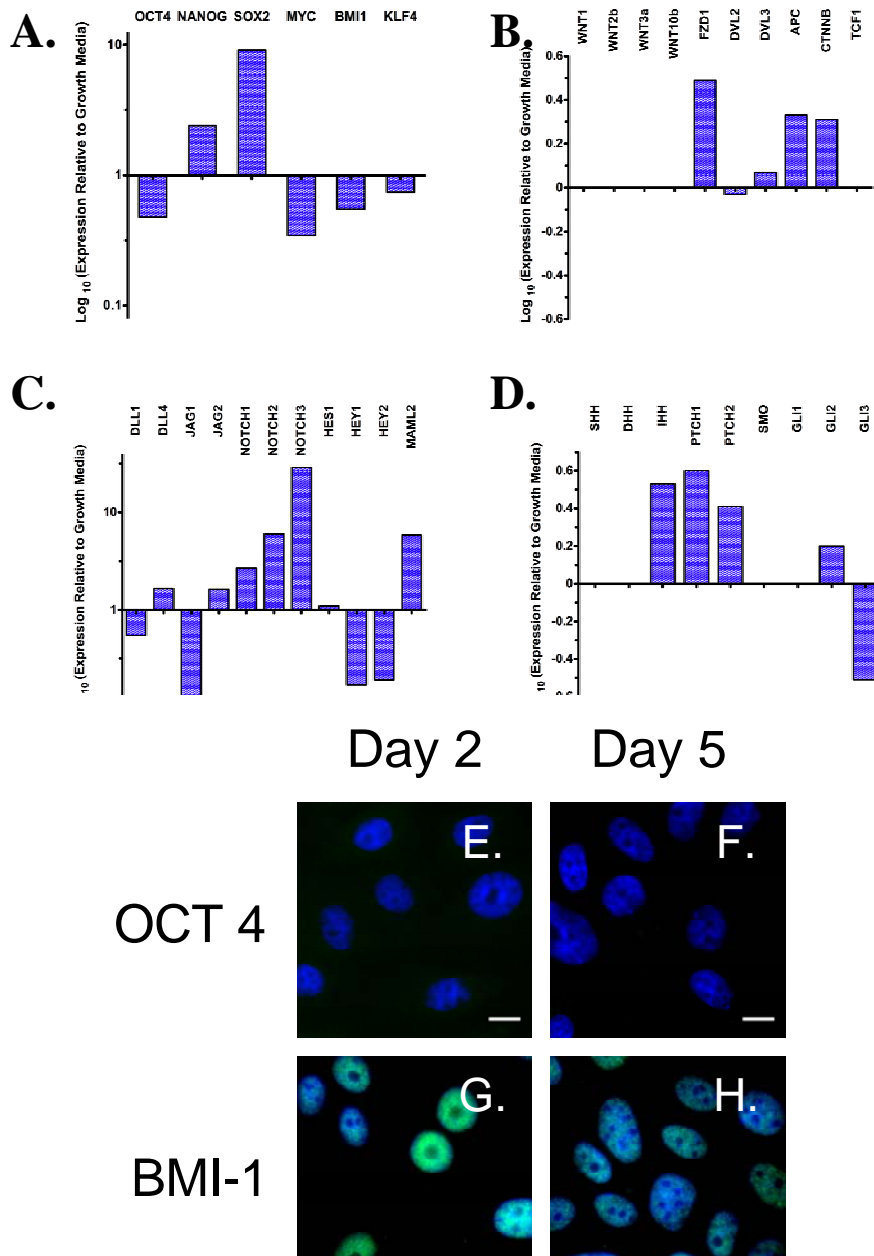


Figure 2.5. Multipotent progenitor maintenance genes and pathways up-regulated in HBEC3 KT cells coincident with marker expression. (A-D) Q-PCR analysis of genes and pathways critical for progenitor maintenance. (A) Genes related to induce pluripotency. (B) Wnt pathway genes. (C) Notch pathway genes. (D) Hedgehog pathway genes. (E-H) Protein expression under quiescent conditions. (E-F) OCT4 is not expressed at either timepoints. (G-H) BMI-1 is expressed and localized to nucleus at both timepoints. Possible decreased expression at five days.

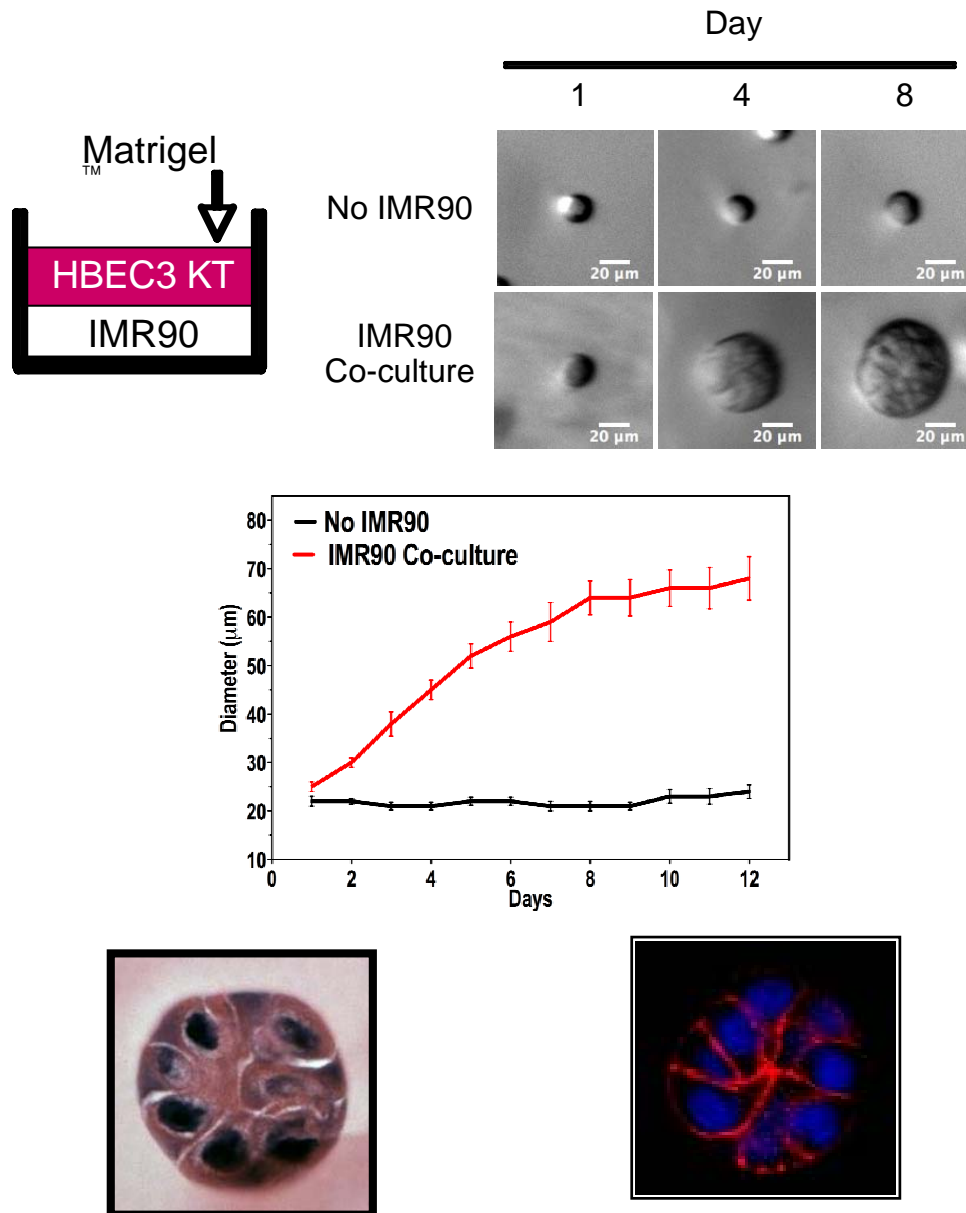


Figure 2.6. HBEC3 KT cells cultured in 3D environment of reconstituted basement membrane form cyst-like structures when co-cultured with IMR90 fetal lung fibroblasts.

(A) Culture scheme. (B) Phase contrast images of HBEC3 KT cells cultured in Matrigel™ with or without IMR90 fibroblast co-culture. (C) Quantitation of growth observed in (B). (D) Representative hematoxylin and eosin staining of HBEC3 KT cyst-like structure after five days of growth. (E) Immunofluorescence staining of E-cadherin in five day HBEC3 KT cyst-like structure.

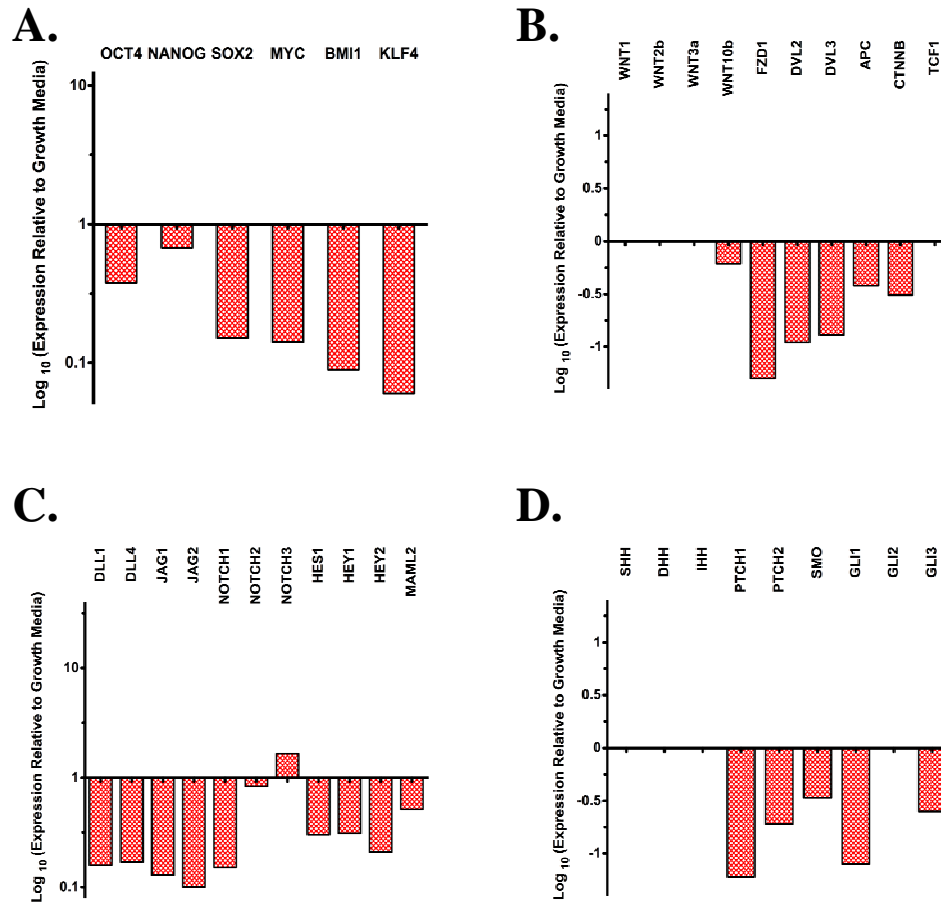


Figure 2.7. Multipotent progenitor maintenance genes and pathways down-regulated in HBEC3 KT cyst-like structures.

(A-D) Culture of HBEC3 KT cells in Matrigel™ with IMR90 fibroblast culture results in down-regulation genes and pathways critical for progenitor maintenance. (A) Genes related to induce pluripotency. (B) Wnt pathway genes. (C) Notch pathway genes. (D) Hedgehog pathway genes. (E-F) Protein expression under quiescent conditions.

D). At this time point these structures, immunofluorescence analysis demonstrates that these structures express SP-A (Figure 2.8 A). The detection of lamellar bodies by transmission electron microscopy suggests the presence of mature SP-A in these structures (Figures 2.8 B and C). If these structures are cultured for nine days, several morphological changes are detected. Some structures contain distinct lumens lined by squamous HBEC3 KT cells (Figure 2.8D). In these structures, SP-A may be detected within the luminal space (Figure 2.8 E). Interestingly, if the HBEC3 KT cells are seeded atop of Matrigel™ in the presence of IMR90 fibroblasts, the HBEC3 KT cells self-assemble into networks of tubular structures (Figure 2.9 A). Small bud-like structures become apparent along the sides of these structures by three to five days of culture (Figures 2.9 B and C).

2.3. Discussion.

Many studies have attempted to elucidate the homeostatic processes in the adult lung and to identify the progenitor cells involved. These studies described that the lung utilizes a maintenance scheme similar to the liver and pancreas and contains several oligopotent progenitor cells (Alison et al., 2004; Dor et al., 2004; Giangreco et al., 2009; Rawlins and Hogan, 2006; Rawlins et al., 2009). It is only during lung development that there exists a multipotent progenitor cell of the lung (Liu and Hogan, 2002; Lu et al., 2008; Rawlins et al., 2007). In this study, we

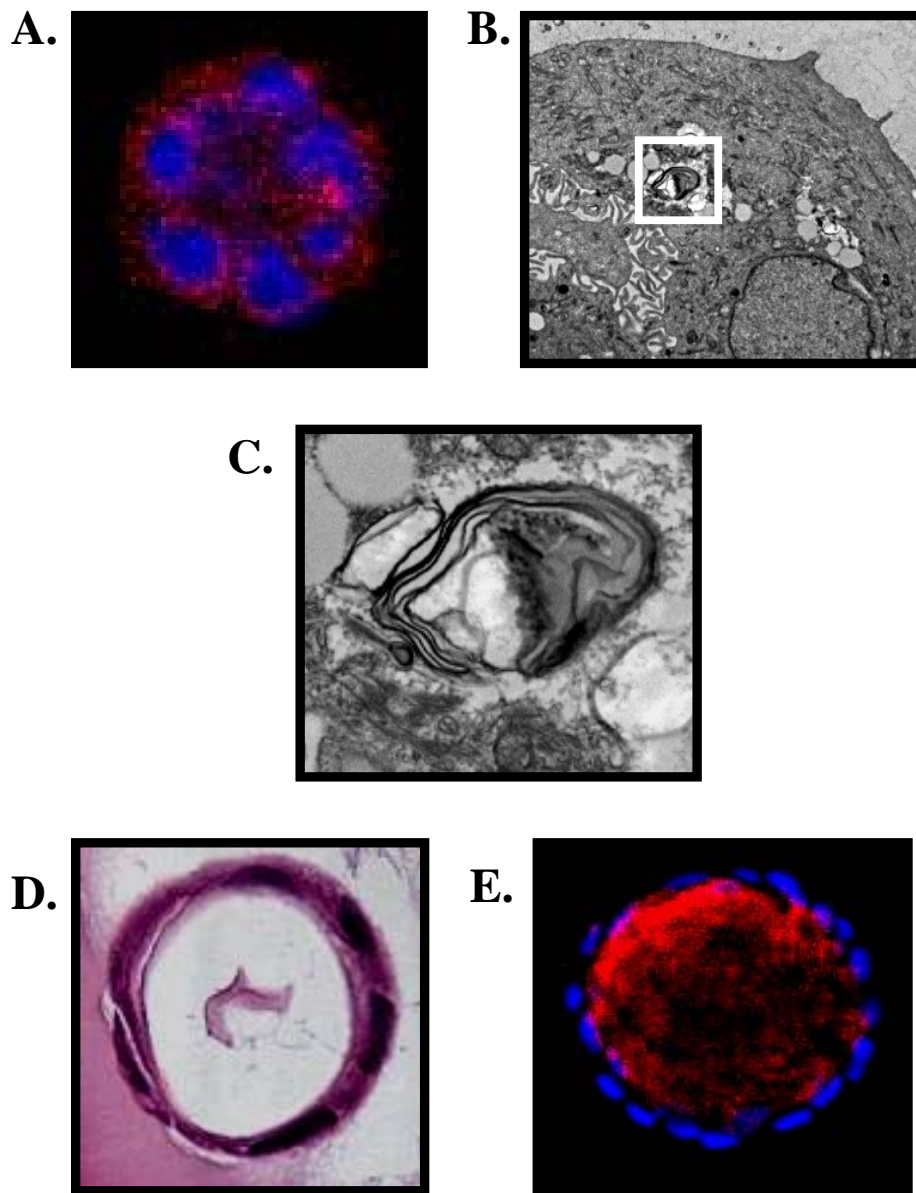


Figure 2.8. Features suggestive of pneumocyte differentiation in HBEC3 KT cyst-like structures.

(A) HBEC3 KT cells grown for five days in Matrigel™ retain punctate SP-A immunofluorescence staining. (B) Transmission electron microscopy reveals presence of lamellar bodies in five day HBEC3 KT cyst-like structures suggestive of Type II pneumocyte differentiation. (C) Higher magnification of inset of (B). (D) Some HBEC3 KT cyst-like structures cultured for nine days are lined with flattened cells surrounding lumen. (E) Immunofluorescence staining in nine day HBEC3 KT cyst-like structures reveals potential luminal localization of SP-A.

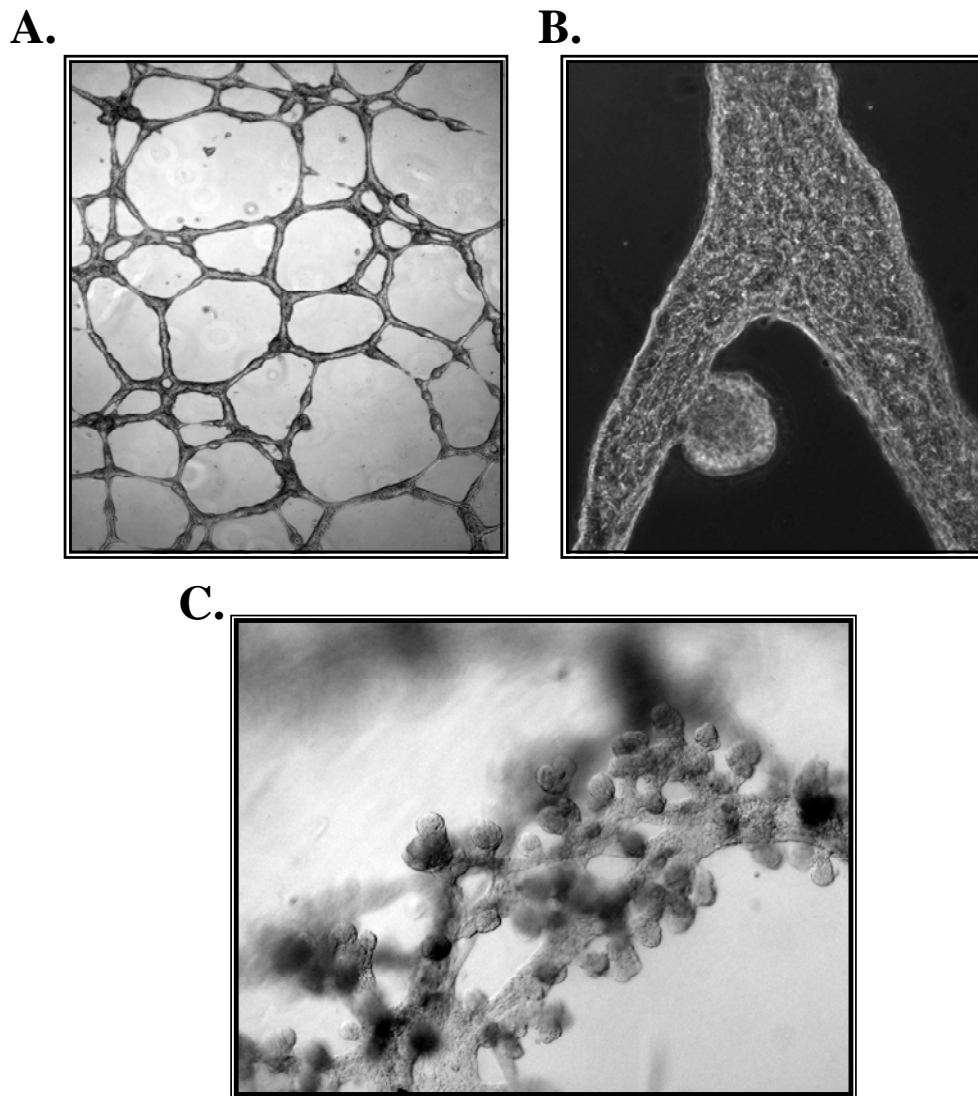


Figure 2.9. Tubule formation and potential branching morphogenesis induced in HBEC3 KT cells cultured on reconstituted basement membrane.

(A) HBEC3 KT cells plated atop of Matrigel™ with IMR90 co-culture self-aggregate into tubules arranged in web-like network. (B) After a few days of culture, small bud-like protrude from web-like structure. (C) By three to five days, bud-like protrusions encompass web-like structures.

demonstrate that the HBEC3 KT cell line is capable of simultaneously expressing markers of multiple cell types of the lung including that of the each facultative stem cells of the lung (Figures 2.1 A – N and 2.2 C - I). This feature of simultaneous expression is novel. Basal cells are known to express both p63 and K14, Clara cells are known to express CC10, SP-A and SP-D, and lastly Type II pneumocytes are known to express CC10, SP-C, SP-A and SP-D (Kalina et al., 1992; Madsen et al., 2000; Rawlins and Hogan, 2006; Rawlins et al., 2009). K19 is reported to be detectable in all epithelial cells of the lung (Nakajima et al., 1998). There are no reports of simultaneous expression of all these markers. Thus, in some respects, the HBEC3 KT cells appear to have properties of a multipotent stem cell.

Previous work from our lab established that the HBEC3 KT cells resemble basal cells, in that it express p63 and retain the capacity to differentiate into ciliated and goblet cells (Vaughan et al., 2006). Basal cells in mice have been shown to differentiate into Clara cells (Borthwick et al., 2001; Rock et al., 2009). Whether human basal cells equally retain this capacity is not known and this potential has not previously been addressed in the HBEC3 KT cell line (Ramirez et al., 2004; Vaughan et al., 2006). Simultaneous expression of both basal and Clara cell markers suggests that at the time of analysis, the HBEC3 KT cells are

in transition between cell types. There is no evidence that a Clara cell may become a basal cell and thus the directionality of this transition would be from a basal cell to a Clara cell. The loss of p63 expression and the enhanced CC10 expression in subsets of HBEC3 KT cells after five days of culture supports this concept (Figures 2.1 A versus H and C versus J). The expression of SP-C in the HBEC3 KT cells, however, precludes this assessment since it is only expressed in Type II pneumocytes (Figures 2.1 D and K and 2.2 E) (Kalina et al., 1992). Thus, the designation of the HBEC3 KT cells as either basal or Clara cells or an oligopotent stem cell may need revision. In addition, freshly isolated human lung basal cells were shown to only differentiate into only ciliated cells *in vitro* and CC10 expression was never detected in these cells (Rock et al., 2009). Since the HBEC3 KT cells can differentiate into both ciliated and goblet cells in some culture conditions and into cell types associated with small bronchioles and alveoli, it suggests that HBEC3 KT cells may not be typical basal cells.

The transcription factor, TTF1, is one of the most critical genes expressed in the lung because of its integral role in all stages of lung development. In the adult lung, it directly regulates expression of several of the markers examined in this study and is expressed only in Type II pneumocytes and Clara cells (Ikeda et al., 1995; Zhou et al., 1996). As such, Type II cells and Clara cells are those in which these markers are detected *in vivo* (Bruno et al., 1995; Ikeda et al., 1995;

Kelly et al., 1996; Maeda et al., 2007; Ray et al., 1996; Zhou et al., 1996). Our observation of transient expression of TTF1 in the HBEC3 KT cells agrees with the detection of CC10, SP-A, SP-C, and SP-D (Figure 2.3A and B). When initially plated at low density, cytoplasmic localization of TTF1 may entirely be due to sequestration during proliferation. As these cells begin to become quiescent, TTF1 appears to translocate into the nucleus and transcribe its target genes (Figure 2.3 A). FOXA2 has been shown to regulate TTF1 *in vitro* and as is down-regulated when TTF1 expression is lost in the HBEC3 KT cells potentially explaining this result (Figure 2.3B and Appendix A) (Ikeda et al., 1996). Further study is required to determine whether TTF1 expression may be maintained in these cells at quiescence. Irrespective, since TTF1 is expressed even transiently in HBEC3 KTs suggests that these cells have characteristics of both central and peripheral airways cells of the lung.

The potential to express markers from every compartment of the lung suggests that, if properly induced, the HBEC3 KT cells may retain the capacity to differentiate into most if not all cell types of the lung (Figures 2.1 A – N and 2.2 C - I). This would imply that the HBEC3 KT cells *in vitro* resemble the embryonic progenitor cells of the developing lung. Our analysis of the gene expression profile of the HBEC3 KT cells under proliferating and quiescent conditions bolsters this argument due to similarities with that characterized for

embryonic progenitors in the mouse (Liu and Hogan, 2002). Q-PCR results also suggest that the HBEC3 KT cells are poised to respond to active developmental cues upon the induction of quiescence (Figure 2.5 A – D). This result, interestingly, corresponds with an increase in the expression of one of the most critical embryonic progenitor markers, ID2 (Figure 2.3B and Appendix A) (Lu et al., 2008; Rawlins and Hogan, 2006). Application of extracellular signals known to be present during the various stages of lung development under these conditions could further illuminate the true potential the HBEC3 KT cell line. In addition, an active role for specific microRNAs in these progenitor cells has also been described and therefore microRNA expression profiling of the HBEC3 KT cell line needs to be evaluated (Lu et al., 2008).

Culture of the HBEC3 KT cells within an alternate 3D environment provides further support for the multipotent capacity of these cells. Lamellar bodies are secretory organelles that in the lung are found exclusively in Type II pneumocytes and are comprised of mature surfactant protein. Detection of lamellar bodies in the 3D cyst-like structures formed by the HBEC3 KT cells by transmission electron microscopy indicates that these cells may be induced to become Type II pneumocytes (Figure 2.8 B and C). Since Type II pneumocytes can differentiate into the flattened Type I pneumocyte, then this may explain the

presence of the squamous cells found in some 3D structures when maintain for nine days in Matrigel™ (Figure 2.8 D).

Overall, our results characterize the HBEC3 KT cells as potentially resembling an embryonic progenitor of the lung and retaining a multipotent capacity *in vitro*. As these cells were derived from the central airways from the adult lung, this suggests that the restrictive potency observed for the facultative stem cells *in vivo* may be due to regulation by the microenvironment. These restrictions would then be alleviated when placed in culture thus permitting their true potency to be assessed. Analysis of several known environmental cues from each compartment such as rigidity of substrate and endothelial crosstalk may provide useful insight into this process. Determining how the lung environment regulates the function of its progenitor cells could also translate into a better understanding of several lung disorders.

2.4. Materials and Methods.

Cell Culture.

HBEC3 KT cells were cultured in Keratinocyte-SFM media (Gibco, Gaithersburg, MD) containing 50 µg/mL bovine pituitary extract (BPE) (Gibco) and 5 ng/mL epidermal growth factor (EGF) (Gibco) at 37°C in 5% CO₂ on

porcine gelatin-coated tissue dishes (Sigma Aldrich, St. Louis, MO) (Ramirez et al., 2004). For *in vitro* differentiation studies, HBEC3 KT cells were cultured in complete ALI media (Fulcher et al., 2005). IMR90 human neo-natal lung fibroblasts were cultured in 4:1 mixture of Dulbecco's Minimal Essential Medium (DMEM) and Medium 199 (Thermo Scientific Hyclone, Rochester, NY) containing 10% Cosmic Calf Serum (Thermo Scientific Hyclone) at 37°C in 2% CO₂.

Immunofluorescence Staining of 2D Cultures.

For 2D analysis, HBEC3 KT cells were seeded into Lab-Tek™ II 8-well chamber slides™ (Thermo Fisher Scientific Nunc™, Rochester, NY) at either low (10,000 cells per well) or high (100,000 cells per well) densities. Cells were washed twice briefly with cold 1X PBS and then fixed at room temperature for 10 minutes in appropriate fixative (cold methanol for cytoskeletal-associated proteins and 4% paraformaldehyde (PFA) for all other proteins). Cells were washed three times in 1X PBS for 5 minutes each and coincidentally permeabilized and blocked at room temperature for 30 minutes with 10% goat serum albumin (GSA) in 1X PBS containing 0.1% bovine serum albumin (BSA) and 0.1% Triton X-100. After permeabilization/blocking, cells were rinsed briefly with 1X PBS and then incubated with primary antibodies (rabbit polyclonal anti-p63 (Santa Cruz Biotechnology, Inc., Santa Cruz, CA; sc-8343), mouse monoclonal anti-K14

(Thermo Fisher Scientific; Cat. #MS-115-P), mouse monoclonal anti-K19 (Santa Cruz; sc-6278), rabbit polyclonal anti-CC10 (Santa Cruz; sc-25554, rabbit polyclonal anti-proSP-C (Chemicon International, Billerica, MA; AB3786, rabbit polyclonal anti-SP-A (gift from Dr. Carole Mendelson, Ph.D., University of Texas Southwestern Medical Center, Dallas, TX), mouse monoclonal anti-SP-D (gift from Dr. Jens Madsen, Ph.D., University of Southampton, Southampton, U.K.), rabbit polyclonal anti-Sox9 (Santa Cruz; sc-20095), mouse monoclonal anti-TTF-1 (Santa Cruz; sc-25331), mouse monoclonal anti-Ki-67 (Santa Cruz; sc-23900), mouse monoclonal anti-OCT3/4 (Santa Cruz; sc-5279), mouse monoclonal anti-BMI-1 (Abcam, Cambridge, MA; ab14389) in a humidified chamber overnight at 4°C. Cells were washed three times at room temperature in 1X PBS (first wash for 10 minutes and 5 minutes each for second and third washes) and then incubated at room temperature with secondary antibodies (Alexa Fluor 488 goat anti-rabbit (Invitrogen; A-11008) or Alexa Fluor 488 goat anti-mouse (Invitrogen; A-11001) in the dark for 45 minutes. Following three washes with 1X PBS at room temperature (first wash for 10 minutes and 5 minutes each for second and third washes), cells were mounted with VECTASHIELD[®] Mounting Medium with DAPI (Vector Laboratories, Burlingame, CA; H-1200), coverslipped, and imaged on Zeiss Axiovert 200M inverted microscope. For 3D structures, 3D cultures were washed twice with 1X PBS and then extracted from Matrigel[™] with Cell Recovery Solution (BD

Biosciences) per the manufacturer's protocol. Extracted 3D structures were seeded into Lab-Tek™ II 8-well chamber slides™ (Thermo Fisher Scientific Nunc™), allowed to adhere to slides for 4 hours, and then fixed for 1 hour with 4% paraformaldehyde at room temperature. 3D structures were then stained according to protocol described for 2D monolayers. Imaging was performed on Leica TCS SP5 confocal microscope.

3D Culture.

Construction of 3D HBEC3 KT cyst-like cultures was performed as previously described for mammary epithelial cells by Lee *et al.* (Lee et al., 2007) with the following modifications. HBEC3 KT cells were suspended in ALI media (Fulcher et al., 2005) at a density of 1.7 million cells per mL. Cell suspension was diluted 1:10 in pre-thawed cold Growth Factor Reduced Matrigel™ Phenol-Red Free (BD Biosciences, San Jose, CA) and seeded into a multi-well plate (BD Falcon, San Jose, CA). Matrigel™ cultures are allowed to gel for 30 minutes at 37°C. After 45 minutes, 100 $\mu\text{L}/\text{cm}^2$ ALI media was added to Matrigel™ cultures. Transwell® permeable inserts (Corning, Lowell, MA) containing 125,000 per cm^2 IMR90 in ALI media were placed on top of cultures to provide growth stimulus. Cultures were grown at 37°C in 5% CO₂ with media changes every 2 days. 3D cultures were maintained for up to 12 days either with or

without IMR90 co-culture. For HBEC3 KT tubule formation, IMR90 fibroblasts were pre-seeded into a multi-well plate (BD Falcon) 48 hours prior to experiment in ALI media. After aspiration of media, pre-thawed cold Growth Factor Reduced Matrigel™ Phenol-Red Free (BD Biosciences) was layered on fibroblasts at volume of 75 $\mu\text{L}/\text{cm}^2$ and allowed to gel for 15 minutes at 37°C. HBEC3 KT cells suspended at 100,000 cells per cm^2 in ALI media were plated on Matrigel™. Cultures were grown at 37°C in 5% CO_2 with media changes every 2 days.

RNA Extraction and Q-PCR

RNA was extracted from HBEC3 KT cells plated in 10cm culture dishes at low or high densities equivalent to that utilized for immunofluorescence with RNeasy Plus Kit (Qiagen, Inc., Valencia, CA) per the manufacturer's protocol. Q-PCR was performed utilizing Applied Biosystems TaqMan® Gene Expression Assay with primers listed in Appendix B.

Microarray Analysis.

Microarrays were done using Illumina HumanRef-8 v3.0 expression beadchips. The protocol from Illumina Total Prep Kit from Ambion was used for labeling and hybridization is done according to manufacturer's (Illumina) instruction using their reagents. Arrays were scanned using beadstation 500 beadarray reader and

acquisitioned with BeadStudio. Data was normalized using the MBCB method (Ding et al., 2008). Significant genes were determined using SAM using a threshold of 2-fold and FDR of 1.0% and clustered using Euclidean distance (Saeed et al., 2003)

CHAPTER THREE.

Characterization of *In Vitro* Transformed HBEC3 KT Population and Clones Isolated in Serum and Serum-free.

3.1. Introduction.

The exposure of the lung tissue to the constant barrage of detrimental agents ultimately succeeds in overwhelming the dynamic repair processes of the lung. Several diseases are known to result from alterations directly or indirectly due to the interruption of normal homeostasis in the lung by this onslaught. Lung cancer is one of the most prevalent of these diseases with estimates of 220,000 new lung cancer cases diagnosed and 159,000 deaths attributed to lung cancer for 2009 in the United States alone. Research into the etiology of lung cancer has revealed many of the molecular alterations that predispose an individual to the onset of some form of lung cancer.

As with all types of cancer, the most critical alterations involve either gain of function in a gene that could promote carcinogenesis or the loss of function in a gene that would normally suppress carcinogenesis. These genes are termed oncogenes and tumor suppressors, respectively, and mutations in both are

generally required for a lesion to become malignant. Multiple genetic alterations in both oncogenes and tumor suppressors are commonly found in the various types of lung cancer. Oncogenic mutations in the *KRAS* gene, whose protein product functions in both mitogenic and pro-survival processes, are found in approximately 30% of lung adenocarcinomas (Sato et al., 2007). In addition, the tumor suppressors *p16* and *p53* commonly sustain loss of function mutations that enable the survival and/or proliferation of any dysregulated cells (Sato et al., 2007).

Much of the research on how each of these genes contributes specifically to the carcinogenic process, however, has been through the analysis of cells or tissues that have already been transformed. The establishment of the immortalized HBEC system described in the preceding chapter enabled a more precise evaluation of the role of specific genes in carcinogenesis. This is with the caveat that these HBEC cells have already lost *p16* function due to the immortalization process. HBEC3 KT cells were manipulated further through the overexpression of an oncogenic *KRAS*^{V12} and/or the knockdown of the tumor suppressor, *p53*. Introduction of both of these alterations into the HBEC3 KT cell line abolishes their differentiation capacity when cultured atop the fibroblast-embedded collagen matrices. These *in vitro* progressed HBEC3 KT cells are also capable of anchorage independent growth, but are not capable of forming tumors

in immunocompromised mice (Sato et al., 2006). Therefore, even with multiple alterations, the normal HBEC3 KT cells require additional “hits” to become transformed.

To elaborate on the previous findings and gain additional insight into the minimal requirements for the transformation of a normal cell, the *in vitro* progressed HBEC3 KT cell line has recently been modified further. By exchanging the overexpression construct that drives $KRAS^{V12}$, these *in vitro* progressed HBEC3 KT cells, in the background of a p53 knockdown, are able to form larger colonies in soft agar in comparison to their previous counterparts. Strikingly, the higher expression $KRAS^{V12}$ in these cells also enables them to form tumors in three of nine immunocompromised mice when injected subcutaneously (Sato, 2009). This tumorigenic frequency is increased slightly to three of seven if the injected cells are derived from the larger soft agar colonies (Sato, 2009).

In addition to modifying the $KRAS^{V12}$ expression levels, another proto-oncogene, *c-Myc*, has been introduced into the HBEC3 KT cell line in conjunction with the higher expression $KRAS^{V12}$ and p53 knockdown. While the introduction of *c-Myc* into these cells increases the soft agar colony formation, it does not affect their tumorigenic capacity (three of ten mice) (Sato, 2009). However, if the typical serum-free media in which these cells are cultured is

substituted with one containing serum, the tumorigenic frequency is significantly increased and seven of seven immunocompromised mice formed tumors. Culture of these *in vitro* transformed HBEC3 KT cells in the presence of serum induces an epithelial-to-mesenchymal transition (EMT) that is evident both morphologically and through altered protein expression (Sato, 2009). Histopathological analysis of the tumors formed from the *in vitro* transformed HBEC3 KT cells has revealed an intriguing and rare phenotype. Although lung cancer in humans has many different subtypes, only one subtype is observed in each lung cancer case. In contrast, the *in vitro* transformed HBEC3 KT cells produced lesions with characteristics of three different lung cancer subtypes within the same lesion (Sato, 2009). This finding suggests that several of the distinct lung tumor subtypes might emerge from the dysregulation of a multipotent progenitor cell of the lung.

Since the culture of the immortalized HBEC cells within a 3D basement membrane environment provides a tractable system to study the differentiation capacity of these cells, this system was utilized to assess how each manipulation alters this capacity. Our findings reveal stark differences between the non-tumorigenic and tumorigenic populations of HBEC 3KT cells when cultured in this context. Within the *in vitro* transformed HBEC3 KT cell line an unappreciated heterogeneity in the invasive capacity of single cells is was

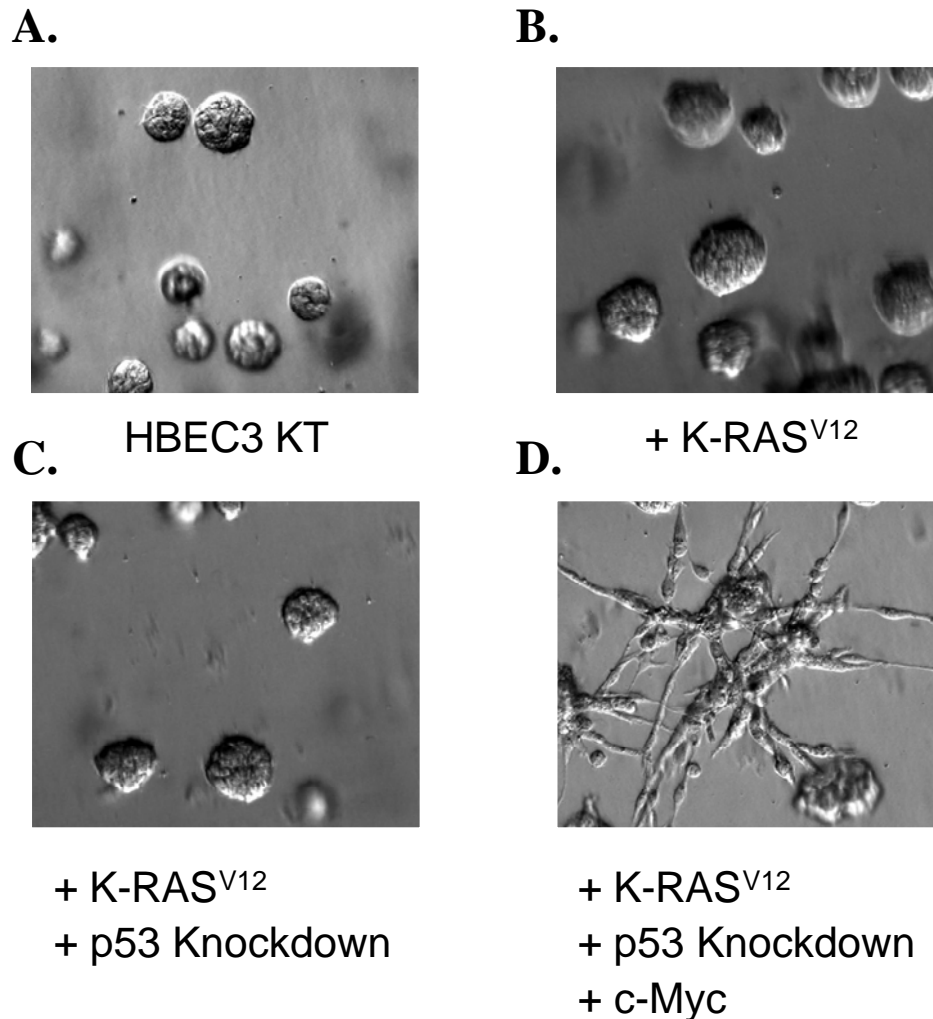


Figure 3.1. *In vitro* transformed HBEC3 KT cells form dysregulated 3D structures when cultured in reconstituted basement membrane.

Culture of normal and *in vitro* manipulated isotypes in Matrigel™ with IMR90 co-culture reveals formation of invasive stellate structures only in *in vitro* transformed HBEC3 KT cells. (A) HBEC3 KT cells. (B) HBEC3 KT cells with *KRAS*^{V12} overexpression. (C) HBEC3 KT cells with *KRAS*^{V12} overexpression and p53 knockdown. (D) HBEC3 KT cells with *KRAS*^{V12} overexpression, p53 knockdown, and *c-Myc* overexpression.

observed. While the characterization of cells isolated from this population suggests some divergence between individual cells, histopathological analysis of tumors from these clones supports the concept that dysregulation of a single cell with multipotent properties can produce several lung cancer subtypes.

3.2. Results.

Analysis of 3D Differentiation Capacity of *in vitro* Transformed HBEC3 KT Cells.

In order to determine the relative influence of each oncogenic manipulation on the differentiation capacity of the HBEC3 KT cell line, each of the manipulated HBEC3 KT cell isotypes were individually cultured within Matrigel™ with IMR90 fibroblasts as described in the preceding chapter. Recapitulating the previous results, the HBEC3 KT cells invariably produce spherical cyst-like structures after five days of growth under these conditions. Introduction of both the higher expression $KRAS^{V12}$ alone or in conjunction with a knockdown of p53 does not affect the capacity of the HBEC3 KT cells to form these regular cyst-like structures (Figure 3.1 and 2.6). The *in vitro* transformed HBEC3 KT cells, which have a knockdown of p53 and overexpression of both $KRAS^{V12}$ and *c-Myc*, on the other hand, form a strikingly aberrant structural

phenotype when cultured under these same conditions. These aberrant structures are each comprised of multiple cells that are configured in a star-like arrangement due to the migration of cells away from the point where each original cell is seeded. Interestingly, this stellar morphology only emerges from approximately 50% of the *in vitro* transformed HBEC3 KT cells seeded within Matrigel™ (Figure 2.1). The other 50% form apparently normal cyst-like structures. Whether these star-like structures contain any intact adherens junctions under these conditions has yet to be determined.

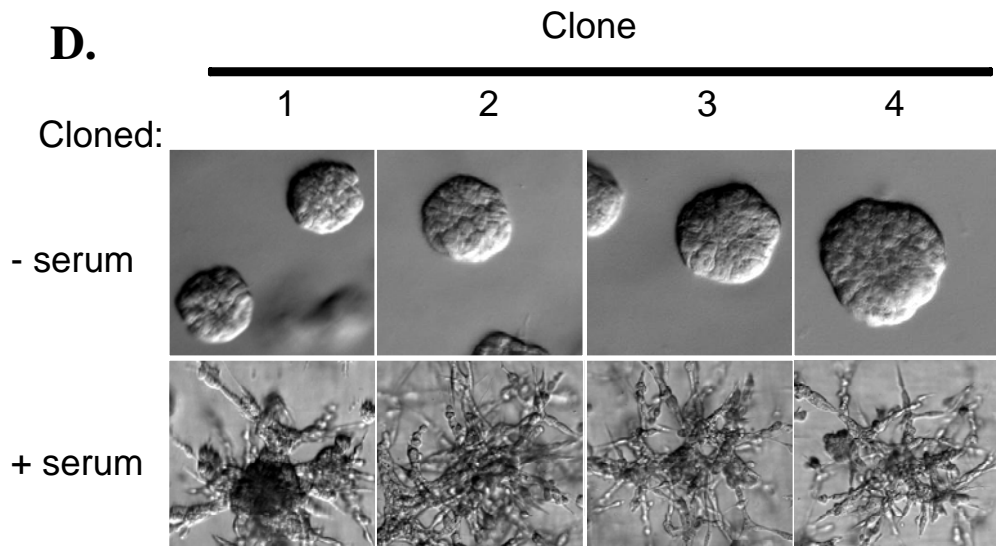
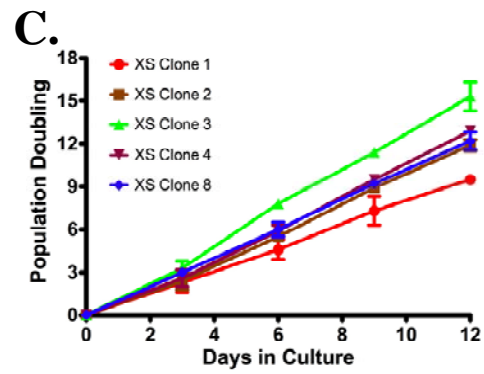
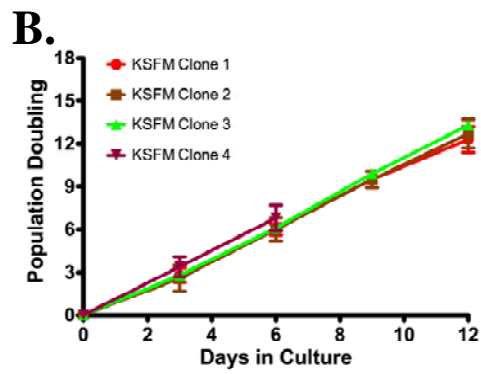
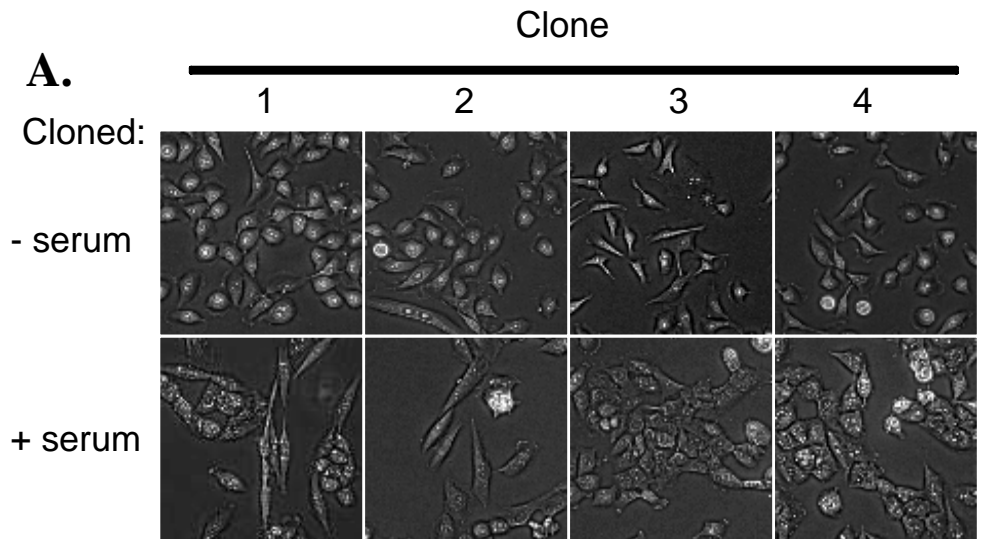
Characterization of *in vitro* Transformed HBEC3 KT Clones Isolated in Presence or Absence of Serum.

The observation from the above experiments that only a proportion of the *in vitro* transformed HBEC3 KT cell population forms the dysregulated structures is intriguing. Since the *in vitro* transformed HBEC3 KT cells are cultured within Matrigel™, the constituent basement membrane proteins, which encase each of the cells, would then have to be degraded in order to permit the migration/invasion of these cells and thus the formation of the star-like structures. While this population is predominantly cultured serum-free, previous work has determined that, if this population is cultured in the presence of serum, an EMT transition occurs and increases in both their ability to grow anchorage

independent and tumorigenic potential are observed (Sato, 2009). Therefore, to determine the effect of serum on the formation of invasive and non-invasive structures, the *in vitro* transformed HBEC3 KT cells were cultured in the presence of serum prior to seeding within Matrigel™.

In order to eliminate a possible selective advantage and population bias provided by the application of serum, the *in vitro* transformed HBEC3 KT cell population was seeded at clonal density in either the presence or absence of serum. Four clones were picked and expanded from the media without serum and eight clones from the media containing serum. During expansion, one of the serum-derived clones underwent a growth arrest state and was eliminated from further analysis. While all of the clones retain the typical cuboidal morphology of an epithelial cell, the clones isolated in the presence of serum appear vacuolated and have more irregular edges in comparison to those isolated in the absence of serum (Figure 3.2 A). All of the serum-derived clones additionally grow in clonal patches, which could be due to the presence of differentiation factors in serum (Figure 3.2 A). Growth rates of these cells are, however, not affected, as they are comparable to the clones isolated under serum-free conditions (Figure 3.2 B).

When each of the expanded clones is cultured within Matrigel™ under the previously described conditions, the variability in structural phenotypes observed



with the original *in vitro* transformed HBEC3 KT cell population is completely lost. Every cell isolated in the absence of serum forms a regular cyst-like structure after five days of growth. In contrast, all of the cells isolated in the presence of serum only form the invasive star-like structures (Figure 3.2 C). To determine whether the above results may be due to serum-induced dysregulation of normal cellular signaling, which has been shown to cause an EMT transition in these cells (Sato, 2009), the serum-free clones were cultured in the presence of serum while the clones isolated with serum were reverted to serum-free media. Each of the clones isolated serum-free rapidly senesce upon exposure to serum (Figure 3.3 B). As expected, the reversion back to serum-free conditions does not elicit the same response from the clones isolated in the presence of serum (Figure 3.3). This transition to serum-free conditions, however, results in permanent visible changes such as a more fibroblastic morphology and lack of forming confluent monolayers (Figure 3.3 A). As the cells reach confluence, cells begin to grow atop of one another. Cells that end up in this secondary layer do not survive

Figure 3.2. Isolation of *in vitro* transformed HBEC3 KT clones in presence of serum enhances formation of dysregulated 3D structural phenotype.

Clones of *in vitro* transformed HBEC3 KT cells were isolated in presence or absence of serum. (A) Phase contrast images of four clones isolated in serum and four clones isolated serum free. (B) Growth curves for clones isolated serum free. (C) Growth curves for clones isolated in presence of serum. Individual serum and serum-free clones were culture in Matrigel™ with IMR90 co-culture. (D) Phase contrast images of structures formed by individual clones after five days of culture in Matrigel™.

for long under these conditions, most likely succumbing to anoikis although this has not been experimentally verified. Growth rate in these cells is not affected by the reversion to serum-free conditions (Figure 3.3 B).

When an exogenous overexpression construct is integrated into a population of cells through retro- or lentiviral infection, variability in expression levels between individual cells inevitably occurs due to factors such as integration sites. In order to determine the extent that the level of exogenous *c-Myc* overexpression has on the emergence of the stellate structures and the resistance to the effects of serum, *c-Myc* protein levels from each of the clones was assessed while in the media that they were isolated. All of the clones have increased *c-Myc* protein levels in comparison to the normal HBEC3 KT cell population (Figure 3.3 C). Within the clones isolated and cultured in the presence of serum, there does not appear to be any distinguishable differences compared to the original *in vitro* transformed HBEC3 KT cell population cultured serum-free. In contrast, three of the serum-free clones have slightly decreased *c-Myc* levels compared to the original population while the fourth serum-free clone expresses *c-Myc* at significantly higher levels than any other sample analyzed (Figure 3.3 C).

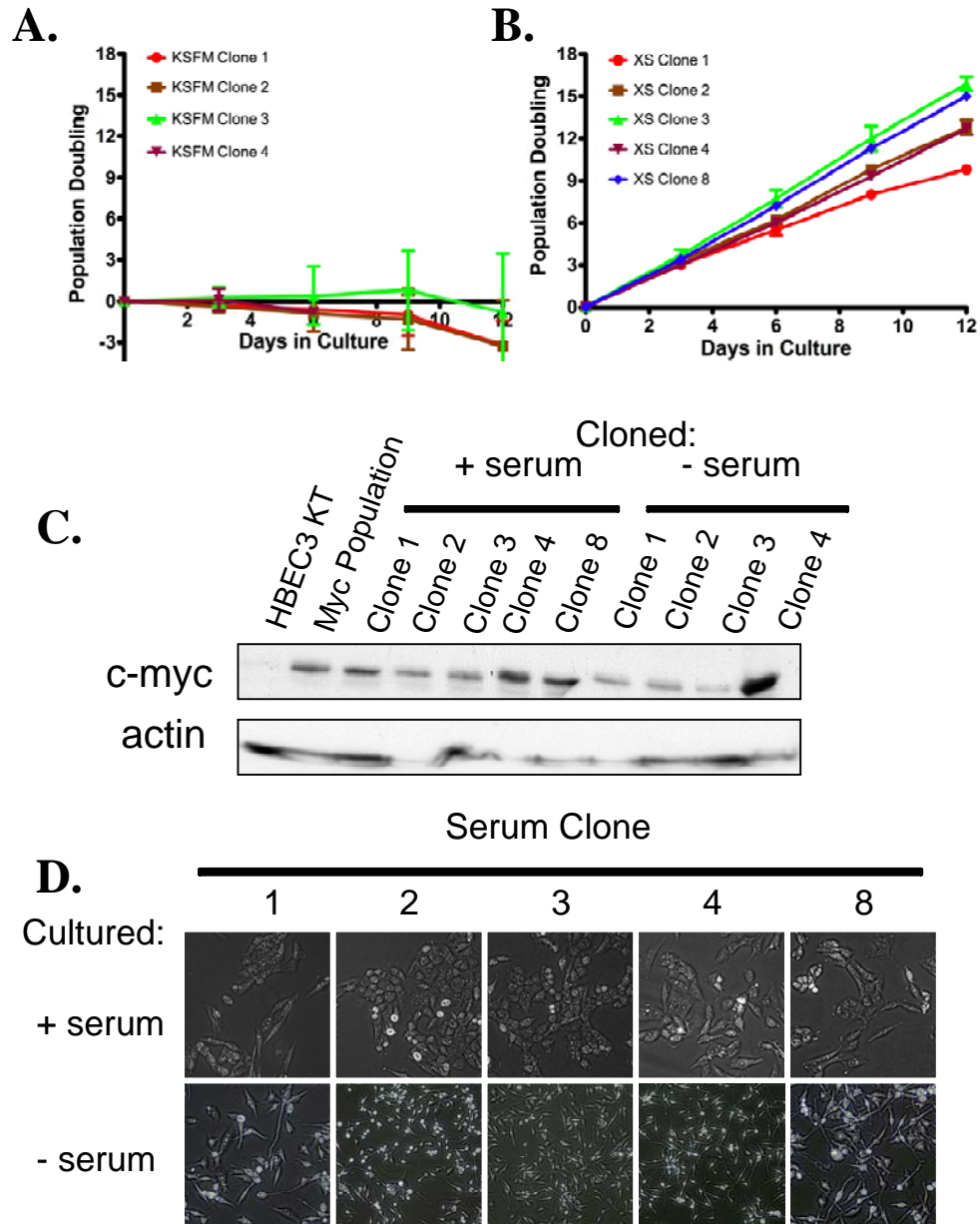


Figure 3.3. Serum exposure selects for cells that resist influence of serum and is independent of c-Myc expression levels.

In vitro transformed HBEC3 KT clones isolated in the presence or absence of serum were converted to cell culture medium without or with serum, respectively. (A) Growth curves for clones isolated serum-free and then exposed to serum. (B) Growth curves from clones isolated in serum and then reverted to serum-free conditions. (C) c-Myc levels in several serum and serum-free clones. (D) Phase contrast images of clones isolated in presence of serum either with or without serum.

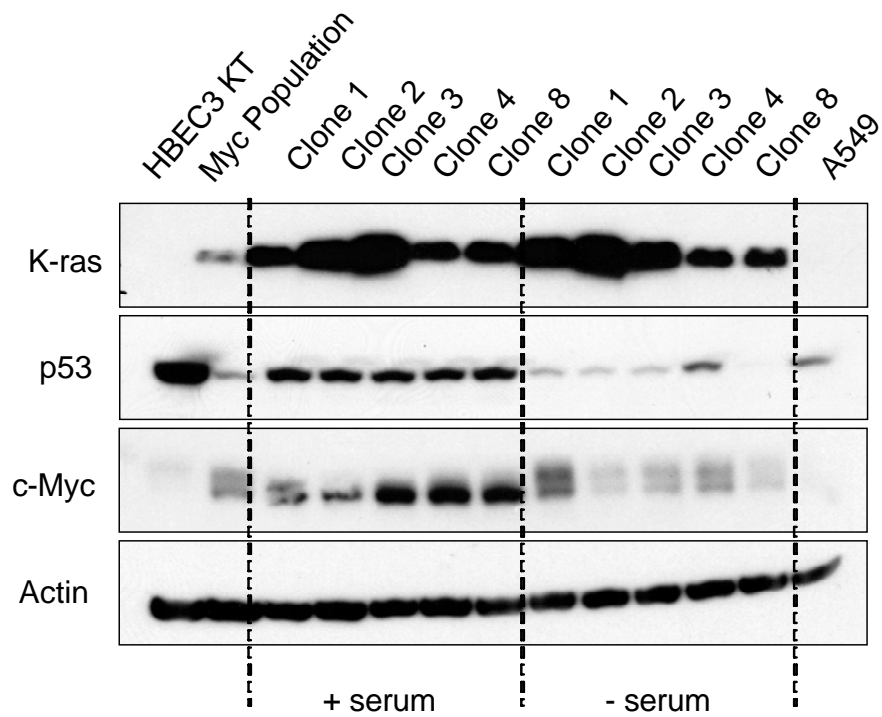


Figure 3.4. Serum exposure either directly or indirectly effects exogenous factors in *in vitro* transformed HBEC3 KT clones isolated in presence of serum.

Western blot of factors introduced into HBEC3 KT cells in *in vitro* transformed clones isolated in the presence serum and maintained in culture medium containing serum or no serum.

Since the addition of serum to the *in vitro* progressed HBEC3 KT population enhanced their tumorigenic potential, their invasive phenotype in Matrigel™, and altered their cellular morphology, we proceeded to determine whether serum might influence the expression of other exogenously expressed genes within these cells. As previously reported, the *in vitro* progressed HBEC3 KT population expresses higher levels of KRAS and c-Myc in addition to a significant knockdown of p53 in comparison to the HBEC3 KT population (Figure 3.4) (Sato, 2009). Of the five clones isolated in serum that were analyzed, all express higher levels of KRAS regardless of whether they were cultured in the presence or absence of serum. The level of p53 in all of these clones, on the other hand, is increased to levels higher than that of the original population only while they are cultured in the presence of serum (Figure 3.4). In the original *in vitro* progressed HBEC3 KT population, c-Myc appears to be post-translationally modified and this persists when the clones that were isolated in serum are reverted to serum-free conditions. This modification is lost in the presence of serum (Figure 3.4).

Evaluation of Tumorigenicity of *In Vitro* Transformed HBEC3 KT Clones Isolated in Serum.

As the xenograft tumors formed when the *in vitro* progressed HBEC3 KT population was injected into mice contained several histological subtypes, we next sought to assess whether this results from variability with the population. Each of the *in vitro* progressed HBEC3 KT clones that were isolated in serum and demonstrated an invasive phenotype when cultured in Matrigel™ were injected subcutaneously into immunocompromised mice. Four of five clones formed tumors.

3.3. Discussion.

The transformation of normal human bronchial epithelial cells through serial introduction of factors known to be important in lung cancer has provided a valuable resource to study cancer progression. Further, enhancement of this phenotype by serum exposure supports a role of the microenvironment on carcinogenesis (Mbeunkui and Johann, 2009; Sato, 2009). Through the application of a 3D differentiation model, we have demonstrated heterogeneity within this transformed population. Only a finite number of individual cells in the *in vitro* progressed HBEC3 KT population when cultured serum-free form an invasive stellate structure within Matrigel™ (Figure 3.1). This conforms with the low tumorigenic potential previously observed with this population cultured serum-free (Sato, 2009). The presence of cells within this population that do not form invasive structures and are not competent to proliferate in the presence of

serum suggests certain cells in this population require additional alterations for transformation and that the application of serum to this population provides a potent selective advantage (Figure 3.1, 3.2 C, and 3.3 B). This serum-induced selection suggests that the increased tumorigenic potential of the *in vitro* progressed HBEC3 KT population after exposure to serum partially results from this selective process (Sato, 2009). Determining precisely the mechanisms and factors involved in this positive and negative resistance would be beneficial in understanding an *in vivo* selection for more malignant tumors.

Isolation of the clones in culture medium supplemented with serum has provided some insight into how the exogenously expressed gene constructs may interact in the context of serum exposure and transformation. When exposed to serum, normal epithelial cells experience growth arrest conceivably due to the presence of TGF- β within serum. This arrest is generally mediated by the induction of the cell cycle inhibitors p21^{CIP1} or p15^{INK4B} (Datto et al., 1995; Reynisdottir et al., 1995). As overexpression of CDK4 in the HBEC3KT cell line should subvert any inhibitory effect of p15^{INK4B} induction, p21^{CIP1}-dependent growth arrest likely predominates. Thus, the reduction of overall p53 protein levels in the HBEC3 KT cells, including the *in vitro* progressed HBEC3 KT population, should alleviate this effect. As there are cells within the *in vitro* progressed HBEC3 KT population that are not capable of growth in the presence

of serum (Figure 3.3 B), evaluation of whether these clones retain higher protein levels of p53 would assist in understanding their serum response.

The dramatically elevated levels of KRAS in all of the *in vitro* progressed HBEC3 KT serum clones may confound the above observations. Oncogenic KRAS is known to phosphorylate p53 inducing its stabilization and the senescence of normal cells (Serrano et al., 1997). Stabilized p53 in this context has been shown to interact with SMAD proteins downstream of activated TGF- β signaling (Cordenonsi et al., 2007). Under serum-free conditions, TGF- β 1 may be induced through constitutive RAS activation and this induction is enhanced with exogenous TGF- β exposure (Geiser et al., 1991; Van Obberghen-Schilling et al., 1988; Yue and Mulder, 2000). Consistent with these findings, overexpression of *KRAS*^{V12} in the HBEC3 KT cells has been shown to induce senescence and this response is diminished in HBEC3 KT cells with knockdown of p53 (Sato, 2009). However, p53 levels do not appear to change upon the introduction of *KRAS*^{V12} and some cells persist upon exposure of the HBEC3 KT population with *KRAS*^{V12} and p53 knockdown to serum (Sato, 2009). Determining whether the phosphorylation status of p53 with the introduction of *KRAS*^{V12} and the overall p53 levels in the serum resistant cells could provide additional insights.

In addition to p53, KRAS also influences the level and activity of c-Myc. Several studies have shown that RAS proteins phosphorylate c-Myc and this in turn affects its stability. Phosphorylation of serine 62 by RAS stabilizes c-Myc while permitting the phosphorylation of threonine 58 by Glycogen synthase kinase 3 beta (GSK3 β), which promotes its degradation (Sears et al., 1999; Sears et al., 2000). In each of the *in vitro* progressed HBEC3 KT serum clones, c-Myc appears to lose a post-translation modification upon serum exposure (Figure 3.4). Evaluation of which residues are phosphorylated and examining how a GSK3 β inhibitor affects these clones is needed in order to determine the role of c-Myc in these cells. If the exposure to serum suppresses the c-Myc degradation in these clones, then this may lead to an increase c-Myc activity in the presence of serum. Higher c-Myc levels could also contribute to the serum resistance in the *in vitro* progressed HBEC3 KT serum clones as the overexpression of c-Myc has been shown to offset the TGF- β mediated inhibition of growth (Alexandrow et al., 1995). Although, knockdown of p53 and c-Myc overexpression still does not prevent growth arrest upon serum exposure in some cells (Figure 3.3 B).

An increase in c-Myc activity may be supported by the increased levels of p53 observed in the *in vitro* progressed HBEC3 KT serum only when exposed to serum (Figure 3.4). c-Myc is known to induce the transcription of p53 by heterodimerization with Max and binding to the p53 promoter (Reisman et al.,

1993). In none of the *in vitro* progressed HBEC3 KT cells or any of the isolated clones does the level of p53 appear to change upon the introduction of c-Myc (Sato, 2009). Only when the *in vitro* progressed HBEC3 KT clones isolated in the presence of serum and are cultured in serum is there an appreciable increase in p53 levels (Figure 3.4). Examining the levels of other known c-Myc targets could further support this hypothesis. Lastly, the evaluation of the *in vivo* tumorigenic potential of the *in vitro* progressed HBEC3 KT clones isolated in serum is ongoing. Results from these studies will assist in integrating the *in vitro* characterization.

3.4. Materials and Methods.

Cell Culture.

HBEC3 KT cells were cultured in Keratinocyte-SFM media (Gibco, Gaithersburg, MD) containing 50 µg/mL bovine pituitary extract (BPE) (Gibco) and 5 ng/mL epidermal growth factor (EGF) (Gibco) at 37°C in 5% CO₂ on porcine gelatin-coated tissue dishes (Sigma Aldrich, St. Louis, MO) (Ramirez et al., 2004). For *in vitro* differentiation studies, HBEC3 KT cells were cultured in complete ALI media (Fulcher et al., 2005). IMR90 human neo-natal lung fibroblasts were cultured in 4:1 mixture of Dulbecco's Minimal Essential Medium (DMEM) and Medium 199 (Thermo Scientific Hyclone, Rochester, NY)

containing 10% Cosmic Calf Serum (Thermo Scientific Hyclone) at 37°C in 2% CO₂.

3D Culture.

Construction of 3D HBEC3 KT cyst-like cultures was performed as previously described for mammary epithelial cells by Lee *et al.* (Lee et al., 2007) with the following modifications. HBEC3 KT cells were suspended in ALI media (Fulcher et al., 2005) at a density of 1.7 million cells per mL. Cell suspension was diluted 1:10 in pre-thawed cold Growth Factor Reduced Matrigel™ Phenol-Red Free (BD Biosciences, San Jose, CA) and seeded into a multi-well plate (BD Falcon, San Jose, CA). Matrigel™ cultures are allowed to gel for 30 minutes at 37°C. After 45 minutes, 100 μL/ cm² ALI media was added to Matrigel™ cultures. Transwell® permeable inserts (Corning, Lowell, MA) containing 125,000 per cm² IMR90 in ALI media were placed on top of cultures to provide growth stimulus. Cultures were grown at 37°C in 5% CO₂ with media changes every 2 days. 3D cultures were maintained for up to 12 days either with or without IMR90 co-culture. For HBEC3 KT tubule formation, IMR90 fibroblasts were pre-seeded into a multi-well plate (BD Falcon) 48 hours prior to experiment in ALI media. After aspiration of media, pre-thawed cold Growth Factor Reduced Matrigel™ Phenol-Red Free (BD Biosciences) was layered on

fibroblasts at volume of 75 $\mu\text{L}/\text{cm}^2$ and allowed to gel for 15 minutes at 37°C. HBEC3 KT cells suspended at 100,000 cells per cm^2 in ALI media were plated on Matrigel™. Cultures were grown at 37°C in 5% CO_2 with media changes every 2 days.

Protein Extraction and Westerns.

Cells pellets were lysed with cold RIPA buffer (50mM Tris, pH 8, 150mM NaCl, 1% NP-40, 0.5% sodium deoxycholate, 0.1% (w/v) SDS) supplemented with 1X Complete protease inhibitor cocktail (Roche Applied Science; Indianapolis, IN) and 1mM phenylmethanesulphonylfluoride by passage through 22G needle. Samples were centrifuged at 10,000 rpm for 10 minutes at 4°C, supernatant collected on ice and protein concentrations were determined by BCA Protein Assay (Thermo Scientific). 15 μg per sample were diluted 1:4 in 4X Laemmli Buffer (250mM Tris, pH 6.8, 8% SDS, 40% (w/v) glycerol, 0.004% (w/v) bromophenol blue) supplemented with 5% β -mercaptoethanol and heated for 5 minutes at 95°C. Samples were run on 10% SDS-PAGE gels for 2 hours at 100V in 1X TGS Buffer. Gels were transferred to PVDF membrane (Immobilon-P; Millipore, Billerica, MA) at 25V overnight at 4°C. Membranes were washed once in 1X PBST (PBS with 0.05% (v/v) Tween-20) then blocked with 5% milk in 1X PBST for 1 hour at room temperature. Primary antibodies (mouse

monoclonal anti-KRAS (Santa Cruz; sc-30; mouse monoclonal anti-c-Myc (Santa Cruz; sc-40; mouse monoclonal anti-p53 (Calbiochem; OP43; mouse monoclonal anti-actin (Sigma Aldrich; A1978) were diluted 1:200 in 5% milk in 1X PBST and incubated with membrane overnight at 4°C. After washing, membranes were incubated with appropriate secondary antibody (mouse/rabbit) for 1 hour at room temperature (anti-actin for 10 minutes). Membranes were washed and then signal was detected with ECL™ Western Detection Reagents (GE Healthcare; Piscataway, NJ) and X-ray film.

CHAPTER FOUR.

Invasive Cancer Induced by Radiation in the LA1 KRAS Mouse

Model of Lung Cancer.

4.1. Introduction.

With longer and deeper missions into space, an increased risk for developing cancer becomes a potential hazard for astronauts. This is predominantly due to the entirely different radiation field to which they will be exposed in space, as compared to terrestrial radiation. There are three forms of space radiation, solar particle events (SPE), galactic cosmic rays (GCR), and electrons and protons trapped within the Earth's Van Allen belts. Of these, exposure to GCR is perceived to be the most detrimental and the most unique. GCR is mostly comprised of atoms ranging from protons to that of high atomic number (Z) atoms such as iron ($^{56}\text{Fe}^-$) that have had their electrons stripped off while being accelerated to high rates of speed. The relative abundance of these particles is roughly the same as they occur naturally with 85% protons, 11% helium, and 2% all other nuclei, which are designated high Z and energy (HZE) particles. All of these charged particles, however, may possess very high amounts

of energy due to their size and extreme rates of speed (Curtis and Letaw, 1989; National Council on Radiation Protection and Measurements., 2006).

Energy deposition by GCR particles is unique in that may be characterized by two components capable of ionization. As the particles traverse matter, large amounts of energy are deposited along the physical track of the particle resulting in a dense “core” of ionization events. The “core” region may be as wide as 0.003 microns depending on the Z and speed of the particle. Secondary electrons, termed delta rays (δ rays), which have been excited by the impacting high-energy particles, radiate away from this core and may proceed to ionize matter as far as 269 microns from the “core” (Brooks et al., 2001). This secondary region is termed the “penumbra”. Due to the diameter of the penumbra, it has been estimated that approximately 32 cells are impacted by a δ rays for every particle hit (Chatterjee and Schaefer, 1976). Due to its composition and method of energy deposition, GCR exposure could thus elicit biological effects that are unique although biological data is limited.

In order to provide adequate radiation protection for astronauts in future space missions, the National Council on Radiation Protection and Measurement (NCRP) established guidelines for limiting excess cancer mortality to 3%. This

percentage is increased to 4.2% if heritable factors and non-fatal cancer is considered (Fry and Nachtwey, 1988; National Council on Radiation Protection and Measurements., 2001, 2006). Current estimates of increased cancer risks from GCR exposure by the National Aeronautics and Space Administration (NASA), states that, above all other forms of cancer, the risk of lung cancer mortality is highest in both males and females after a single mission. However, as biological data is limited, these estimates have relied entirely on extrapolation of data from various sources and require more in depth empirical investigation.

Lung cancer is a compelling model for space radiation risk assessment since, aside from being estimated to have the highest risk of mortality from space radiation exposure, it is one of the most prevalent form of cancer in both men and women overall. In 2009, it is estimated that there will be approximately 220,000 new lung cancer cases diagnosed and 159,000 deaths attributed to lung cancer in the United States alone (ACS, 2009). Research into the etiology of lung cancer has revealed many of the molecular alterations that predispose an individual to the onset of some form of lung cancer. While inactivation or bypass of p16^{INK4A}, mutations in p53, and the expression of telomerase activity are almost universal changes in lung cancer, oncogenic *KRAS* mutations have been observed in approximately 20-30% of NSCLCs. The importance of oncogenic *KRAS* mutation in lung cancer is supported by the development of lung cancer in

transgenic mouse models in which oncogenic *KRAS* is expressed in the murine lung (Fisher et al., 2001; Jackson et al., 2001; Johnson et al., 2001).

One such transgenic mouse model (LA1 *KRAS*) harbors a latent G12D allele integrated into the endogenous *KRAS* locus (Johnson et al., 2001). Activation of the latent G12D oncogene occurs spontaneously and stochastically throughout animal development. Every LA1 *KRAS* animal develops alveolar type II lineage lung cancer with multiple lesions and dies before an approximate age of five hundred days (Figure 4.1 A and B). Death is presumably due to substantial tumor burden in the lung impacting upon pulmonary function.

Although the expression of oncogenic *KRAS* is sufficient to induce lung cancer in the LA1 *KRAS* model, careful histopathological examination reveals that only 20% of these animals develop invasive carcinoma (Figure 4.1 C and Table 4.1). The majority of the lesions in these animals range from early lesions such as alveolar epithelial hyperplasia to well defined adenomas in the distal lung. This is suggestive that intact barriers to malignancy remain and additional alterations are required, which is consistent with a multi-step carcinogenic process (Vogelstein and Kinzler, 1993). It is therefore conceivable that radiation could provide the additional hit required and thus making the LA1 *KRAS* mouse model of lung cancer ideal for the study of space radiation effects on lung cancer

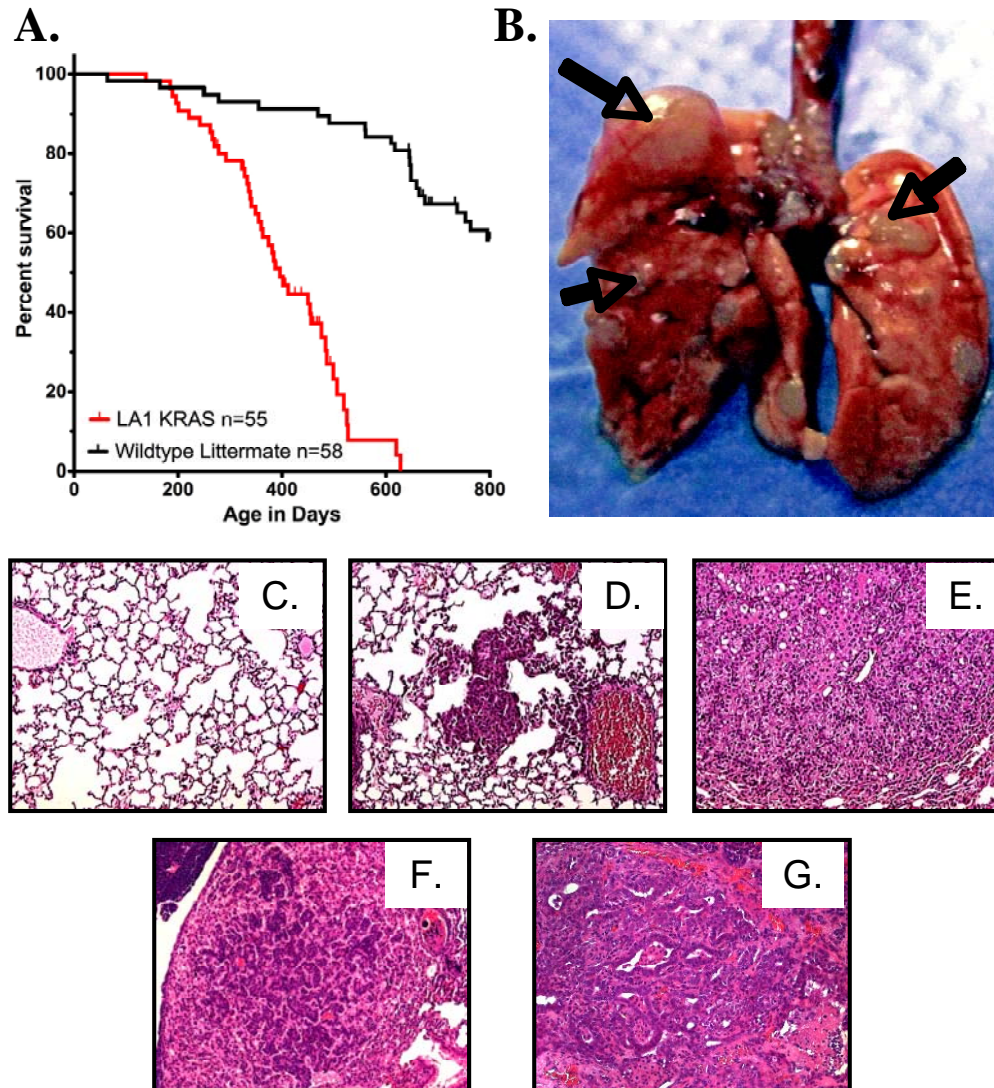


Figure 4.1. Characteristics of LA1 KRAS mouse model of lung cancer.

Expression of oncogenic KRAS G12D in LA1 KRAS mouse model results in significantly shortened lifespan compared to wildtype littermates (A; $P < 0.0001$) and extensive tumor burden in lung (B). (C – G) Lung cancer progression in LA1 KRAS mice mimics that seen in humans. (C) Normal lung. (D) Early alveolar hyperplasia. (E) Adenoma. (F) Adenoma with atypia. (G) Invasive carcinoma.

progression.

4.2. Results.

Effect of Acute or Fractionated Doses of 1.0 Gy X-rays or ^{56}Fe - Particles on Wildtype and LA1 KRAS Mice.

LA1 KRAS mice and wildtype littermates were irradiated with 1.0 Gy dose of X-rays or 1.0 GeV ^{56}Fe - particles. Radiation was administered as either an acute dose or fractionated into five consecutive daily 0.2 Gy doses (Figure 4.2). Irrespective of how the radiation is administered, 1.0 Gy dose of X-ray irradiation does not affect the overall survival of LA1 KRAS or wildtype littermate animals (Figures 4.3 A and C). ^{56}Fe - particle irradiation equally does not affect the survival of wildtype littermate mice (Figure 4.3 B). The survival of LA1 KRAS mice, on the other hand, is significantly decreased upon exposure to either a fractionated or acute dose of 1.0 Gy ^{56}Fe - particles (Figure 4.3 D).

As the shortened lifespan in the LA1 KRAS mice is presumed to be due the substantial tumor burden in the lung, the number of tumors per lung was analyzed to determine if irradiation might be initiating more lesions. Unirradiated LA1 KRAS mice develop over their lifespan approximately thirty-five lesions per lung with a broad range of variability. The incidence of tumors in the LA1 KRAS mice is not affected by any radiation type or radiation scheme tested (Figure 4.4

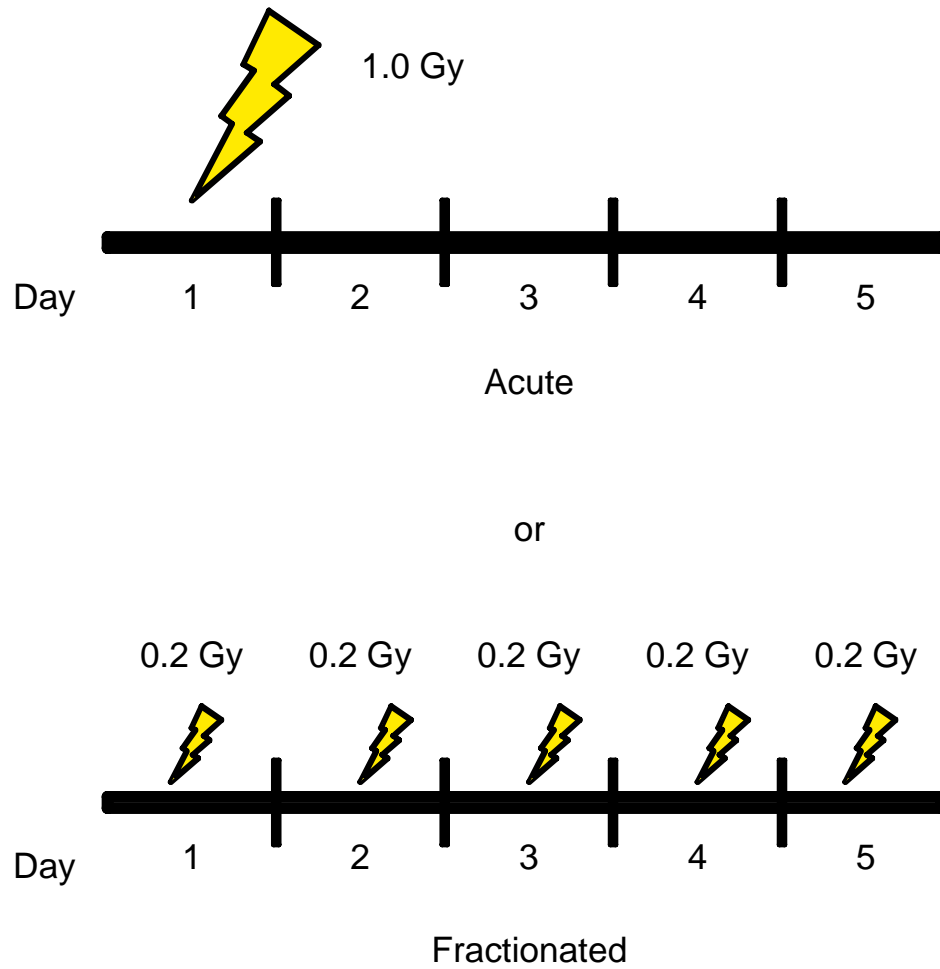


Figure 4.2. Irradiation Scheme.

LA1 KRAS and wildtype littermate mice were irradiated with either an acute or fractionated (0.2 Gy per day for five consecutive days) 1.0 Gy dose of radiation.

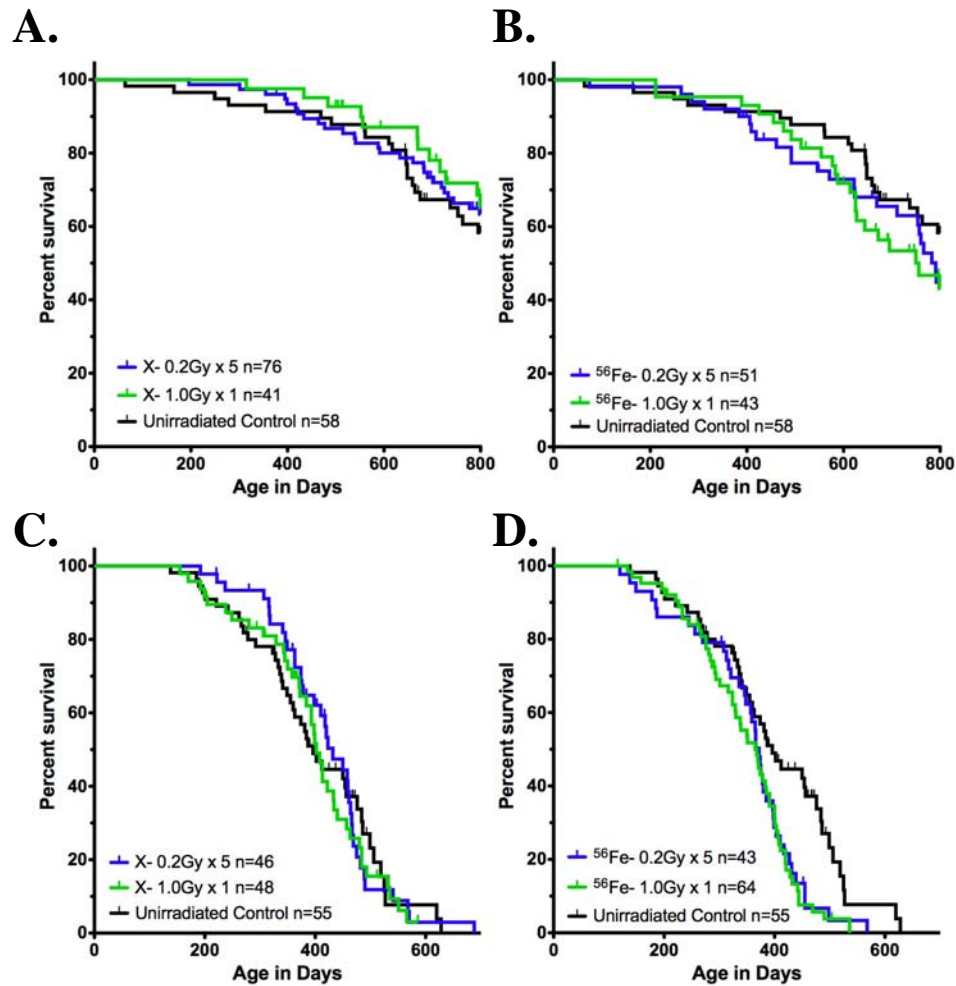


Figure 4.3. 1.0 Gy dose of ^{56}Fe particle irradiation significantly decreases lifespan of LA1 K-ras mice.

LA1 KRAS and wildtype littermate mice were irradiated with either a fractionated or acute dose of 1.0 Gy X-rays or ^{56}Fe - particles. Animal survival was monitored post-irradiation. (A- D) Kaplan-Meier survival curves of (A) wildtype littermate mice irradiated with 1.0 Gy X-rays compared to unirradiated controls (p -value not significant for either irradiation regimen). (B) wildtype littermate mice irradiated with 1.0 Gy ^{56}Fe - particles compared to unirradiated controls (p -value not significant for either irradiation regimen). (C) LA1 KRAS mice irradiated with 1.0 Gy X-rays compared to unirradiated controls (p -value not significant for either irradiation regimen). (D) LA1 KRAS mice irradiated with 1.0 Gy ^{56}Fe - particles compared to unirradiated controls ($p \leq 0.01$ for fractionated dose; $p \leq 0.001$ for acute dose).

B). While some wildtype littermate animals spontaneously develop one or two lesions in the lung, irradiation does not initiate additional lesions in the wildtype mice at the irradiation doses examined (Figure 4.4 A).

To determine whether irradiation influences the progression of pre-initiated lesions in the LA1 KRAS mice, histopathological examination of each mouse lung was performed. Of note was the overall incidence of invasive carcinoma in these animals. Approximately 20% of all unirradiated LA1 KRAS mice have tumors that have progressed to invasive carcinoma. These carcinomas are characterized with tumor cells with high nuclear to cytoplasmic ratios, definite nuclear pleomorphism, and lost much, if not all, of their differentiation capacity. The surrounding stroma is also frequently activated by these carcinomas. Various carcinomas also demonstrate a metastatic potential (Figure 4.5 A – H). Irradiation of these mice with either an acute or fractionated dose of 1.0 Gy X-rays or an acute dose of 1.0 Gy ^{56}Fe - particles does not alter this incidence (21% on average for all groups). Fractionation of the 1.0 Gy dose (0.2 Gy per day for five consecutive days) of ^{56}Fe - particles, however, significantly increases the incidence of invasive carcinoma to approximately 40% (Table 4.1).

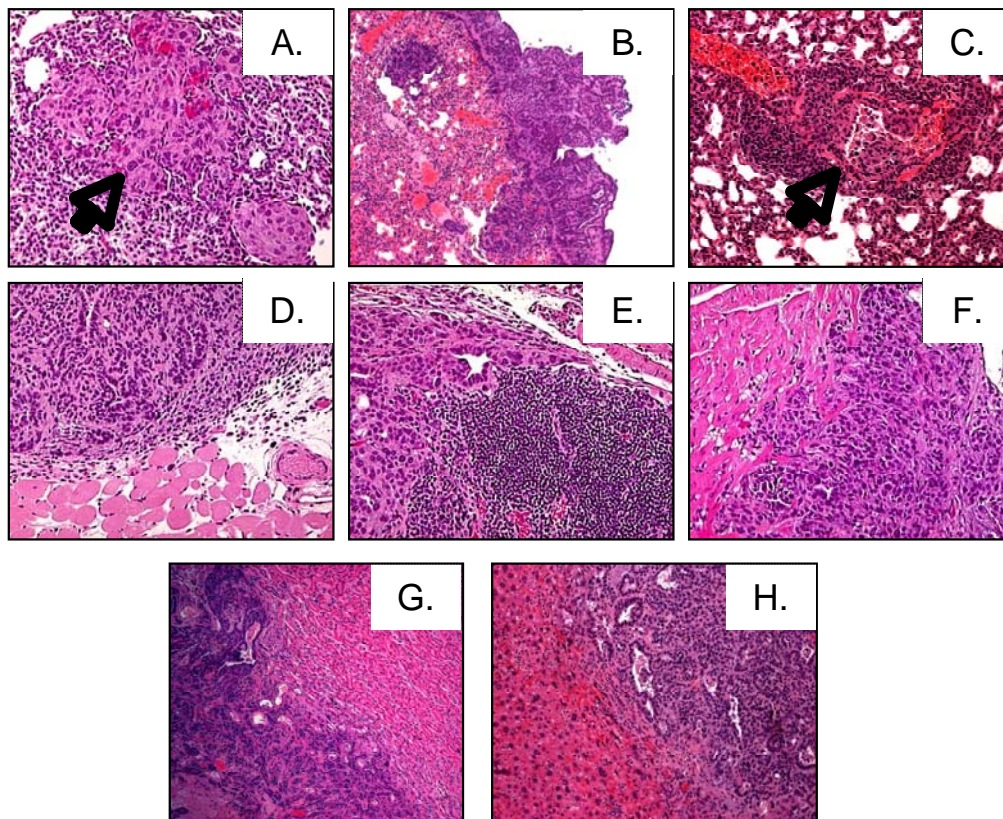


Figure 4.5. Histological features of invasive adenocarcinomas.

Some adenocarcinomas demonstrate abrupt adenoma to carcinoma transition (A), invasion of pleural surface (B), intravasation (C), implantation on intercostal muscle (D), invasion of hilar node (E), invasion of heart (F), metastasis to kidney (G), and metastasis to liver (H).

Experimental Group	N	Percent Invasive Carcinoma
Unirradiated Control	49	20%
Acute Dose X-ray	43	21%
Fractionated Dose X-ray	43	21%
Acute Dose ⁵⁶ Fe-	56	21%
Fractionated Dose ⁵⁶ Fe-	38	40% *

Table 4.1. Lifetime carcinoma incidence in unirradiated and LA1 KRAS mice irradiated with either an acute or fractionated 1.0 Gy dose of X-ray or ⁵⁶Fe- particles.

Percentage of total lungs assessed with invasive carcinoma (* denotes $p \leq 0.05$ compared to all other groups).

Since the survival of both ⁵⁶Fe- irradiated cohorts is significantly shortened, the same analysis was performed utilizing an age cutoff approximately equivalent to that of the maximal lifespan of these cohorts. The incidence of invasive carcinoma in the ⁵⁶Fe- particle irradiated mice changes minimally with this adjustment to 20% for an acute dose and 38% for a fractionated dose. At this time point, 16% of unirradiated LA1 KRAS mice have invasive carcinoma and this is not significantly affected with either an acute or fractionated dose of X-rays (18% for both groups) (Table 4.2).

Radiation is known to impact the health of mice by other means such as the induction of lymphoma (Kaplan, 1948). The incidence of lymphoma, leukemia, myeloproliferative disease, and pneumonia were thus examined in

Experimental Group	N	Percent Invasive Carcinoma
Unirradiated Control	43	16%
Acute Dose X-ray	38	18%
Fractionated Dose X-ray	39	18%
Acute Dose ⁵⁶ Fe-	54	20%
Fractionated Dose ⁵⁶ Fe-	37	38%

Table 4.2. Carcinoma incidence in unirradiated and LA1 KRAS mice irradiated with either an acute or fractionated 1.0 Gy dose of X-ray or ⁵⁶Fe- particles adjusted for survival.

Percentage of lungs within age criteria with invasive carcinoma (* denotes $p \leq 0.05$ compared to unirradiated control).

order to determine if these factors contributed to the decreased survival of the ⁵⁶Fe- particle irradiated cohorts. Both unirradiated LA1 KRAS and wildtype littermate animals are mildly susceptible to lymphoma (16% and 10%, respectively) (Figure 4.6 A). Irradiation of wildtype mice, but not LA1 KRAS mice, with an acute dose of ⁵⁶Fe- particles significantly decreases the incidence of lymphoma. Lymphoma incidence in no other experimental groups appears to be influenced by irradiation (Figure 4.6 A). Overall, the incidence of leukemia and pneumonia, while significantly elevated in the LA1 KRAS mice compared wildtype littermates (12% vs. 0% and 51% vs 20%, respectively), also changes with irradiation (Figure 4.6 B and C). This also occurs with another hematopoietic disorder, myeloproliferative disease, that which LA1 KRAS mice are mildly susceptible (9%) (Figure 4.6 D). In addition, wildtype mice have an increased incidence of pre-cancerous lesions in the liver compared to LA1 KRAS

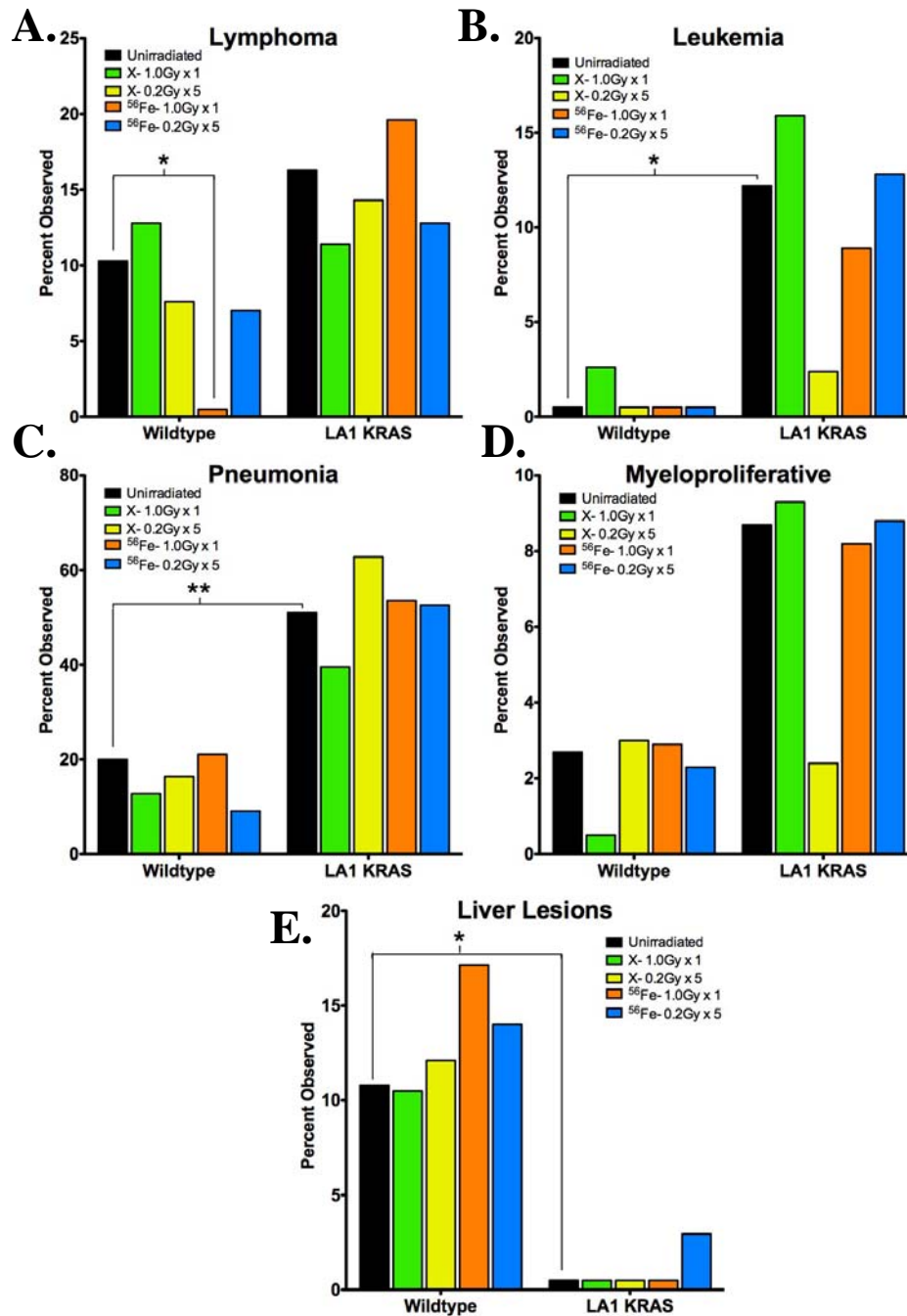


Figure 4.6. Incidence of several non-lung related factors detrimental to murine health.

Percent of lymphoma (A), leukemia (B), pneumonia (C), myeloproliferative disease (D), or benign lesion in liver (E) in unirradiated and irradiated LA1 KRAS and wildtype littermate mice (* denotes $p < 0.05$; ** denotes $p < 0.01$).

mice and this is mildly increased only upon irradiation with an acute dose of ^{56}Fe - particles compared to unirradiated animals (17% versus 11%, respectively) (Figure 4.6 E).

Genomic Analysis of Pulmonary Radiation Response.

To evaluate how a fractionated dose of ^{56}Fe - particles significantly increases the incidence of invasive carcinoma in LA1 KRAS mice, whole genome microarray analysis was performed. We extracted RNA from whole lungs of LA1 KRAS and wildtype littermate mice irradiated with a fractionated dose of 1.0 Gy ^{56}Fe - particles one year post-irradiation. RNA was also extracted from age-matched unirradiated LA1 KRAS and wildtype mice. Comparison of gene expression profiles between irradiated and unirradiated LA1 KRAS mice with a t-test and a threshold of $p \leq 0.01$ resulted in 1631 genes differentially expressed (Figure 4.7 and Appendix C). Gene ontology (GO) term enrichment analysis of these genes was performed utilizing the gene functional classification tool on the database for annotation, visualization, and integrated discovery (DAVID) (Huang da et al., 2009; Huang da et al., 2007). Clusters were enriched in 864 annotation terms and pathways such as those concerning protein metabolism, intercellular signaling including RAS, and inflammatory pathways (Appendix D). Since inflammation has been reported to influence both the onset and progression of cancer, including oncogenic KRAS initiated tumors; a subset was created utilizing

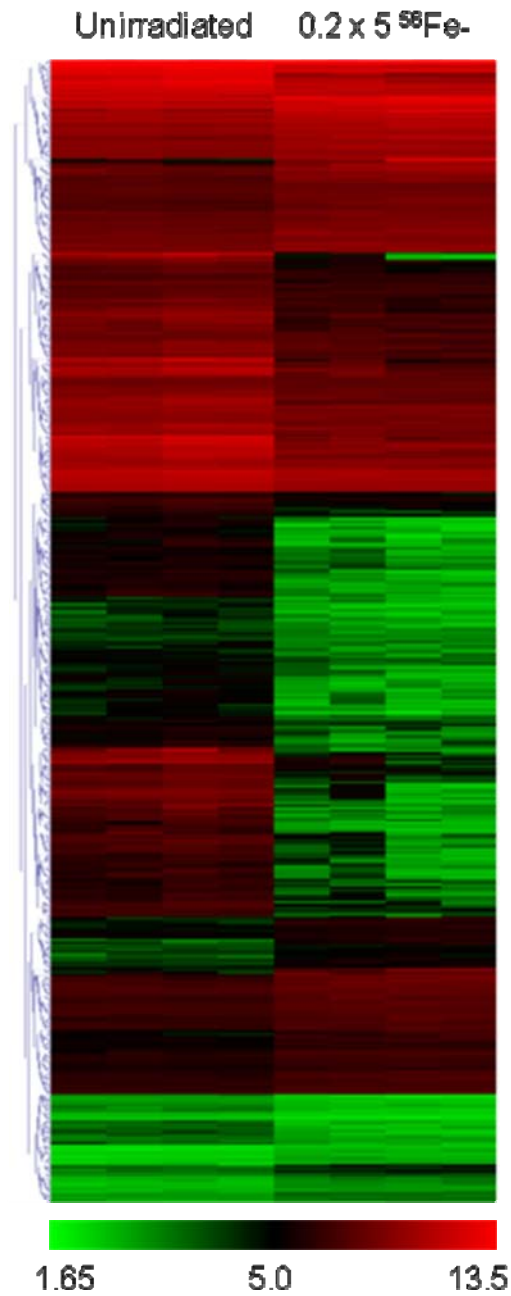


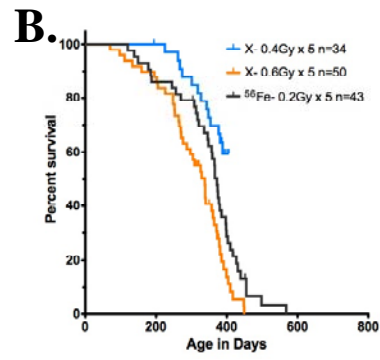
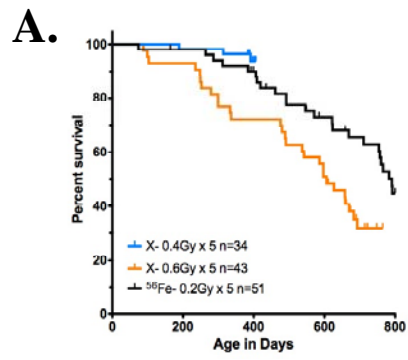
Figure 4.7. Whole lung microarray analysis one year post-irradiation.

RNA was extracted from whole lungs of LA1 KRAS one year after irradiation with fractionated dose (0.2Gy per day for 5 days) of 1.0 Gy ⁵⁶Fe- particles and compared to RNA from whole lungs of age matched unirradiated LA1 KRAS mice. 1631 genes differentially expressed (analysis with t-test and threshold of

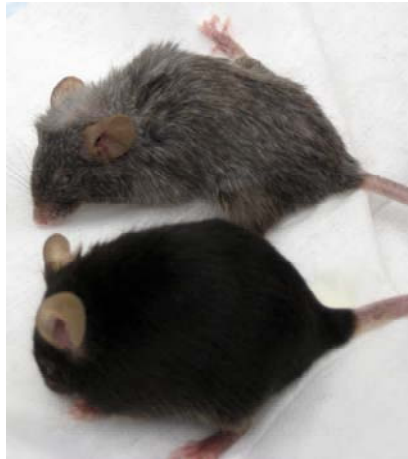
GO term associated with inflammation and analyzed (de Visser et al., 2006; Granville et al., 2009; Ji et al., 2006; Meira et al., 2008). 200 GO terms were enriched with a p-value of $p \leq 0.05$ by this reanalysis including several for various developmental processes and for the activation and maturation of the adaptive immune response (Appendix E).

Determination of Relative Biological Effect of ^{56}Fe - Particle Compared to X-ray Irradiation.

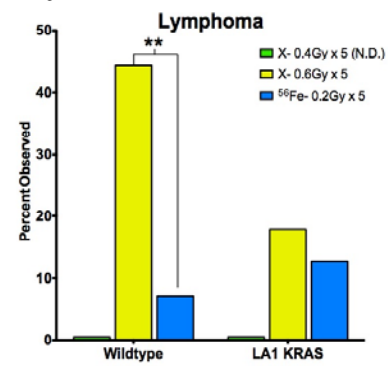
To determine whether a higher fractionated dose of X-rays is capable of phenocopying the effect observed with a 1.0 Gy fractionated dose of ^{56}Fe -particles, LA1 KRAS and wildtype littermate mice were irradiated with a fractionated dose of either 2.0 Gy or 3.0 Gy X-rays. Both LA1 KRAS and wildtype littermate mice irradiated with a fractionated 3.0 Gy dose of X-rays have significantly decreased survival compared to those irradiated with a fractionated dose of 1.0 Gy ^{56}Fe - particles (Figure 4.8 A and B). Irradiated mice demonstrate features associated with radiation toxicity and premature aging such as fur graying, kyphosis, and cataracts (Figure 4.8 C). Histopathological examination of the tumors in these LA1 KRAS mice irradiated with a fractionated 3.0 Gy dose of X-rays reveals a slightly elevated incidence of invasive carcinoma (26%; Table 4.3). Wildtype littermate mice, but not LA1 KRAS, have significantly a higher incidence of lymphoma (Figure 4.8 D). Incidence of leukemia, pneumonia, and



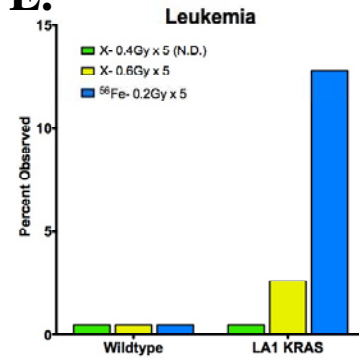
C.



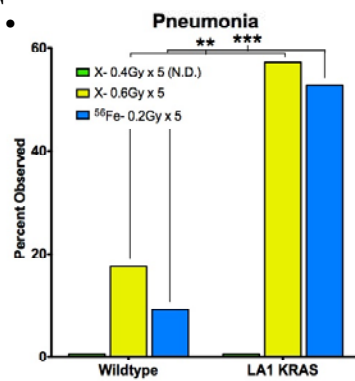
D.



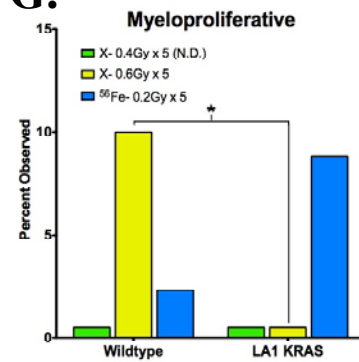
E.



F.



G.



myeloproliferative disease are not affected (Figures 4.8 E – G). The fractionated 2.0 Gy X-ray irradiation experiments are ongoing.

Determination of Relative Biological Effect of Fractionating ^{56}Fe - Particle Irradiation.

As the fractionation of a 1.0 Gy ^{56}Fe - particle dose of radiation significantly increases the incidence of carcinoma while an acute dose only has a minimal effect, we sought to determine the effect of other acute and fractionated irradiation schemes. LA1 KRAS and wildtype littermate animals were thus irradiated with ten 0.1 Gy doses of ^{56}Fe - particles over a twelve day interval or 5 0.1 Gy doses of ^{56}Fe - particles over a five day interval. Survival of both LA1 KRAS and wildtype littermate animals was identical to that of a 1.0 Gy dose of ^{56}Fe - particles administered in five 0.2 Gy fractions and as an acute dose (Figure 4.9 A and B). Currently, there is a modest effect on the incidence of invasive

Figure 4.8. Irradiation with a fractionated dose of 3.0 Gy dose of X-rays significantly affects survival and health of LA1 KRAS and wildtype littermate mice.

LA1 KRAS and wildtype littermate mice were irradiated with fractionated 2.0 Gy (0.4 Gy per day for five consecutive days) and 3.0 Gy (0.6 Gy per day for five consecutive days). (A) Kaplan-Meier survival curve of wildtype littermate mice. (B) Kaplan-Meier survival curve of LA1 KRAS mice. (C) Representative picture of LA1 KRAS mice either unirradiated (lower) or irradiated with fractionated 3.0 Gy dose of X-rays (upper). (D – G) Incidence of factors known to influence murine health. (D) Lymphoma. (E) Leukemia. (F) Pneumonia. (G) Myeloproliferative disease. (* denotes $p \leq 0.05$; ** denotes $p \leq 0.01$)

Experimental Group	Overall Incidence of Invasive Carcinoma	Adjusted Incidence of Invasive Carcinoma
Fractionated 1.0 Gy Dose ⁵⁶ Fe-	40% (n=38)	36.4% (n=33)
Fractionated 2.0 Gy Dose X-	N.D.	N.D.
Fractionated 3.0 Gy Dose X-	26.2 (n=42)	26.2% (n=42)

Table 4.3. Lifetime and survival adjusted carcinoma incidence in LA1 KRAS mice irradiated with either a fractionated 2.0 Gy or 3.0 Gy dose of X-rays compared to a fractionated 1.0 Gy dose of ⁵⁶Fe- particles.

carcinoma (24%), but the histopathological analysis is ongoing and incomplete (Table 4.4). The fractionated 0.5 Gy dose of ⁵⁶Fe- particles is also ongoing.

In order to determine whether the lower fractionated dosages are sufficient to elicit an effect as single doses, LA1 KRAS and wildtype littermate mice were irradiated with either a 0.1 Gy or 0.2 Gy doses of ⁵⁶Fe- particles. While it appears that there will be a dose dependence on the survival of both LA1 KRAS and wildtype littermate animals, both of these experiments are also in progress (Figure 4.10).

4.3. Discussion.

Expression of oncogenic KRAS in murine lung initiates the formation of lesions that mimic early lung cancer progression in humans and permits evaluation of lung cancer progression *in vivo*. In order to determine if radiation

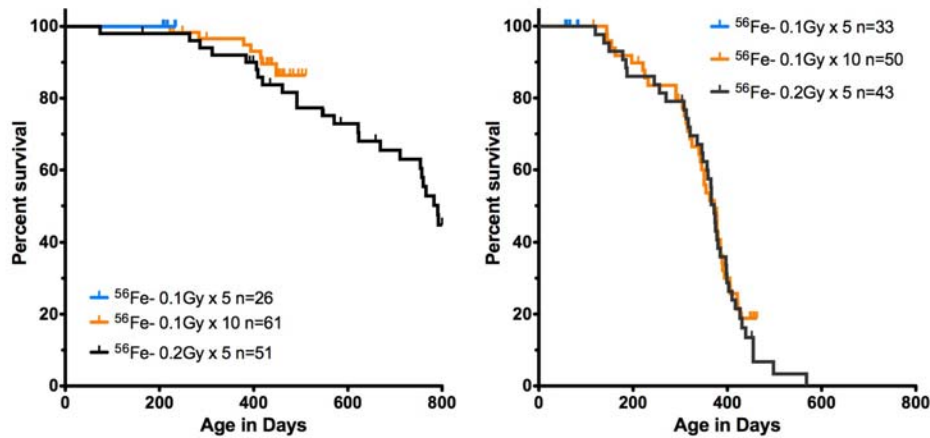


Figure 4.9. Fractionation of 1.0 Gy dose of ^{56}Fe - particles into ten 0.1 Gy doses impacts survival of LA1 KRAS and wildtype littermate mice identically to acute and five 0.2 Gy fractionation regimen.

may influence the initiation or progression of lung cancer, we irradiated the LA1 KRAS mouse model with a 1.0 Gy dose of different radiation qualities and dose regimens (Figure 4.2). Survival differences are apparent and are dependent on radiation quality. LA1 KRAS animals irradiated with ^{56}Fe - particles have a significantly decreased lifespan compared to unirradiated controls regardless of whether the dose was acute or fractionated (Figures 4.3 B and D) In contrast, X-ray irradiation does not affect lifespan except at the highest dosage tested (3.0 Gy) (Figures 4.3 A and C and 4.8 A and B). Histopathological analysis of tumors from KRAS mice irradiated with a fractionated dose of ^{56}Fe - particles demonstrate a dramatic progression in grade of lesion compared to all other

Experimental Group	Overall Incidence of Invasive Carcinoma	Adjusted Incidence of Invasive Carcinoma
Five 0.2 Gy Doses of ^{56}Fe -	40% (n=38)	38.7% (n=31)
Five 0.1 Gy Doses of ^{56}Fe -	N.D.	N.D.
Ten 0.1 Gy Doses of ^{56}Fe -	24.0 (n=25)	24.0% (n=25)

Table 4.4. Lifetime and survival adjusted carcinoma incidence in LA1 KRAS mice irradiated with five or ten 0.1 Gy doses of ^{56}Fe - particles compared to five 0.2 Gy doses of ^{56}Fe - particles.

groups. In all established mouse models of lung cancer, including the LA1 KRAS mouse, advanced lesions such as invasive adenocarcinoma occurs only in approximately 20% of animals, suggesting that intact barriers to invasive cancer remain. Importantly, LA1 KRAS mice that received a fractionated 1.0 Gy dose of ^{56}Fe - particles (but not single dose) showed a significant increase in the incidence of invasive adenocarcinomas (~40% overall) (Tables 4.1 and 4.2). These results were unexpected since a fractionated dose of terrestrial radiation is generally thought as sparing.

These results suggest that radiation exposure affects lifespan and carcinogenesis distinctly. The lethality observed in the LA1 KRAS mice from a 1.0 Gy whole body dose of high-energy ^{56}Fe - particles could be in part due to a systemic effect on the animal. Several biological systems are already impacted by the activation

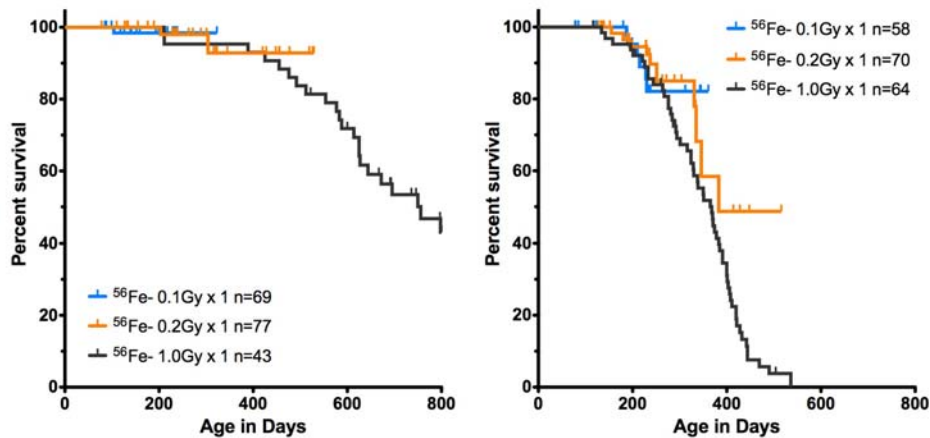


Figure 4.10. Current survival of LA1 KRAS and wildtype littermate mice irradiated with either an acute dose of 0.1 Gy or 0.2 Gy ^{56}Fe - particles.

of oncogenic KRAS in these animals compared to wildtype littermate (Figure 4.4 B, C and D). A 1.0 Gy dose of ^{56}Fe - particles, regardless of whether fractionated or not, could then potentially synergize with these health conditions in the LA1 KRAS mice leading to the observed decrease in lifespan. While we did not see a radiation effect on the health factors assessed, this hypothesis is supported by the similar decrease in LA1 KRAS lifespan observed from the fractionation of a 1.0 Gy dose of ^{56}Fe - particles into ten 0.1 Gy doses. Further, determination whether there exists a dose dependence from acute exposures on this phenotype has yet to be established due to ongoing experimentation.

The absence of an effect on lifespan by a 1.0 Gy dose of X-ray radiation may be due to the differences between ^{56}Fe - particles and X-rays in both the method of energy deposition and LET (Figure 4.3 A and C). These differences are known to minimize radiation effects, such as DNA damage and cell survival, from electromagnetic radiation compared to that of high-energy particles (Brooks et al., 2001; Hall and Giaccia, 2006). Thus, higher dosages of X-rays are required to elicit a similar biological effect (Hall and Giaccia, 2006). Conforming with this concept is the significant decrease in lifespan, in both LA1 KRAS and wildtype littermate mice, observed with a fractionated 3.0 Gy dose of X-rays (Figures 4.8 A and B).

As the increased incidence of invasive carcinoma was observed only in the LA1 KRAS animals that received a fractionated dose of ^{56}Fe - particles, this implies that mechanism behind this effect could be distinguishable from that causing the decrease in lifespan. Fractionation of radiation exposure can have a sparing effect and induce both bystander and radio-protective effects on cells and tissues (Hall and Giaccia, 2006; Prise and O'Sullivan, 2009; Qutob et al., 2006). Therefore, the fractionation of the ^{56}Fe - particle irradiation could allow tumor cells or cells within the microenvironment to persist after receiving the total 1.0 Gy dose. These cells could in turn either influence their surroundings or, if within the tumor cells, have acquired the necessary genomic instability for

transformation (Limoli et al., 2000; Morgan et al., 2002). Results from the in progress ten fraction (0.1 Gy per day) 1.0 Gy total dose experiment, in addition to the higher fractionated X-ray experiments will assist in understanding this role and whether there is an LET dependence.

One bystander effect detected through our genomic analysis and is known to influence carcinogenesis is that of inflammation (Appendices C - E) (de Visser et al., 2006; Granville et al., 2009; Ji et al., 2006; Meira et al., 2008). In order to further evaluate this possibility cohorts of LA1 KRAS and wildtype littermate mice were irradiated with either a fractionated or acute dose of 1.0 Gy ^{56}Fe -particles. RNA and plasma will be extracted two months post-irradiation from these animals and analyzed with a focus on altered inflammatory responses. Wildtype littermate animals will allow us to evaluate the dependence of a pre-initiated lesion for any dysregulation of the immune response.

Overall, we have demonstrated that radiation exposure may lead to several biological effects whose severity may be dependent on radiation quality. The potential to impact the overall lifespan of irradiated animals is greater with high-energy ^{56}Fe -particle exposure compared to a comparable dose of X-rays. This effect is further enhanced by the presence of a lesion that influences the health of an animal. In the context of pre-cancerous lesions, the fractionation of ^{56}Fe -

particle irradiation promotes the progression of these lesions to malignancy. Understanding how radiation exposure causes this progression is critical for NAASA as the average age of an American astronaut during their first mission in space is 42 and the presence of undetected pre-cancerous lesions increases with age.

4.4. Materials and Methods.

LA1 K-ras Mice.

The LA1 K-ras mouse model of lung cancer backcrossed into the C57/B6 and 129sv mouse backgrounds and method of genotyping have been previously described (Johnson et al., 2001). Animals are housed in a specific pathogen free (SPF) facility at the University of Texas Southwestern Medical Center at Dallas (UTSW). All animal husbandry has been performed according to the pair-wise breeding scheme between a heterozygous and wildtype animal of the same background.

Irradiation.

For ^{56}Fe - particle irradiation, LA1 K-ras and wildtype littermate animals, ages 5 weeks to 15 weeks, were shipped to the Brookhaven National Laboratory (BNL) on Long Island, NY. Animals were irradiated at the NASA Space Radiation

Laboratory (NSRL) at BNL with 1.0 GeV ^{56}Fe - particles at a dose rate of 0.2 Gy/min. Radiation doses were either administered acutely (0.1 Gy, 0.2 Gy, 1.0 Gy) or fractionated (0.1 Gy/day for 5 days, 0.2 Gy/day for 5 days or 0.1 Gy/day for ten days). Mice were then returned to the UTSW SPF facility and monitored twice daily until death or euthanasia due to health concerns. For X-ray irradiation, LA1 K-ras and wildtype littermate animals, ages 5 weeks to 15 weeks, were irradiated with 250-kV X-rays using an X-RAD 320 irradiator (Precision X-ray, Inc., North Branford, CT) at UTSW at a dose rate of approximately 0.14 Gy/min. Radiation doses were either administered acutely (1.0 Gy) or fractionated (0.2 Gy/day for 5 days, 0.4 Gy/day for 5 days, or 0.6 Gy/day for 5 days). Mice were then monitored twice daily in the UTSW SPF facility until death or euthanasia due to health concerns.

Lung Tumor Evaluation and Histology.

At death, carcasses are necropsied, the lungs removed, and visible tumor nodules on both dorsal and ventral pleural surfaces are documented, enumerated, and measured. Lungs are inflated by intra-tracheal infusion with 10% neutral buffered formalin (NBF), the trachea clamped, and then the whole lung is immersion-fixed overnight in 10% NBF. Gross examination of other tissues occurs at this time and relevant tissues, such as liver, kidney, and spleens, are extracted and immersion-fixed in 10% NBF overnight. Remaining carcasses are also individually fixed and

stored in case other tissues require analysis. The lungs and other tissues are paraffin embedded, cut at 5 microns, and stained with Hematoxylin and Eosin (H&E) for histopathological assessment by NSCOR investigator Dr. James Richardson.

Lung Tissue and Blood Collection for Array Analysis.

Age matched LA1 K-ras animals were either irradiated with an acute dose of 1.0 Gy ^{56}Fe - particles, a five-day fractionated dose of 1.0 Gy ^{56}Fe - particles, or left unirradiated. At five weeks or one year post-irradiation, animals were anesthetized with an intraperitoneal injection of a Ketamine, Xylazine, and Acepromazine mixture (Dosage: 100 mg/kg, 10 mg/kg, and 2 mg/kg, respectively). Cardiac puncture was performed immediately after anesthetization. Following cardiac puncture, animals were euthanized via cervical dislocation and the left lung lobe was extracted and flash frozen in liquid nitrogen.

RNA Extraction and Microarray Analysis.

Frozen lung tissue was homogenized and RNA extracted utilizing the Qiagen RNeasy Plus Kit (Qiagen, Inc.) per manufacturer's protocol. Microarrays were done using Illumina MouseWG-6 v2.0 Expression BeadChips. The protocol from Illumina Total Prep Kit from Ambion was used for labeling and hybridization is done according to manufacturer's (Illumina) instruction using their reagents.

Arrays were scanned using beadstation 500 beadarray reader and acquisitioned with BeadStudio. Data was normalized using the MBCB method (Ding et al., 2008). Significant genes were determined using a t-test with a threshold of $p > 0.01$ and clustered using Euclidean distance (Saeed et al., 2003)

Statistics.

In order to determine cohort size, power analysis was performed utilizing a two-tailed logrank (Mantel-Cox) test and a median survival of 300 days for the LA1 KRAS mice (Johnson et al., 2001). Forty-five animals were found to be sufficient to detect a 150 day change in survival with a power of 0.85%. This analysis was performed again once we established a median survival of 370 days with the animals raised in our facility. A change in survival of 120 days was found to be detectable with a cohort of forty-five LA1 KRAS mice. Analysis of Kaplan-Meier survival curves was also performed utilizing the logrank test. Comparisons of histological results were through two-tailed chi-square tests as no expectation of how the irradiated sample population would vary from the unirradiated sample population.

CHAPTER FIVE.

Discussion and Future Directions.

Radiation exposure is known to have detrimental biological effects such as an increased risk of cancer. Analysis of several human populations exposed to radiation has provided a foundation for this concept. In addition, these human epidemiological studies have demonstrated that the lung is particularly susceptible to the carcinogenic effects of radiation (Denman et al., 2003; Little, 2009; Preston et al., 2007; Reynolds et al., 2000b; Suit et al., 2007). Integration of the cancer stem cell (CSC) concept would imply that radiation either directly targets a tissue stem cell or manipulates a differentiated cell to re-acquire stem-like properties (Eramo et al., 2008; Visvader and Lindeman, 2008). Although, the stem cell niche intricately regulates tissue stem cells, radiation could also influence lung carcinogenesis by affecting the microenvironment. Therefore, a more complete understanding of lung homeostasis and repair is critical for a proper evaluation of the susceptibility of the lung to radiation-induced carcinogenesis.

The lung is currently characterized to have an atypical mechanism for regulation of homeostasis and repair compared to highly proliferative stem cell compartments such as the blood, skin, and GI track. The lung appears to rely on

multiple quiescent facultative stem cells that are situated throughout the lung. These cells rapidly regenerate the lung after injury, but are compartmentally restricted in the cell types they are capable of regenerating (Adamson and Bowden, 1974; Aso et al., 1976; Evans et al., 1975; Hong et al., 2004a; Rawlins et al., 2009; Reynolds et al., 2000a; Reynolds et al., 2000b; Rock et al., 2009). How and when this restriction is established is not known, but may involve an interaction with the microenvironment as has been shown with other tissue stem cells. Therefore, regardless if radiation-induced carcinogenesis is due to a direct or indirect effect on a tissue stem cell, there are several radiation targets in the lung that could lead to cancer. The histological subtype of resultant lung cancer could then be related to the compartment in which the dysregulated cell is located. In the Life Span Study (LSS) cohort of Hiroshima and Nagasaki atomic bomb survivors, the risks for all the major histological subtypes of lung cancer are increased with the risk for adenocarcinoma predominating (Land et al., 1993). As adenocarcinoma arises primarily from the distal compartment, this increased risk may be attributed to the larger surface area of the distal compartment relative to the central compartment. Although, external factors such as smoking could influence this result (Pierce et al., 2003).

The establishment of the HBEC3 KT line has provided a useful reagent for evaluating the effects of radiation exposure on lung cancer and the role of stem

cells since they were described to resemble the facultative basal cells (Ramirez et al., 2004; Vaughan et al., 2006). Further, introduction of factors known to be important in lung cancer were shown to gradually transform these cells (Sato, 2009; Sato et al., 2006). Tumors formed from these transformed HBEC3 KT cells consist of a mixed histology, which supports the CSC hypothesis. This study also indicated that serum exposure plays a critical role in the enhancement of this transformation (Sato, 2009). Thus, carcinogenesis in the HBEC system may be regulated by both intrinsic and extrinsic factors.

In this body of work, I have characterized that the HBEC3 KT cell line is multipotent. These cells appear to retain the capacity to differentiate into most, if not all, of the cell types of the lung in *in vitro* assays. This supports the concept that each facultative stem cell of the lung is restricted by external factors such as their microenvironment. Future manipulation of the specific culture conditions in which the cells are maintained or differentiated could provide a mechanistic understanding of how the lung tissue stem cells are regulated and how this role changes during the transformation process.

Another possibility is that the transformation of these cells could result in carcinomas characteristic of both central and distal airways. Currently, all histological subtypes within tumors from the transformed HBEC3 KT cells are

related to the central compartment (Sato, 2009). Whether this represents an intrinsic feature of these cells since they were derived from the central compartment or a response to extrinsic factors such as the culture conditions prior to injection or the site of injection has yet to be established.

Determining how intrinsic and extrinsic factors coalesce in regulating the HBEC3 KT cells is also important for the interpretation of radiation effects on these cells and the lung as a whole. If the regulation of these cells *in vitro* differs from that *in vivo*, then any observed effect may not directly translate to an *in vivo* situation. For example, radiation exposure should affect the lung microenvironment simultaneous with the epithelium. This could lead to a dysregulated stromal compartment that promotes a permissive environment for carcinogenesis to occur or synergize in combination with an existing or radiation-induced epithelial alteration. The differential effect of serum on the tumorigenic potential of the transformed HBEC3 KT cells and on the factors introduced to these cells compared to that of the normal HBEC3 KT cells supports this notion (Figure 3.4) (Sato, 2009). Therefore, the response of a pre-initiated or progressed cell may differ from that of a normal cell and both responses may be dependent on the relative condition *in vivo* at the time of exposure.

The increased incidence of invasive lung cancer observed in irradiated LA1 KRAS mice also suggests a critical extrinsic influence. Expression of oncogenic KRAS in the lung epithelium not only activates proliferative and survival pathways directly leading to lesions in the lung, but indirectly leads to a dysregulated inflammatory response (Granville et al., 2009; Ji et al., 2006). Radiation could further dysregulate the microenvironment surrounding these pre-initiated lesions and thus influence their progression. As this increased incidence was observed only when high-energy radiation was administered as a fractionated dose, this implies that more cells were affected by but not killed by the radiation. These cells could then affect their surroundings and influence carcinogenesis. Evaluating whether the initiation of a lesion after irradiation of the microenvironment leads to a similar phenotype would help determine if we can separate the microenvironment from the direct effect on the epithelial compartment.

Taken together, the results contained in the preceding chapters suggest the progenitor cells of lung retain a multipotent capacity, but are highly responsive to and restricted by extrinsic signals from their environment. Dysregulation of this signaling is received differently depending on whether these cells contain or do not contain intrinsic alterations. The increased risk of cancer in the lung from radiation exposure could very well be due to a composite of radiation effects on

the epithelial and stromal compartments. Further analysis of the interplay between these two compartments is then required to determine what reciprocal effects occur in response to changes in a single compartment whether induced by radiation exposure or not.

**APPENDIX A. GENES WITH SIGNIFICANT EXPRESSION CHANGES
IN QUIESCENT VERSUS PROLIFERATING HBEC3 KT CELLS.**

Gene	Fold Change	Gene	Fold Change
A2ML1	41.1	C1R	2.2
ABCC3	0.1	C21orf91	2.6
ABHD5	6.8	C22orf36	0.1
ABHD6	2.4	C5orf32	0.1
ABLIM1	7.2	C7orf49	0.4
ACP6	0.5	C9orf37	0.2
ACPP	8.8	CACNA2D3	2.8
ADH7	35.9	CALM1	2.9
ADRB2	8.0	CAPNS2	41.1
AGPAT9	0.1	CAPRN2	0.3
ALDH3B2	115.0	CATSPER1	0.4
ALDH5A1	4.3	CCBP2	5.7
ANGPT1	2.3	CCDC109B	0.1
ANK3	2.7	CCDC3	14.4
ANKRD22	9.4	CD1D	0.4
ANKRD35	41.5	CD276	0.3
ANXA3	0.2	CD36	30.9
ARG2	0.2	CD40	0.3
ARL5A	6.3	CD99	0.1
ATP10B	35.6	CDH4	0.1
ATP1A1	3.2	CDKN2B	6.2
ATP1B3	5.8	CERCAM	0.2
ATP2C2	2.1	CES2	4.3
ATP6V0E1	3.1	CGB5	0.2
AXL	0.1	CIB1	0.2
BAIAP2L2	0.4	CLDN23	0.3
BBOX1	21.0	CLIP2	0.2
BCL11B	7.9	CMTM7	0.0
BCL2L11	0.4	COL4A4	2.0
BMP6	0.2	CPA4	116.6
BNIP1	18.1	CPE	5.5
BOLA2	0.4	CRABP2	21.5
C10orf35	0.2	CSRP1	0.1
C10orf99	339.0	CSTA	30.4
C11orf73	0.4	CTF1	0.3
C12orf39	0.1	CXCL14	32.4
C16orf52	0.2	CYCS	4.1
C16orf58	0.4	CYLN2	0.2

Gene	Fold Change	Gene	Fold Change
CYP27B1	0.1	FSCN1	0.2
CYP2C18	12.8	GAS1	49.4
CYP3A5	3.5	GBP2	6.9
CYP4F11	0.1	GBP6	24.1
CYP4F12	13.2	GDPD3	9.6
CYP4F2	0.2	GGH	6.4
CYP4F3	9.9	GJA1	7.7
DSC2	7.9	GLIPR1L2	0.5
DSC3	4.3	GLTP	4.0
DUSP1	2.7	GNAI2	0.4
ECOP	0.4	GNG11	0.1
EFEMP2	0.2	GNL1	0.3
EGR1	0.5	GPM6B	5.7
ELF3	10.4	GRHL1	3.0
ELFN2	0.3	GRHL3	8.1
EMP3	0.1	GSTA2	2.1
EMR2	4.0	GSTA4	7.8
EPHA4	9.9	HERC6	5.9
EPPB9	0.3	HEY1	0.3
ERCC1	0.3	HIGD1A	3.8
ERN1	0.2	HIST1H1C	4.1
ETV4	0.1	HIST1H2AC	10.2
ETV5	0.0	HIST1H2BD	11.1
EXPH5	2.9	HIST1H2BK	7.2
FAM113B	0.1	HLA-A	0.4
FAM122A	2.7	HMGA2	0.1
FAM3D	5.3	HMGCS2	8.1
FAM69B	0.3	HNRNPH2	2.3
FAM86C	0.5	HOM-TES-103	0.3
FBXO17	0.3	HOPX	160.3
FCHO1	0.2	HSD11B2	19.4
FGFR3	22.3	HYI	0.2
FHL1	0.1	IFFO	0.1
FLG	3.7	IGFBP5	2.8
FLJ20021	0.3	IGFBP6	0.0
FLJ40504	0.1	IGFBP7	0.1
FLJ41603	7.0	IL13RA2	0.0
FLVCR2	9.4	INCA	4.4
FLYWCH1	0.2	IRX3	3.2
FOXA2	0.0	ITGA3	0.3
FOXO3	2.6	ITGB4	0.3
FOXQ1	17.6	ITGB5	0.1

Gene	Fold Change	Gene	Fold Change
ITM2C	0.2	LOX	33.4
ITPR3	0.4	LRRC26	11.0
KAL1	6.8	LRRC29	0.2
KCTD14	0.2	LYPD3	31.3
KHDRBS3	0.2	MACROD1	0.1
KIAA1622	0.3	MAD2L2	0.2
KLHL24	3.9	MAFB	41.9
KLK10	4.6	MAP3K7IP3	2.2
KLK12	3.0	MEGF9	2.6
KLK7	26.7	METTL7A	10.2
KLK8	57.7	MMP1	0.0
KLRG2	3.9	MST1R	0.4
KRT1	73.8	MT1F	0.1
KRT10	6.1	MTMR11	0.3
KRT13	227.5	MUC1	9.5
KRT4	327.4	MUC15	6.9
KRT7	0.4	MYADM	0.1
KRT80	6.2	MYCBP	2.3
KRTDAP	417.3	NCALD	11.8
LAMA3	0.3	NKX3-1	0.2
LAMC2	0.2	NMU	18.8
LASS3	11.6	NOD2	9.3
LETM2	0.1	OR7E156P	0.3
LGALS1	0.3	PBX4	0.4
LIPE	0.4	PCNXL2	0.4
LMCD1	0.2	PDCD4	11.9
LOC147645	2.8	PDLIM7	0.1
LOC342897	24.8	PERP	3.1
LOC389641	0.3	PFN1	0.4
LOC389816	12.8	PHC2	0.3
LOC401152	3.7	PHF19	0.3
LOC441019	0.2	PI3	29.3
LOC441282	28.5	PJCG6	2.1
LOC57228	5.7	PLA2G4F	21.6
LOC606724	0.4	PPAP2C	0.3
LOC641835	7.3	PPARGC1A	10.3
LOC642299	5.1	PPARGC1B	2.3
LOC644640	0.1	PPFIBP2	4.8
LOC644689	0.1	PRDM10	2.3
LOC646407	0.5	PRDM13	0.1
LOC646723	0.2	PRDM8	0.1
LOC652097	7.2	PRMT1	0.2

Gene	Fold Change	Gene	Fold Change
PRODH	13.9	SOX9	0.1
PROS1	15.1	SPINK5	8.1
PRR3	0.3	SPRR1A	435.0
PRSS2	0.2	SPRR1B	83.6
PRSS3	0.1	SPRR3	408.7
PTP4A3	0.2	SPTLC3	7.4
PTTG2	0.4	ST3GAL2	0.3
PYCR1	0.2	STX19	11.4
RAB17	0.3	SUPT3H	0.4
RAB25	2.9	SYNGR3	0.3
RAC2	0.1	TACSTD2	3.2
RAET1L	6.4	TAGLN3	0.1
RBM15B	2.3	TFPI2	0.0
RCAN1	5.4	TFRC	7.8
RDH12	16.4	TMEM156	0.1
RICS	3.5	TMEM39B	0.4
RP9	0.4	TMEM63C	4.9
RPL34	4.3	TMPRSS4	2.8
RPTN	27.9	TNFRSF6B	0.0
RPUSD3	0.3	TPCN2	0.4
S100A7	50.7	TPD52L2	0.4
SBSN	139.6	TRIM29	7.3
SC65	0.5	TRIM47	0.1
SCNN1B	12.6	TSPAN4	0.2
SEMA3B	0.1	TUBB3	0.3
SEMA6A	4.5	TUBG2	0.2
SERPINB13	79.6	TWIST2	0.2
SERPINB3	270.6	UCN	0.4
SFTPD	82.4	UGT1A6	16.2
SFTPG	2.7	UPP1	0.0
SGK	26.7	VILL	6.3
SGPP2	20.7	VNN3	2.4
SH2B3	0.2	VTCN1	4.9
SIGIRR	0.3	WBSCR27	0.1
SIPA1L2	10.3	WNT4	45.3
SLC3A2	0.3	ZBTB16	8.3
SLMO1	0.3	ZC3HAV1L	0.4
SLPI	3.5	ZNF598	0.3
SMOX	0.1	ZNF750	24.5
SMPDL3A	4.1		

(Significant genes were determined using SAM using a threshold of 2-fold and FDR of 1.0% and clustered using Euclidean distance)

**APPENDIX B. MAINTENANCE GENE AND PATHWAY GENE LIST
FOR TAQMAN® ASSAY WITH CORRESPONDING IDENTIFIERS.**

Gene	Refseq #	TaqMan Assay #
SHH	NM_000193	Hs00179843_m1
DHH	NM_021044	Hs00368305_m1
IHH	NM_002181	Hs01081801_m1
PTCH1	NM_000264	Hs00181117_m1
PTCH2	NM_003738.3	Hs00184804_m1
SMO	NM_005631	Hs00170665_m1
GLI1	NM_005269	Hs00171790_m1
GLI2	NM_005270	Hs00257977_m1
GLI2	NM_000168	Hs00609233_m1
DLL1	NM_005618	Hs00194509_m1
DLL3	NM_016941	Hs00213561_m1
DLL4	NM_019074	Hs00184092_m1
JAG1	NM_000214	Hs00164982_m1
JAG2	NM_002226	Hs00171432_m1
NOTCH1	NM_017617	Hs00413187_m1
NOTCH2	NM_024408	Hs00225747_m1
NOTCH3	NM_000435	Hs00166432_m1
NOTCH4	NM_004557	Hs00270200_m1
HES1	NM_005524	Hs00172878_m1
HEY1	NM_012258	Hs00232618_m1
HEY2	NM_012259	Hs00232622_m1
MAML2	NM_032427.1	Hs00287205_m1
ASCL1	NM_004316.3	Hs002699_m1
WNT1	NM_005430	Hs00180529_m1
WNT2b	NM_024494.1	Hs00257131_m1
WNT3a	NM_033131.2	Hs00263977_m1
WNT10b	NM_003394.2	Hs00559664_m1
FZD1	NM_003505	Hs00268943_s1
DVL2	NM_004422.2	Hs00182901_m1
DVL3	NM_004423.3	Hs00610263_m1
APC	NM_000038	Hs00181051_m1
B-CAT	NM_001904	Hs00170025_m1
TCF1	NM_000545	Hs00167041_m1
OCT4	NM_002701	Hs01895061_u1
NANOG	NM_024865	Hs02387400_g1
SOX2	NM_003106	Hs00602736_s1
MYC	NM_002467	Hs00153408_m1
BMI1	NM_005180	Hs00180411_m1
KLF4	NM_004235	Hs00358836_m1

**APPENDIX C. 1671 GENES DIFFERENTIALLY EXPRESSED IN LA1
KRAS MICE COMPARED TO UNIRRADIATED CONTROLS ONE
YEAR AFTER FRACTIONATED 1.0 GY DOSE OF ⁵⁶FE- PARTICLE
IRRADIATION.**

Gene	Gene	Gene	Gene
1810008N23RIK	2610507B11RIK	4930463G05RIK	6430562A12RIK
1810037C20RIK	2700078E11RIK	4930486L24RIK	6530401D06RIK
1810054D07RIK	2810004N23RIK	4930504E06RIK	6720407G21RIK
1810055E12RIK	2810025M15RIK	4930526H21RIK	6720487G11RIK
1810073N04RIK	2810029C07RIK	4930534B04RIK	6820408C15RIK
2010002M12RIK	2810032G03RIK	4930535E21RIK	8030447N19RIK
2010004N17RIK	2810037O22RIK	4930538K18RIK	8030474H12RIK
2010005O13RIK	2810402A17RIK	4930579J09RIK	8430403J19RIK
2010200O16RIK	2810403A07RIK	4930599N23RIK	8430419L09RIK
2010204O13RIK	2810405J23RIK	4932409I22RIK	8430421H08RIK
2200001I15RIK	2810410P22RIK	4932425I24RIK	8430426J06RIK
2210414H16RIK	2810453H10RIK	4932441J05RIK	8430438E03RIK
2300002D11RIK	2810484G07RIK	4932443I19RIK	9030003C19RIK
2300005B03RIK	2900006K08RIK	4933417E01RIK	9030409G11RIK
2310003C23RIK	2900026A02RIK	4933424B01RIK	9130019P16RIK
2310004I03RIK	2900027G03RIK	4933425L06RIK	9130020K20RIK
2310007A19RIK	2900041M22RIK	4933427C01RIK	9130230L23RIK
2310008H09RIK	2900090M10RIK	4933428D01RIK	9130415E20RIK
2310015A05RIK	3010015K02RIK	4933428G20RIK	9330158H04RIK
2310016C08RIK	3110001A13RIK	4933430H15RIK	9330162L04RIK
2310039L15RIK	3110007F17RIK	5031436O03RIK	9430008C03RIK
2310047B19RIK	3110040N11RIK	5330439J01RIK	9430015L11RIK
2310047M10RIK	3110048E14RIK	5430433E21RIK	9430020K01RIK
2310056P07RIK	3110053B16RIK	5530401N12RIK	9430073N08RIK
2310061F22RIK	3300002A11RIK	5730406F04RIK	9530027K23RIK
2410002F23RIK	3632451O06RIK	5730408I11RIK	9630032J03RIK
2410004A20RIK	4432404P07RIK	5730502D15RIK	9630050M13RIK
2410004P03RIK	4432405B04RIK	5730596K20RIK	9630058J23RIK
2410016F01RIK	4631416I11RIK	5830420C15RIK	9830002I17RIK
2410019A14RIK	4631423B10RIK	5930404K09RIK	9930039L23RIK
2410066E13RIK	4632408I12RIK	5930434B04RIK	A030005L19RIK
2410091C18RIK	4632413C10RIK	6030408B16RIK	A130010C12RIK
2510002D24RIK	4832408C21RIK	6030458C11RIK	A130010J15RIK
2610020O08RIK	4833441J24RIK	6030495B01RIK	A230059K20RIK
2610021K21RIK	4921507O14RIK	6230400G14RIK	A330021E22RIK
2610024G14RIK	4921511C04RIK	6330405H19	A330042I21RIK
2610024H22RIK	4921528H16RIK	6330500D04RIK	A430083B19RIK
2610024N24RIK	4921531P07RIK	6430402L23RIK	A430088H15RIK
2610204M08RIK	4922501L14RIK	6430521C12RIK	A430091O22RIK
2610301N02RIK	4930438O05RIK	6430531B16RIK	A4GALT
2610304F08RIK	4930451C15RIK	6430537H07RIK	A530021P12RIK
2610312E17RIK	4930455F23RIK	6430548M08RIK	A630056H20RIK

Gene	Gene	Gene	Gene
A730017C20RIK	AMPD2	BBS4	C730026O12RIK
A730049B06RIK	AMPH	BBS9	C79267
A830026L17RIK	ANKRD1	BC008163	CABLES1
A830030H10RIK	ANKRD17	BC020535	CACNA1D
A830054O07RIK	ANKRD28	BC024537	CALCRL
A930017M01RIK	ANKRD45	BC026439	CALML4
A930023F05RIK	ANXA8	BC027231	CALR
AA407270	AOX1	BC028528	CALU
AA536749	AQP1	BC029169	CAMTA1
ABHD5	ARF5	BC030183	CASC1
ABHD7	ARHGAP20	BC030396	CASKIN1
ABI3	ARHGAP24	BC034090	CASP3
ABI3BP	ARHGAP25	BC038167	CBFA2T2
ABRA	ARHGEF15	BC049806	CBR1
ACOT2	ARHGEF19	BC050196	CBX5
ACOT8	ARHGEF3	BC051019	CC2D2A
ACSL3	ARL5A	BC055107	CCBP2
ACTC1	ARMC4	BCAS2	CCDC100
ACYP1	ARMCX1	BMP1	CCDC103
ADAM3	ARRDC3	BMP6	CCDC108
ADAMTS15	ART3	BMPR1B	CCDC111
ADCK5	ART4	BNIP1	CCDC113
ADCY2	ASAH3L	BNIP2	CCDC39
ADCY4	ASCC1	BRI3	CCDC40
ADCY8	ATF2	BRI3BP	CCDC41
ADD3	ATP13A2	BXDC1	CCDC78
ADPRHL1	ATP1A2	C030003H22RIK	CCDC96
ADRB1	ATP2B2	C030003M13RIK	CCNT2
AFAP1	ATP8B1	C030045D06RIK	CCRL2
AGR3	AU016693	C030048B08RIK	CCT6A
AGRP	AU021034	C030048H21RIK	CD209F
AI507611	AV249152	C130008L17RIK	CD27
AI850995	AW548124	C130064E22RIK	CD40
AIM1	B130007O15RIK	C130065N10RIK	CD40LG
AK129341	B230363H02RIK	C130072A16RIK	CD47
AK7	B230373P09RIK	C130078N17RIK	CD97
AKAP12	B230396O12RIK	C1QTNF2	CDC42EP4
AKAP14	B430105G09RIK	C1QTNF3	CDH5
AKAP2	B430109P06RIK	C230053B09RIK	CDH8
AKR1C19	B430217B02RIK	C230069K22RIK	CDK2
AKT3	B430302L04RIK	C230070D10RIK	CDKL2
ALG12	B430305P08RIK	C430046P22RIK	CDKL4
ALG8	B430320J11RIK	C530047J20RIK	CDKN2D
ALG9	B930011A14RIK	C5AR1	CEACAM1
ALOX12	B930044G13RIK	C630013B14RIK	CENTD2
ALOXE3	B930095G15RIK	C630024B01RIK	CENTD3
AMIGO2	BACH2	C7	CEP1
AMPD1	BARX2	C730009F21RIK	CEP63

Gene	Gene	Gene	Gene
CES6	D430034D15RIK	E130203B14RIK	FABP3
CETN3	D4BWG1540E	E330009P21RIK	FAIM
CFDP1	D530004J12RIK	E330018D03RIK	FAIM2
CFTR	D530030K12RIK	EARS2	FANCC
CHD1	D530033A12RIK	EDG2	FARSA
CHRM2	D5WSU178E	EDIL3	FAS
CHRNA10	D630022P03RIK	EDNRA	FBLN1
CHST3	D7ERTD70E	EDNRB	FBXL12
CHST7	D830005N24RIK	EEF1E1	FBXL13
CHST8	D830044I16RIK	EFCAB1	FBXL17
CIDEA	D9WSU20E	EFCAB3	FBXL5
CIDEC	DAD1	EFHD1	FBXO15
CIRH1A	DCAMKL1	EFNA5	FBXO16
CLCN4-2	DCBLD2	EFR3A	FGD6
CLDN11	DDX27	EFTUD1	FGF10
CLDN15	DDX3Y	EG241041	FGFR1OP
CLDN2	DES	EG277333	FGL1
CLDN5	DGKB	EG433144	FHL1
CLEC1A	DGKG	EG623230	FIS1
CLEC3B	DGKH	EG635702	FKBP14
CLNS1A	DIRAS2	EG638695	FMNL2
CNRIP1	DIRC2	EG665378	FMO2
CNTFR	DKKL1	EGFL7	FN1
CNTN1	DLL4	EGFLAM	FNDC7
COL17A1	DMWD	EGLN3	FOLH1
COL8A2	DNAHC11	EHMT1	FOXA3
COPZ1	DNAHC2	EIF1B	FOXC1
COX4I2	DNAHC5	EIF2S2	FOXI1
CP	DNAHC9	EIF3S4	FPR1
CPSF4L	DNAJB13	EIF4G1	FRRS1
CRISPLD2	DNAJC5B	EIF5	FSIP1
CRLF3	DNALI1	ELA1	FUT10
CTRB1	DNM2	ELMOD1	FUT8
CTSA	DNTTIP2	ELTD1	FXR1H
CUGBP1	DOC2B	EMG1	FZD3
CYP2B10	DOCK6	ENG	G630024G08RIK
CYP4B1	DPT	ENO1	G630026M10RIK
CYTL1	DPYSL5	EPAS1	GAB3
D030034I04RIK	DSCR6	EPB4.1L2	GABRP
D030069G17RIK	DSG2	EPB4.1L5	GADD45B
D10ERTD641E	DST	EPHA1	GALK1
D12ERTD553E	DTNBP1	EPHB4	GALNTL2
D130084M03RIK	DUSP14	ERCC8	GART
D14ERTD449E	DYDC2	ERGIC2	GAS2L1
D15ERTD621E	E030019B06RIK	EXDL2	GATA2
D19WSU162E	E030025D05RIK	EXOSC2	GATA3
D330027H18RIK	E030044B06RIK	EXOSC6	GCG
D430013K02	E130012A19RIK	F830048D03RIK	GCNT2

Gene	Gene	Gene	Gene
GCS1	GRIA1	HSD11B1	KLF13
GDF1	GRIA3	HSD17B12	KLF2
GDPD2	GRIP1	HSD3B2	KLF9
GEMIN6	GRK4	HSPA4	KLHDC8A
GFER	GRWD1	HSPA9	KLHDC9
GIT2	GSDMDC1	HSPB7	KLHL29
GJA4	GSPT2	HUS1	KLHL5
GLB1L2	GSS	ICAM2	KLK1
GLT25D2	GSTK1	ID2	KLK1B21
GLT8D2	GSTP1	IDH1	KLRA16
GM101	GTF2E2	IDS	KNDC1
GM106	GTF3C4	IFIT2	KNG1
GM1574	GUCY1A3	IFNA13	KNG2
GM1661	GUCY1B3	IFT172	KRTAP17-1
GM1673	GYK	IGF2BP1	KY
GM1752	GYP A	IGSF10	LAMA2
GM281	GZMM	IHPK3	LAMC3
GM525	H1FX	IL12A	LARP4
GM527	H2-T24	IL15	LARP5
GM705	HARBI1	IL16	LARP6
GM815	HCN4	IL17RC	LASS2
GM867	HDGF	INPP5A	LAYN
GM969	HEATR3	IQCA	LBX2
GM973	HECW2	IQCG	LIX1
GMPS	HEPH	IRAK4	LNX2
GNA11	HERPUD1	IRF3	LOC100038894
GNAI2	HEY2	ISLR	LOC100039001
GNG8	HHEX	ITCH	LOC100039175
GNL3	HIBADH	ITGAE	LOC100039479
GNS	HIGD1A	ITPKB	LOC100039660
GOT1L1	HIST1H1C	IVNS1ABP	LOC100041388
GP1BB	HIST1H2AC	JUN	LOC100043332
GP5	HIST1H2BE	KANK4	LOC100044829
GP6	HNF4A	KBTBD10	LOC100044934
GP9	HOOK1	KCNA6	LOC100044948
GPATCH4	HOOK2	KCNH3	LOC100045284
GPD2	HOPX	KCNJ12	LOC100045776
GPIHBP1	HOXA2	KCNK3	LOC100045967
GPLD1	HOXA3	KCNK6	LOC100046457
GPM6A	HOXA5	KCNMB4	LOC100046959
GPM6B	HOXB2	KCTD12	LOC100046963
GPR116	HOXB5	KCTD20	LOC100047193
GPR153	HOXB6	KCTD6	LOC100047369
GPR22	HOXD9	KCTD9	LOC100047583
GPR27	HPCAL4	KIF27	LOC100047915
GPRC6A	HPRT1	KIF9	LOC100048056
GPS2	HS3ST6	KIT	LOC100048116
GRAP	HS6ST2	KITL	LOC100048169

Gene	Gene	Gene	Gene
LOC100048331	LOC631037	MCPT4	MYL4
LOC100048332	LOC633238	MDH1B	MYL7
LOC100048534	LOC633945	MDM1	MYL9
LOC100048807	LOC638024	MDN1	MYOZ2
LOC213043	LOC664837	MED16	MYRIP
LOC216397	LOC666025	MED8	NAP1L5
LOC218877	LOC666403	MEF2C	NAT12
LOC219049	LOC667609	MEIS1	NDE1
LOC224163	LOC668387	MEIS2	NDN
LOC225609	LOC669168	MEMO1	NECAP1
LOC229810	LOC670044	MESP1	NEDL2
LOC231936	LOC673352	MET	NEK11
LOC234050	LPHN3	METTTL1	NEK9
LOC234882	LRFN3	METTTL4	NEO1
LOC234915	LRRC18	MFAP2	NETO2
LOC238943	LRRC23	MGC41689	NFATC1
LOC239559	LRRC34	MIB2	NFIB
LOC269919	LRRC36	MIF	NFKBIA
LOC333670	LRRC46	MLF1	NHLRC1
LOC333744	LRRC48	MMP23	NHLRC2
LOC380653	LRRC50	MOBKL1A	NIP7
LOC380665	LRRC51	MORN3	NLRP3
LOC380927	LRRC8A	MPL	NNAT
LOC381000	LRRFIP2	MPP3	NOC4L
LOC381105	LSG1	MPP6	NOS1AP
LOC381132	LSM6	MRAS	NOV
LOC381146	LSR	MRGPRB8	NOXA1
LOC381256	LTBP4	MRGPRF	NPAL1
LOC381260	LTBR	MRPL35	NPAL2
LOC381265	LTK	MRPS18B	NPHP4
LOC381284	LUC7L	MRPS25	NPR3
LOC381546	LUC7L2	MSH3	NPY1R
LOC381670	LYPD2	MSL2	NR2F6
LOC382237	LYSMD2	MSL2L1	NR6A1
LOC382646	LYVE1	MTAP	NRGN
LOC383948	LYZL4	MTAP2	NT5DC2
LOC385217	M6PR	MTAP4	NTN4
LOC385390	MACF1	MTAP6	NUB1
LOC385905	MAFK	MTAP7D3	NUMB
LOC386078	MAMDC2	MUC16	NUP50
LOC386094	MAN1A2	MXD3	NYX
LOC386233	MAP3K3	MXD4	OGN
LOC386254	MAP3K6	MYBBP1A	OLFM1
LOC386289	MAP4K2	MYBPHL	OLFML3
LOC386413	MAPT	MYD116	OLFR1084
LOC386534	MB	MYH10	OLFR1297
LOC545481	MBTD1	MYL1	OLFR1465
LOC623006	MCFD2	MYL3	OLFR1477

Gene	Gene	Gene	Gene
OLFR399	PLEKHA6	PSP	RNF170
OMP	PLEKHG1	PTGER2	RNF5
OTOP3	PLEKHG6	PTGIS	ROBO2
OTUD7B	PLOD2	PTPDC1	RPA1
OTX1	PLSCR4	PTPRB	RPAP1
P2RY5	PLTP	PTPRK	RPGR
P4HB	PNMA1	PTPRZ1	RPL37
PACSIN3	PODXL2	PTTG1IP	RPL7L1
PAF1	POFUT1	QPCT	RPRML
PAG1	POLR2A	RAB28	RPS13
PAPPA	POPDC2	RAB3C	RRAGB
PCBP3	POPDC3	RAB8A	RRBP1
PCDH20	PPA1	RABGGTB	RRP15
PCDH9	PPA2	RAGE	RSAD1
PCDHA6	PPAP2A	RAMP1	RSHL3
PCDHA7	PPAT	RAMP3	RSL1D1
PCDHAC2	PPBP	RARA	RTDR1
PCDHB15	PPIL6	RARS	RTKN2
PCGF6	PPM1E	RARS2	RTP1
PCMT1	PPM1F	RASA4	RUFY1
PCNX	PPP1R13B	RASL10A	RUNX1T1
PCOLCE2	PPP1R14A	RASL10B	RUSC2
PCYT1B	PPP1R2	RASSF4	RYK
PDDC1	PPP2R5C	RASSF5	SAMHD1
PDE3A	PPS	RASSF7	SBDS
PDGFC	PRDM6	RBM13	SCAMP5
PDGFRA	PRDX3	RBM47	SCGB3A2
PDSS1	PRDX4	RBMX	SCGN10
PDZD2	PRICKLE1	RCAN2	SCL0001284.1_18
PECAM1	PRKAA1	RCSD1	SCL0001333.1_125
PEO1	PRKCBP1	RECK	SCL000179.1_19
PER1	PRKCZ	REPS1	SCL0002507.1_236
PEX2	PRKG1	RFWD3	SCL0002785.1_49
PGAM1	PRKG2	RGS12	SCL000959.1_2
PGCP	PRMT3	RGS2	SCN2B
PGM2L1	PRMT6	RGS5	SCN3A
PGM5	PRMT7	RGS9	SCN7A
PHACTR1	PRPF8	RHBDL2	SCRN1
PHB2	PRR18	RHBDL3	SCUBE2
PI16	PRRG1	RHEB	SDK1
PIGF	PRRX2	RHOB	SDPR
PIGL	PRSS16	RHOBTB2	SDSL
PIGZ	PRX	RHOD	SEC61A1
PIP4K2A	PSCD3	RHOT2	SEC63
PKIA	PSMB7	RIBC1	SEL1L
PKNOX2	PSMD14	RIOK3	SEMA3B
PKP2	PSMD5	RLF	SEMA3C
PLA2G6	PSME4	RNF121	SENP5

Gene	Gene	Gene	Gene
SERPINA3C	SMR1	TBCD	TRAPPC3
SERPINB5	SMTN	TBX5	TREML1
SESN1	SMYD2	TCAP	TRIM10
SFRP2	SNCA	TCF23	TRIM2
SFT2D2	SNCG	TCP1	TRIM27
SFXN1	SND1	TCTE1	TRIM37
SGCB	SNORA65	TCTE3	TRO
SGIP1	SNRK	TCTEX1D4	TRPC4AP
SGK1	SNX13	TEK	TRPM5
SGTB	SNX21	TEKT1	TRPV4
SH3BP5L	SOBP	TG	TRRP1
SH3GLB1	SOX11	TGFBR3	TSC22D3
SH3YL1	SOX13	TGM1	TSFM
SHANK3	SOX7	THBS2	TSGA10
SHE	SPAG4	THSD1	TSHZ1
SHISA2	SPAG6	TICAM1	TSHZ3
SIPA1L1	SPAG8	TIE1	TSNAXIP1
SIX1	SPATA18	TIMP4	TSPAN18
SKIV2L	SPATA4	TLR7	TSPAN4
SLAIN2	SPCS3	TM4SF4	TSPAN7
SLAMF1	SPEER4C	TMCC2	TTC18
SLC10A6	SPINK2	TMEM100	TTC25
SLC10A7	SPINK4	TMEM166	TTC27
SLC13A4	SPNB1	TMEM167	TTC28
SLC16A9	SPON2	TMEM17	TTC29
SLC23A1	SPR	TMEM204	TTC30A1
SLC24A3	SRD5A1	TMEM35	TTC30B
SLC25A10	SRGN	TMEM41A	TTC9C
SLC25A18	SRPK3	TMEM55B	TTL10
SLC30A2	SRPX	TMEM66	TTL9
SLC30A6	SRXN1	TMOD2	TUBA8
SLC38A2	SSPN	TMTC1	TUFM
SLC40A1	ST3GAL4	TNA	TULP1
SLC4A4	ST6GAL1	TNFRSF11B	TULP3
SLC6A2	ST8SIA2	TNFRSF1B	TWIST2
SLC7A10	STAB1	TNIK	TYKI
SLC9A2	STARD13	TNN	TYMS
SLC9A3R2	STARD8	TNP2	UBE2E3
SLCO4A1	STK16	TNRC6C	UBE2F
SLIT3	STK33	TNS1	UBE2O
SLN	STRBP	TOM1L2	UBE2Q2
SLU7	STX8	TOMM40	UBFD1
SLURP1	SULT4A1	TOR1B	UBL3
SMAD6	SYF2	TPM2	UBXD5
SMARCA2	SYT5	TPRGL	UCK2
SMCR7L	SYTL4	TRAF4	UCP2
SMOC2	TARS2	TRAK2	UEVLD
SMPDL3A	TBC1D24	TRAP1A	UFSP2

Gene	Gene	Gene	Gene
ULK4	VPS26	WNT4	ZFP174
UNC45B	VPS54	XAB1	ZFP213
UNC5C	VSNL1	XIST	ZFP27
UPK3B	VSTM2A	XKRX	ZFP276
USP10	VTI1B	XPNPEP2	ZFP422-RS1
USP8	VWA3A	XPOT	ZFP474
USP9X	WDR24	XRCC2	ZFP496
USPL1	WDR43	XRCC6	ZFP523
V1RE10	WDR51B	YIPF3	ZFP533
VAMP2	WDR59	YRDC	ZFP598
VAMP4	WDR66	ZBTB16	ZFP618
VAV3	WDR69	ZC3H15	ZFP641
VDAC3	WDR74	ZCRB1	ZFP787
VEGFC	WDR92	ZDHHC5	ZMYND10
VGLL4	WFDC1	ZEB1	ZMYND12
VPREB1	WFDC13	ZEB2	ZNF512B
VPREB3	WFDC6B	ZFAND2A	ZSWIM2
VPS16	WNT10B	ZFP1	

APPENDIX D. ENRICHED ANNOTATION TERMS FROM GENES SIGNIFICANTLY CHANGED IN LA1 KRAS MOUSE LUNGS ONE YEAR AFTER FRACTIONATED 1.0 GY DOSE OF ⁵⁶FE- PARTICLE IRRADIATION.

Category	Term	p-value
SP_PIR_KEYWORDS	activator	0.0000
UP_SEQ_FEATURE	active site:Proton acceptor	0.0000
SP_PIR_KEYWORDS	alternative splicing	0.0053
SP_PIR_KEYWORDS	aminoacyl-tRNA synthetase	0.0001
SP_PIR_KEYWORDS	aminopeptidase	0.0046
SP_PIR_KEYWORDS	ATP	0.0000
SP_PIR_KEYWORDS	atp-binding	0.0000
UP_SEQ_FEATURE	binding site:ATP	0.0000
UP_SEQ_FEATURE	binding site:Glutamate	0.0073
SP_PIR_KEYWORDS	calcium	0.0000
UP_SEQ_FEATURE	calcium-binding region:3	0.0121
SP_PIR_KEYWORDS	carbohydrate metabolism	0.0134
SP_PIR_KEYWORDS	carboxypeptidase	0.0125
SP_PIR_KEYWORDS	cell adhesion	0.0000
SP_PIR_KEYWORDS	cell junction	0.0000
SP_PIR_KEYWORDS	Coiled coil	0.0003
UP_SEQ_FEATURE	compositionally biased region:Arg/Ser-rich	0.0063
UP_SEQ_FEATURE	compositionally biased region:Poly-Ser	0.0052
SP_PIR_KEYWORDS	cytoplasm	0.0037
SP_PIR_KEYWORDS	cytoplasmic vesicle	0.0000
COG_ONTOLOGY	Cytoskeleton	0.0007
SP_PIR_KEYWORDS	Developmental protein	0.0000
UP_SEQ_FEATURE	disulfide bond	0.0002
SP_PIR_KEYWORDS	DNA binding	0.0000
UP_SEQ_FEATURE	DNA-binding region:HMG box	0.0130
UP_SEQ_FEATURE	DNA-binding region:Homeobox	0.0000
UP_SEQ_FEATURE	domain:AGC-kinase C-terminal	0.0000
UP_SEQ_FEATURE	domain:EF-hand 1	0.0000
UP_SEQ_FEATURE	domain:EF-hand 2	0.0000
UP_SEQ_FEATURE	domain:EF-hand 3	0.0000
UP_SEQ_FEATURE	domain:EGF-like 1	0.0000
UP_SEQ_FEATURE	domain:EGF-like 2; calcium-binding	0.0000
UP_SEQ_FEATURE	domain:EGF-like 3; calcium-binding	0.0001
UP_SEQ_FEATURE	domain:EGF-like 4; calcium-binding	0.0001
UP_SEQ_FEATURE	domain:EGF-like 5; calcium-binding	0.0130
UP_SEQ_FEATURE	domain:EGF-like 6; calcium-binding	0.0104
UP_SEQ_FEATURE	domain:EGF-like 7; calcium-binding	0.0104
UP_SEQ_FEATURE	domain:EGF-like 8; calcium-binding	0.0084
UP_SEQ_FEATURE	domain:EGF-like 9; calcium-binding	0.0057
UP_SEQ_FEATURE	domain:F-box	0.0000
UP_SEQ_FEATURE	domain:Fibronectin type-III 1	0.0019
UP_SEQ_FEATURE	domain:Fibronectin type-III 2	0.0019
UP_SEQ_FEATURE	domain:GPS	0.0104

Category	Term	p-value
UP_SEQ_FEATURE	domain:Ig-like C2-type 1	0.0028
UP_SEQ_FEATURE	domain:Ig-like C2-type 2	0.0028
UP_SEQ_FEATURE	domain:Ig-like C2-type 4	0.0070
UP_SEQ_FEATURE	domain:PH	0.0109
UP_SEQ_FEATURE	domain:Protein kinase	0.0000
UP_SEQ_FEATURE	domain:SAM	0.0067
UP_SEQ_FEATURE	domain:TAFH	0.0109
SP_PIR_KEYWORDS	egf-like domain	0.0000
SP_PIR_KEYWORDS	endoplasmic reticulum	0.0031
SP_PIR_KEYWORDS	er-golgi transport	0.0000
SP_PIR_KEYWORDS	Exonuclease	0.0101
SP_PIR_KEYWORDS	Exosome	0.0028
COG_ONTOLOGY	General function prediction only	0.0022
SP_PIR_KEYWORDS	glycoprotein	0.0000
UP_SEQ_FEATURE	glycosylation site:N-linked (GlcNAc...)	0.0000
SP_PIR_KEYWORDS	glycosyltransferase	0.0002
GOTERM_BP_ALL	GO:0000041~transition metal ion transport	0.0004
GOTERM_BP_ALL	GO:0000074~regulation of progression through cell cycle	0.0004
GOTERM_CC_ALL	GO:0000119~mediator complex	0.0058
GOTERM_BP_ALL	GO:0000122~negative regulation of transcription from RNA polymerase II promoter	0.0000
GOTERM_CC_ALL	GO:0000178~exosome (RNase complex)	0.0044
GOTERM_BP_ALL	GO:0000226~microtubule cytoskeleton organization and biogenesis	0.0000
GOTERM_BP_ALL	GO:0000245~spliceosome assembly	0.0000
GOTERM_MF_ALL	GO:0000287~magnesium ion binding	0.0002
GOTERM_BP_ALL	GO:0000375~RNA splicing, via transesterification reactions	0.0001
GOTERM_BP_ALL	GO:0000398~nuclear mRNA splicing, via spliceosome	0.0001
GOTERM_BP_ALL	GO:0001501~skeletal development	0.0000
GOTERM_CC_ALL	GO:0001518~voltage-gated sodium channel complex	0.0145
GOTERM_MF_ALL	GO:0001584~rhodopsin-like receptor activity	0.0064
GOTERM_MF_ALL	GO:0001653~peptide receptor activity	0.0000
GOTERM_BP_ALL	GO:0001655~urogenital system development	0.0093
GOTERM_BP_ALL	GO:0001657~ureteric bud development	0.0145
GOTERM_BP_ALL	GO:0001822~kidney development	0.0072
GOTERM_BP_ALL	GO:0001974~blood vessel remodeling	0.0033
GOTERM_BP_ALL	GO:0003002~regionalization	0.0089
GOTERM_MF_ALL	GO:0003677~DNA binding	0.0000
GOTERM_MF_ALL	GO:0003690~double-stranded DNA binding	0.0051
GOTERM_MF_ALL	GO:0003713~transcription coactivator activity	0.0007
GOTERM_MF_ALL	GO:0003723~RNA binding	0.0000
GOTERM_MF_ALL	GO:0003743~translation initiation factor activity	0.0000
GOTERM_MF_ALL	GO:0003746~translation elongation factor activity	0.0008
GOTERM_MF_ALL	GO:0003924~GTPase activity	0.0000
GOTERM_MF_ALL	GO:0004175~endopeptidase activity	0.0000
GOTERM_MF_ALL	GO:0004177~aminopeptidase activity	0.0000
GOTERM_MF_ALL	GO:0004221~ubiquitin thiolesterase activity	0.0000

Category	Term	p-value
GOTERM_MF_ALL	GO:0004252~serine-type endopeptidase activity	0.0000
GOTERM_MF_ALL	GO:0004293~tissue kallikrein activity	0.0068
GOTERM_MF_ALL	GO:0004672~protein kinase activity	0.0000
GOTERM_MF_ALL	GO:0004674~protein serine/threonine kinase activity	0.0000
GOTERM_MF_ALL	GO:0004693~cyclin-dependent protein kinase activity	0.0000
GOTERM_MF_ALL	GO:0004713~protein-tyrosine kinase activity	0.0000
GOTERM_MF_ALL	GO:0004714~transmembrane receptor protein tyrosine kinase activity	0.0000
GOTERM_MF_ALL	GO:0004721~phosphoprotein phosphatase activity	0.0000
GOTERM_MF_ALL	GO:0004722~protein serine/threonine phosphatase activity	0.0085
SP_PIR_KEYWORDS	er-golgi transport	0.0000
SP_PIR_KEYWORDS	Exonuclease	0.0101
GOTERM_MF_ALL	GO:0004725~protein tyrosine phosphatase activity	0.0002
GOTERM_MF_ALL	GO:0004812~aminoacyl-tRNA ligase activity	0.0000
GOTERM_MF_ALL	GO:0004814~arginine-tRNA ligase activity	0.0009
GOTERM_MF_ALL	GO:0004842~ubiquitin-protein ligase activity	0.0000
GOTERM_MF_ALL	GO:0004843~ubiquitin-specific protease activity	0.0000
GOTERM_MF_ALL	GO:0004866~endopeptidase inhibitor activity	0.0000
GOTERM_MF_ALL	GO:0004867~serine-type endopeptidase inhibitor activity	0.0000
GOTERM_MF_ALL	GO:0004872~receptor activity	0.0000
GOTERM_MF_ALL	GO:0004888~transmembrane receptor activity	0.0000
GOTERM_MF_ALL	GO:0004930~G-protein coupled receptor activity	0.0000
GOTERM_MF_ALL	GO:0004962~endothelin receptor activity	0.0104
GOTERM_MF_ALL	GO:0005083~small GTPase regulator activity	0.0000
GOTERM_MF_ALL	GO:0005085~guanyl-nucleotide exchange factor activity	0.0000
GOTERM_MF_ALL	GO:0005088~Ras guanyl-nucleotide exchange factor activity	0.0000
GOTERM_MF_ALL	GO:0005089~Rho guanyl-nucleotide exchange factor activity	0.0000
GOTERM_MF_ALL	GO:0005216~ion channel activity	0.0000
GOTERM_MF_ALL	GO:0005230~extracellular ligand-gated ion channel activity	0.0037
GOTERM_MF_ALL	GO:0005244~voltage-gated ion channel activity	0.0000
GOTERM_MF_ALL	GO:0005248~voltage-gated sodium channel activity	0.0001
GOTERM_MF_ALL	GO:0005249~voltage-gated potassium channel activity	0.0000
GOTERM_MF_ALL	GO:0005261~cation channel activity	0.0000
GOTERM_MF_ALL	GO:0005267~potassium channel activity	0.0000
GOTERM_MF_ALL	GO:0005272~sodium channel activity	0.0000
GOTERM_MF_ALL	GO:0005342~organic acid transmembrane transporter activity	0.0040
GOTERM_MF_ALL	GO:0005506~iron ion binding	0.0135
GOTERM_MF_ALL	GO:0005509~calcium ion binding	0.0000
GOTERM_MF_ALL	GO:0005519~cytoskeletal regulatory protein binding	0.0038

Category	Term	p-value
GOTERM_MF_ALL	GO:0005524~ATP binding	0.0000
GOTERM_MF_ALL	GO:0005525~GTP binding	0.0000
GOTERM_CC_ALL	GO:0005634~nucleus	0.0000
GOTERM_CC_ALL	GO:0005654~nucleoplasm	0.0000
GOTERM_CC_ALL	GO:0005667~transcription factor complex	0.0000
GOTERM_CC_ALL	GO:0005681~spliceosome	0.0000
GOTERM_CC_ALL	GO:0005737~cytoplasm	0.0008
GOTERM_CC_ALL	GO:0005739~mitochondrion	0.0000
GOTERM_CC_ALL	GO:0005740~mitochondrial envelope	0.0000
GOTERM_CC_ALL	GO:0005743~mitochondrial inner membrane	0.0000
GOTERM_CC_ALL	GO:0005783~endoplasmic reticulum	0.0104
GOTERM_CC_ALL	GO:0005794~Golgi apparatus	0.0000
GOTERM_CC_ALL	GO:0005840~ribosome	0.0000
GOTERM_CC_ALL	GO:0005856~cytoskeleton	0.0000
GOTERM_CC_ALL	GO:0005874~microtubule	0.0000
GOTERM_CC_ALL	GO:0005875~microtubule associated complex	0.0000
GOTERM_CC_ALL	GO:0005886~plasma membrane	0.0000
GOTERM_CC_ALL	GO:0005887~integral to plasma membrane	0.0000
GOTERM_BP_ALL	GO:0006022~aminoglycan metabolic process	0.0093
GOTERM_BP_ALL	GO:0006029~proteoglycan metabolic process	0.0107
GOTERM_BP_ALL	GO:0006082~organic acid metabolic process	0.0012
GOTERM_BP_ALL	GO:0006139~nucleobase, nucleoside, nucleotide and nucleic acid metabolic process	0.0000
GOTERM_BP_ALL	GO:0006259~DNA metabolic process	0.0001
GOTERM_BP_ALL	GO:0006260~DNA replication	0.0004
GOTERM_BP_ALL	GO:0006261~DNA-dependent DNA replication	0.0001
GOTERM_BP_ALL	GO:0006281~DNA repair	0.0006
GOTERM_BP_ALL	GO:0006298~mismatch repair	0.0034
GOTERM_BP_ALL	GO:0006351~transcription, DNA-dependent	0.0000
GOTERM_BP_ALL	GO:0006355~regulation of transcription, DNA-dependent	0.0000
GOTERM_BP_ALL	GO:0006357~regulation of transcription from RNA polymerase II promoter	0.0000
GOTERM_BP_ALL	GO:0006364~rRNA processing	0.0000
GOTERM_BP_ALL	GO:0006366~transcription from RNA polymerase II promoter	0.0000
GOTERM_BP_ALL	GO:0006397~mRNA processing	0.0000
GOTERM_BP_ALL	GO:0006399~tRNA metabolic process	0.0000
GOTERM_BP_ALL	GO:0006413~translational initiation	0.0000
GOTERM_BP_ALL	GO:0006418~tRNA aminoacylation for protein translation	0.0000
GOTERM_BP_ALL	GO:0006420~arginyl-tRNA aminoacylation	0.0009
GOTERM_BP_ALL	GO:0006446~regulation of translational initiation	0.0061
GOTERM_BP_ALL	GO:0006457~protein folding	0.0000
GOTERM_BP_ALL	GO:0006464~protein modification process	0.0000
GOTERM_BP_ALL	GO:0006468~protein amino acid phosphorylation	0.0000
GOTERM_BP_ALL	GO:0006470~protein amino acid dephosphorylation	0.0000
GOTERM_BP_ALL	GO:0006486~protein amino acid glycosylation	0.0001
GOTERM_BP_ALL	GO:0006508~proteolysis	0.0000
GOTERM_BP_ALL	GO:0006511~ubiquitin-dependent protein catabolic process	0.0000

Category	Term	p-value
GOTERM_BP_ALL	GO:0006512~ubiquitin cycle	0.0000
GOTERM_BP_ALL	GO:0006519~amino acid and derivative metabolic process	0.0003
GOTERM_BP_ALL	GO:0006520~amino acid metabolic process	0.0002
GOTERM_BP_ALL	GO:0006793~phosphorus metabolic process	0.0000
GOTERM_BP_ALL	GO:0006811~ion transport	0.0000
GOTERM_BP_ALL	GO:0006812~cation transport	0.0000
GOTERM_BP_ALL	GO:0006813~potassium ion transport	0.0000
GOTERM_BP_ALL	GO:0006814~sodium ion transport	0.0000
GOTERM_BP_ALL	GO:0006816~calcium ion transport	0.0121
GOTERM_BP_ALL	GO:0006826~iron ion transport	0.0001
GOTERM_BP_ALL	GO:0006886~intracellular protein transport	0.0054
GOTERM_BP_ALL	GO:0006888~ER to Golgi vesicle-mediated transport	0.0001
GOTERM_BP_ALL	GO:0006891~intra-Golgi vesicle-mediated transport	0.0035
GOTERM_BP_ALL	GO:0006974~response to DNA damage stimulus	0.0009
GOTERM_BP_ALL	GO:0006996~organelle organization and biogenesis	0.0000
GOTERM_BP_ALL	GO:0007010~cytoskeleton organization and biogenesis	0.0000
GOTERM_BP_ALL	GO:0007017~microtubule-based process	0.0000
GOTERM_BP_ALL	GO:0007018~microtubule-based movement	0.0000
GOTERM_BP_ALL	GO:0007156~homophilic cell adhesion	0.0001
GOTERM_BP_ALL	GO:0007165~signal transduction	0.0010
GOTERM_BP_ALL	GO:0007166~cell surface receptor linked signal transduction	0.0001
GOTERM_BP_ALL	GO:0007167~enzyme linked receptor protein signaling pathway	0.0009
GOTERM_BP_ALL	GO:0007169~transmembrane receptor protein tyrosine kinase signaling pathway	0.0012
GOTERM_BP_ALL	GO:0007185~transmembrane receptor protein tyrosine phosphatase signaling pathway	0.0056
GOTERM_BP_ALL	GO:0007186~G-protein coupled receptor protein signaling pathway	0.0000
GOTERM_BP_ALL	GO:0007242~intracellular signaling cascade	0.0000
GOTERM_BP_ALL	GO:0007243~protein kinase cascade	0.0063
GOTERM_BP_ALL	GO:0007264~small GTPase mediated signal transduction	0.0000
GOTERM_BP_ALL	GO:0007265~Ras protein signal transduction	0.0000
GOTERM_BP_ALL	GO:0007266~Rho protein signal transduction	0.0000
GOTERM_BP_ALL	GO:0007399~nervous system development	0.0010
GOTERM_BP_ALL	GO:0007417~central nervous system development	0.0005
GOTERM_BP_ALL	GO:0007423~sensory organ development	0.0036
GOTERM_BP_ALL	GO:0007507~heart development	0.0000
GOTERM_BP_ALL	GO:0007517~muscle development	0.0005
GOTERM_MF_ALL	GO:0008017~microtubule binding	0.0000
GOTERM_CC_ALL	GO:0008021~synaptic vesicle	0.0000
GOTERM_CC_ALL	GO:0008076~voltage-gated potassium channel complex	0.0000
GOTERM_MF_ALL	GO:0008092~cytoskeletal protein binding	0.0000
GOTERM_BP_ALL	GO:0008104~protein localization	0.0006

Category	Term	p-value
GOTERM_MF_ALL	GO:0008134~transcription factor binding	0.0000
GOTERM_MF_ALL	GO:0008146~sulfotransferase activity	0.0019
GOTERM_MF_ALL	GO:0008233~peptidase activity	0.0000
GOTERM_MF_ALL	GO:0008234~cysteine-type peptidase activity	0.0000
GOTERM_MF_ALL	GO:0008236~serine-type peptidase activity	0.0000
GOTERM_MF_ALL	GO:0008238~exopeptidase activity	0.0001
GOTERM_MF_ALL	GO:0008270~zinc ion binding	0.0000
GOTERM_BP_ALL	GO:0008277~regulation of G-protein coupled receptor protein signaling pathway	0.0073
GOTERM_MF_ALL	GO:0008324~cation transmembrane transporter activity	0.0000
GOTERM_BP_ALL	GO:0008380~RNA splicing	0.0000
GOTERM_MF_ALL	GO:0008459~chondroitin 6-sulfotransferase activity	0.0104
GOTERM_MF_ALL	GO:0008565~protein transporter activity	0.0003
GOTERM_MF_ALL	GO:0008565~protein transporter activity	0.0014
GOTERM_BP_ALL	GO:0009057~macromolecule catabolic process	0.0000
GOTERM_BP_ALL	GO:0009059~macromolecule biosynthetic process	0.0000
GOTERM_BP_ALL	GO:0009100~glycoprotein metabolic process	0.0005
GOTERM_BP_ALL	GO:0009101~glycoprotein biosynthetic process	0.0002
GOTERM_BP_ALL	GO:0009308~amine metabolic process	0.0006
GOTERM_BP_ALL	GO:0009792~embryonic development ending in birth or egg hatching	0.0074
GOTERM_BP_ALL	GO:0009887~organ morphogenesis	0.0000
GOTERM_BP_ALL	GO:0009888~tissue development	0.0059
GOTERM_BP_ALL	GO:0009892~negative regulation of metabolic process	0.0000
GOTERM_BP_ALL	GO:0009893~positive regulation of metabolic process	0.0000
GOTERM_BP_ALL	GO:0009952~anterior/posterior pattern formation	0.0148
GOTERM_BP_ALL	GO:0009966~regulation of signal transduction	0.0000
GOTERM_BP_ALL	GO:0014706~striated muscle development	0.0066
GOTERM_MF_ALL	GO:0015026~coreceptor activity	0.0014
GOTERM_BP_ALL	GO:0015031~protein transport	0.0004
GOTERM_MF_ALL	GO:0015071~protein phosphatase type 2C activity	0.0046
GOTERM_MF_ALL	GO:0015075~ion transmembrane transporter activity	0.0000
GOTERM_MF_ALL	GO:0015267~channel activity	0.0000
GOTERM_MF_ALL	GO:0015276~ligand-gated ion channel activity	0.0002
GOTERM_MF_ALL	GO:0015291~secondary active transmembrane transporter activity	0.0001
GOTERM_MF_ALL	GO:0015293~symporter activity	0.0000
GOTERM_CC_ALL	GO:0015629~actin cytoskeleton	0.0002
GOTERM_CC_ALL	GO:0015630~microtubule cytoskeleton	0.0000
GOTERM_MF_ALL	GO:0015631~tubulin binding	0.0000
GOTERM_BP_ALL	GO:0015672~monovalent inorganic cation transport	0.0000
GOTERM_BP_ALL	GO:0015674~di-, tri-valent inorganic cation transport	0.0029
GOTERM_CC_ALL	GO:0015934~large ribosomal subunit	0.0132
GOTERM_CC_ALL	GO:0016021~integral to membrane	0.0000

Category	Term	p-value
GOTERM_CC_ALL	GO:0016023~cytoplasmic membrane-bound vesicle	0.0000
GOTERM_BP_ALL	GO:0016044~membrane organization and biogenesis	0.0009
GOTERM_BP_ALL	GO:0016070~RNA metabolic process	0.0000
GOTERM_BP_ALL	GO:0016071~mRNA metabolic process	0.0000
GOTERM_BP_ALL	GO:0016072~rRNA metabolic process	0.0000
GOTERM_BP_ALL	GO:0016192~vesicle-mediated transport	0.0000
GOTERM_MF_ALL	GO:0016301~kinase activity	0.0000
GOTERM_BP_ALL	GO:0016310~phosphorylation	0.0000
GOTERM_BP_ALL	GO:0016311~dephosphorylation	0.0000
GOTERM_BP_ALL	GO:0016337~cell-cell adhesion	0.0000
GOTERM_CC_ALL	GO:0016459~myosin complex	0.0000
GOTERM_MF_ALL	GO:0016462~pyrophosphatase activity	0.0000
GOTERM_BP_ALL	GO:0016481~negative regulation of transcription	0.0000
GOTERM_CC_ALL	GO:0016591~DNA-directed RNA polymerase II, holoenzyme	0.0045
GOTERM_MF_ALL	GO:0016757~transferase activity, transferring glycosyl groups	0.0000
GOTERM_MF_ALL	GO:0016758~transferase activity, transferring hexosyl groups	0.0002
GOTERM_MF_ALL	GO:0016772~transferase activity, transferring phosphorus-containing groups	0.0000
GOTERM_MF_ALL	GO:0016773~phosphotransferase activity, alcohol group as acceptor	0.0000
GOTERM_MF_ALL	GO:0016782~transferase activity, transferring sulfur-containing groups	0.0028
GOTERM_MF_ALL	GO:0016788~hydrolase activity, acting on ester bonds	0.0000
GOTERM_MF_ALL	GO:0016790~thiolester hydrolase activity	0.0000
GOTERM_MF_ALL	GO:0016791~phosphoric monoester hydrolase activity	0.0000
GOTERM_MF_ALL	GO:0016817~hydrolase activity, acting on acid anhydrides	0.0000
GOTERM_MF_ALL	GO:0016818~hydrolase activity, acting on acid anhydrides, in phosphorus-containing anhydrides	0.0000
GOTERM_MF_ALL	GO:0016875~ligase activity, forming carbon-oxygen bonds	0.0000
GOTERM_MF_ALL	GO:0016876~ligase activity, forming aminoacyl-tRNA and related compounds	0.0000
GOTERM_MF_ALL	GO:0016879~ligase activity, forming carbon-nitrogen bonds	0.0000
GOTERM_MF_ALL	GO:0016881~acid-amino acid ligase activity	0.0000
GOTERM_MF_ALL	GO:0017076~purine nucleotide binding	0.0000
GOTERM_MF_ALL	GO:0017111~nucleoside-triphosphatase activity	0.0000
GOTERM_MF_ALL	GO:0017171~serine hydrolase activity	0.0000
GOTERM_MF_ALL	GO:0019001~guanyl nucleotide binding	0.0000
GOTERM_BP_ALL	GO:0019219~regulation of nucleobase, nucleoside, nucleotide and nucleic acid metabolic process	0.0000
GOTERM_BP_ALL	GO:0019538~protein metabolic process	0.0000
GOTERM_BP_ALL	GO:0019752~carboxylic acid metabolic process	0.0012

Category	Term	p-value
GOTERM_MF_ALL	GO:0019783~small conjugating protein-specific protease activity	0.0000
GOTERM_MF_ALL	GO:0019787~small conjugating protein ligase activity	0.0000
GOTERM_CC_ALL	GO:0019866~organelle inner membrane	0.0000
GOTERM_MF_ALL	GO:0019887~protein kinase regulator activity	0.0114
GOTERM_BP_ALL	GO:0019941~modification-dependent protein catabolic process	0.0000
GOTERM_MF_ALL	GO:0019955~cytokine binding	0.0092
GOTERM_BP_ALL	GO:0022607~cellular component assembly	0.0001
GOTERM_BP_ALL	GO:0022613~ribonucleoprotein complex biogenesis and assembly	0.0000
GOTERM_BP_ALL	GO:0022618~protein-RNA complex assembly	0.0000
GOTERM_MF_ALL	GO:0022803~passive transmembrane transporter activity	0.0000
GOTERM_MF_ALL	GO:0022804~active transmembrane transporter activity	0.0011
GOTERM_MF_ALL	GO:0022832~voltage-gated channel activity	0.0000
GOTERM_MF_ALL	GO:0022834~ligand-gated channel activity	0.0002
GOTERM_MF_ALL	GO:0022836~gated channel activity	0.0000
GOTERM_MF_ALL	GO:0022838~substrate specific channel activity	0.0000
GOTERM_MF_ALL	GO:0022843~voltage-gated cation channel activity	0.0000
GOTERM_MF_ALL	GO:0022891~substrate-specific transmembrane transporter activity	0.0000
GOTERM_BP_ALL	GO:0030001~metal ion transport	0.0000
GOTERM_CC_ALL	GO:0030054~cell junction	0.0001
GOTERM_CC_ALL	GO:0030135~coated vesicle	0.0000
GOTERM_CC_ALL	GO:0030136~clathrin-coated vesicle	0.0000
GOTERM_BP_ALL	GO:0030154~cell differentiation	0.0002
GOTERM_BP_ALL	GO:0030163~protein catabolic process	0.0000
GOTERM_BP_ALL	GO:0030166~proteoglycan biosynthetic process	0.0067
GOTERM_BP_ALL	GO:0030203~glycosaminoglycan metabolic process	0.0093
GOTERM_CC_ALL	GO:0030286~dynein complex	0.0003
GOTERM_MF_ALL	GO:0030414~protease inhibitor activity	0.0000
GOTERM_MF_ALL	GO:0030554~adenyl nucleotide binding	0.0000
GOTERM_BP_ALL	GO:0030705~cytoskeleton-dependent intracellular transport	0.0000
GOTERM_BP_ALL	GO:0030878~thyroid gland development	0.0000
GOTERM_MF_ALL	GO:0030955~potassium ion binding	0.0000
GOTERM_MF_ALL	GO:0030983~mismatched DNA binding	0.0018
GOTERM_CC_ALL	GO:0031224~intrinsic to membrane	0.0000
GOTERM_CC_ALL	GO:0031226~intrinsic to plasma membrane	0.0000
GOTERM_BP_ALL	GO:0031323~regulation of cellular metabolic process	0.0000
GOTERM_BP_ALL	GO:0031324~negative regulation of cellular metabolic process	0.0000
GOTERM_BP_ALL	GO:0031325~positive regulation of cellular metabolic process	0.0000
GOTERM_MF_ALL	GO:0031402~sodium ion binding	0.0000
GOTERM_CC_ALL	GO:0031410~cytoplasmic vesicle	0.0000

Category	Term	p-value
GOTERM_MF_ALL	GO:0031420~alkali metal ion binding	0.0000
GOTERM_CC_ALL	GO:0031966~mitochondrial membrane	0.0000
GOTERM_CC_ALL	GO:0031981~nuclear lumen	0.0000
GOTERM_CC_ALL	GO:0031988~membrane-bound vesicle	0.0000
GOTERM_MF_ALL	GO:0032553~ribonucleotide binding	0.0000
GOTERM_MF_ALL	GO:0032555~purine ribonucleotide binding	0.0000
GOTERM_MF_ALL	GO:0032559~adenyl ribonucleotide binding	0.0000
GOTERM_MF_ALL	GO:0032561~guanyl ribonucleotide binding	0.0000
GOTERM_BP_ALL	GO:0032774~RNA biosynthetic process	0.0000
GOTERM_BP_ALL	GO:0032940~secretion by cell	0.0000
GOTERM_CC_ALL	GO:0033279~ribosomal subunit	0.0003
GOTERM_BP_ALL	GO:0035023~regulation of Rho protein signal transduction	0.0000
GOTERM_BP_ALL	GO:0035136~forelimb morphogenesis	0.0029
GOTERM_BP_ALL	GO:0035270~endocrine system development	0.0002
GOTERM_BP_ALL	GO:0042254~ribosome biogenesis and assembly	0.0000
GOTERM_BP_ALL	GO:0042471~ear morphogenesis	0.0042
GOTERM_MF_ALL	GO:0042578~phosphoric ester hydrolase activity	0.0000
GOTERM_BP_ALL	GO:0042592~homeostatic process	0.0148
GOTERM_BP_ALL	GO:0042692~muscle cell differentiation	0.0072
GOTERM_BP_ALL	GO:0043009~chordate embryonic development	0.0070
GOTERM_BP_ALL	GO:0043038~amino acid activation	0.0000
GOTERM_BP_ALL	GO:0043039~tRNA aminoacylation	0.0000
GOTERM_MF_ALL	GO:0043169~cation binding	0.0000
GOTERM_CC_ALL	GO:0043231~intracellular membrane-bound organelle	0.0000
GOTERM_CC_ALL	GO:0043232~intracellular non-membrane-bound organelle	0.0000
GOTERM_BP_ALL	GO:0043283~biopolymer metabolic process	0.0000
GOTERM_BP_ALL	GO:0043285~biopolymer catabolic process	0.0000
GOTERM_BP_ALL	GO:0043405~regulation of MAP kinase activity	0.0007
GOTERM_BP_ALL	GO:0043406~positive regulation of MAP kinase activity	0.0060
GOTERM_BP_ALL	GO:0043412~biopolymer modification	0.0000
GOTERM_BP_ALL	GO:0043413~biopolymer glycosylation	0.0001
GOTERM_BP_ALL	GO:0043549~regulation of kinase activity	0.0095
GOTERM_MF_ALL	GO:0043565~sequence-specific DNA binding	0.0000
GOTERM_MF_ALL	GO:0043566~structure-specific DNA binding	0.0117
GOTERM_BP_ALL	GO:0043583~ear development	0.0087
GOTERM_BP_ALL	GO:0043632~modification-dependent macromolecule catabolic process	0.0000
GOTERM_BP_ALL	GO:0043687~post-translational protein modification	0.0000
GOTERM_BP_ALL	GO:0044248~cellular catabolic process	0.0000
GOTERM_BP_ALL	GO:0044249~cellular biosynthetic process	0.0000
GOTERM_BP_ALL	GO:0044257~cellular protein catabolic process	0.0000
GOTERM_BP_ALL	GO:0044260~cellular macromolecule metabolic process	0.0000
GOTERM_BP_ALL	GO:0044265~cellular macromolecule catabolic process	0.0000
GOTERM_BP_ALL	GO:0044267~cellular protein metabolic process	0.0000

Category	Term	p-value
GOTERM_CC_ALL	GO:0044428~nuclear part	0.0000
GOTERM_CC_ALL	GO:0044429~mitochondrial part	0.0000
GOTERM_CC_ALL	GO:0044430~cytoskeletal part	0.0000
GOTERM_CC_ALL	GO:0044431~Golgi apparatus part	0.0007
GOTERM_CC_ALL	GO:0044444~cytoplasmic part	0.0000
GOTERM_CC_ALL	GO:0044451~nucleoplasm part	0.0000
GOTERM_CC_ALL	GO:0044459~plasma membrane part	0.0000
GOTERM_BP_ALL	GO:0045005~maintenance of fidelity during DNA-dependent DNA replication	0.0036
GOTERM_BP_ALL	GO:0045045~secretory pathway	0.0000
GOTERM_BP_ALL	GO:0045449~regulation of transcription	0.0000
GOTERM_BP_ALL	GO:0045595~regulation of cell differentiation	0.0030
GOTERM_BP_ALL	GO:0045859~regulation of protein kinase activity	0.0085
GOTERM_BP_ALL	GO:0045892~negative regulation of transcription, DNA-dependent	0.0000
GOTERM_BP_ALL	GO:0045893~positive regulation of transcription, DNA-dependent	0.0000
GOTERM_BP_ALL	GO:0045934~negative regulation of nucleobase, nucleoside, nucleotide and nucleic acid metabolic process	0.0000
GOTERM_BP_ALL	GO:0045935~positive regulation of nucleobase, nucleoside, nucleotide and nucleic acid metabolic process	0.0000
GOTERM_BP_ALL	GO:0045941~positive regulation of transcription	0.0000
GOTERM_BP_ALL	GO:0045944~positive regulation of transcription from RNA polymerase II promoter	0.0002
GOTERM_BP_ALL	GO:0046578~regulation of Ras protein signal transduction	0.0000
GOTERM_MF_ALL	GO:0046872~metal ion binding	0.0000
GOTERM_MF_ALL	GO:0046873~metal ion transmembrane transporter activity	0.0000
GOTERM_BP_ALL	GO:0046907~intracellular transport	0.0000
GOTERM_MF_ALL	GO:0046914~transition metal ion binding	0.0000
GOTERM_MF_ALL	GO:0046915~transition metal ion transmembrane transporter activity	0.0142
GOTERM_MF_ALL	GO:0046943~carboxylic acid transmembrane transporter activity	0.0038
GOTERM_MF_ALL	GO:0046983~protein dimerization activity	0.0128
GOTERM_BP_ALL	GO:0048193~Golgi vesicle transport	0.0000
GOTERM_BP_ALL	GO:0048489~synaptic vesicle transport	0.0058
GOTERM_BP_ALL	GO:0048513~organ development	0.0000
GOTERM_BP_ALL	GO:0048518~positive regulation of biological process	0.0000
GOTERM_BP_ALL	GO:0048519~negative regulation of biological process	0.0000
GOTERM_BP_ALL	GO:0048522~positive regulation of cellular process	0.0000
GOTERM_BP_ALL	GO:0048523~negative regulation of cellular process	0.0000
GOTERM_BP_ALL	GO:0048598~embryonic morphogenesis	0.0000
GOTERM_BP_ALL	GO:0048731~system development	0.0000
GOTERM_BP_ALL	GO:0048732~gland development	0.0000

Category	Term	p-value
GOTERM_BP_ALL	GO:0048878~chemical homeostasis	0.0045
GOTERM_BP_ALL	GO:0050801~ion homeostasis	0.0026
GOTERM_BP_ALL	GO:0051056~regulation of small GTPase mediated signal transduction	0.0000
GOTERM_BP_ALL	GO:0051338~regulation of transferase activity	0.0104
GOTERM_BP_ALL	GO:0051603~proteolysis involved in cellular protein catabolic process	0.0000
GOTERM_BP_ALL	GO:0051726~regulation of cell cycle	0.0004
GOTERM_BP_ALL	GO:0065003~macromolecular complex assembly	0.0001
SP_PIR_KEYWORDS	golgi apparatus	0.0000
SP_PIR_KEYWORDS	g-protein coupled receptor	0.0144
SP_PIR_KEYWORDS	GTP-binding	0.0000
SP_PIR_KEYWORDS	guanine-nucleotide releasing factor	0.0001
SP_PIR_KEYWORDS	Homeobox	0.0000
SP_PIR_KEYWORDS	hydrolase	0.0000
SP_PIR_KEYWORDS	initiation factor	0.0000
SP_PIR_KEYWORDS	ion transport	0.0000
SP_PIR_KEYWORDS	Ionic channel	0.0000
INTERPRO	IPR000047:Helix-turn-helix motif, lambda-like repressor	0.0004
INTERPRO	IPR000152:Aspartic acid and asparagine hydroxylation site	0.0000
INTERPRO	IPR000203:GPS	0.0009
INTERPRO	IPR000210:BTB/POZ-like	0.0005
INTERPRO	IPR000215:Protease inhibitor I4, serpin	0.0117
INTERPRO	IPR000219:DH	0.0001
INTERPRO	IPR000222:Protein phosphatase 2C, manganese/magnesium aspartate binding site	0.0031
INTERPRO	IPR000242:Protein-tyrosine phosphatase, receptor/non-receptor type	0.0104
INTERPRO	IPR000387:Protein-tyrosine phosphatase, Tyr-specific/dual-specificity type	0.0001
INTERPRO	IPR000499:Endothelin receptor	0.0132
INTERPRO	IPR000504:RNA recognition motif, RNP-1	0.0000
INTERPRO	IPR000608:Ubiquitin-conjugating enzyme, E2	0.0015
INTERPRO	IPR000719:Protein kinase, core	0.0000
INTERPRO	IPR000742:EGF-like, type 3	0.0000
INTERPRO	IPR000795:Protein synthesis factor, GTP-binding	0.0001
INTERPRO	IPR000832:GPCR, family 2, secretin-like	0.0000
INTERPRO	IPR000961:Protein kinase, C-terminal	0.0000
INTERPRO	IPR001125:Recoverin	0.0000
INTERPRO	IPR001245:Tyrosine protein kinase	0.0000
INTERPRO	IPR001254:Peptidase S1 and S6, chymotrypsin/Hap	0.0009
INTERPRO	IPR001278:Arginyl-tRNA synthetase, class Ic	0.0008
INTERPRO	IPR001314:Peptidase S1A, chymotrypsin	0.0008
INTERPRO	IPR001356:Homeobox	0.0000
INTERPRO	IPR001394:Peptidase C19, ubiquitin carboxyl-terminal hydrolase 2	0.0000
INTERPRO	IPR001412:Aminoacyl-tRNA synthetase, class I	0.0001
INTERPRO	IPR001440:Tetratricopeptide TPR-1	0.0000
INTERPRO	IPR001660:Sterile alpha motif SAM	0.0139

Category	Term	p-value
INTERPRO	IPR001680:WD40 repeat	0.0000
INTERPRO	IPR001806:Ras GTPase	0.0000
INTERPRO	IPR001810:Cyclin-like F-box	0.0000
INTERPRO	IPR001827:Homeobox protein, antennapedia type	0.0000
INTERPRO	IPR001841:Zinc finger, RING-type	0.0000
INTERPRO	IPR001878:Zinc finger, CCHC-type	0.0121
INTERPRO	IPR001881:EGF-like calcium-binding	0.0000
INTERPRO	IPR001909:KRAB box	0.0067
INTERPRO	IPR001932:Protein phosphatase 2C-related	0.0045
INTERPRO	IPR002048:Calcium-binding EF-hand	0.0000
INTERPRO	IPR002126:Cadherin	0.0000
INTERPRO	IPR002290:Serine/threonine protein kinase	0.0000
INTERPRO	IPR002343:Paraneoplastic encephalomyelitis antigen	0.0035
INTERPRO	IPR002350:Proteinase inhibitor II, Kazal	0.0071
INTERPRO	IPR002735:Translation initiation factor IF2/IF5	0.0005
INTERPRO	IPR002893:Zinc finger, MYND-type	0.0040
INTERPRO	IPR002917:GTP-binding protein, HSR1-related	0.0000
INTERPRO	IPR003131:Potassium channel, voltage dependent, Kv, tetramerisation	0.0000
INTERPRO	IPR003307:eIF4-gamma/eIF5/eIF2-epsilon	0.0017
INTERPRO	IPR003578:Ras small GTPase, Rho type	0.0003
INTERPRO	IPR003598:Immunoglobulin subtype 2	0.0046
INTERPRO	IPR003894:TAFH/NHR1	0.0129
INTERPRO	IPR003961:Fibronectin, type III	0.0068
INTERPRO	IPR004160:Translation elongation factor EFTu/EF1A, C-terminal	0.0094
INTERPRO	IPR004273:Dynein heavy chain	0.0077
INTERPRO	IPR004882:LUC7 related	0.0050
INTERPRO	IPR005225:Small GTP-binding protein domain	0.0000
INTERPRO	IPR005289:GTP-binding	0.0059
INTERPRO	IPR005821:Ion transport	0.0000
INTERPRO	IPR006073:GTP1/OBG	0.0129
INTERPRO	IPR006209:EGF-like	0.0000
INTERPRO	IPR006210:EGF	0.0000
INTERPRO	IPR006630:RNA-binding protein Lupus La	0.0018
INTERPRO	IPR006985:Receptor activity modifying protein	0.0001
INTERPRO	IPR007087:Zinc finger, C2H2-type	0.0000
INTERPRO	IPR007484:Peptidase M28	0.0011
INTERPRO	IPR008266:Tyrosine protein kinase, active site	0.0000
INTERPRO	IPR008271:Serine/threonine protein kinase, active site	0.0000
INTERPRO	IPR008636:HOOK	0.0018
INTERPRO	IPR008909:DALR anticodon binding	0.0012
INTERPRO	IPR008957:Fibronectin, type III-like fold	0.0069
INTERPRO	IPR009071:High mobility group box, HMG	0.0141
INTERPRO	IPR010526:Sodium ion transport-associated	0.0106
INTERPRO	IPR011333:BTB/POZ fold	0.0110
INTERPRO	IPR011704:ATPase associated with various cellular activities, AAA-5	0.0071
INTERPRO	IPR011990:Tetratricopeptide-like helical	0.0000

Category	Term	p-value
INTERPRO	IPR011991:Winged helix repressor DNA-binding	0.0125
INTERPRO	IPR011992:EF-Hand type	0.0000
INTERPRO	IPR012287:Homeodomain-related	0.0000
INTERPRO	IPR012677:Nucleotide-binding, alpha-beta plait	0.0000
INTERPRO	IPR013026:Tetratricopeptide region	0.0000
INTERPRO	IPR013032:EGF-like region	0.0000
INTERPRO	IPR013087:Zinc finger, C2H2-type/integrase, DNA-binding	0.0000
INTERPRO	IPR013088:Zinc finger, NHR/GATA-type	0.0123
INTERPRO	IPR013091:EGF calcium-binding	0.0000
INTERPRO	IPR013105:Tetratricopeptide TPR2	0.0000
INTERPRO	IPR013164:Cadherin, N-terminal	0.0104
INTERPRO	IPR013289:Eight-Twenty-One	0.0086
INTERPRO	IPR013594:Dynein heavy chain, N-terminal region 1	0.0041
INTERPRO	IPR013602:Dynein heavy chain, N-terminal region 2	0.0041
INTERPRO	IPR013753:Ras	0.0000
INTERPRO	IPR013761:Sterile alpha motif-type	0.0091
INTERPRO	IPR014045:Protein phosphatase 2C, N-terminal	0.0042
INTERPRO	IPR014729:Rossmann-like alpha/beta/alpha sandwich fold	0.0001
INTERPRO	IPR014896:NHR2-like	0.0086
INTERPRO	IPR015655:Protein phosphatase 2C	0.0038
INTERPRO	IPR015721:Rho GTP exchange factor	0.0026
INTERPRO	IPR015880:Zinc finger, C2H2-like	0.0001
SP_PIR_KEYWORDS	iron	0.0107
SP_PIR_KEYWORDS	Iron transport	0.0001
SP_PIR_KEYWORDS	kinase	0.0000
SP_PIR_KEYWORDS	ligase	0.0001
UP_SEQ_FEATURE	lipid moiety-binding region:S-geranylgeranyl cysteine	0.0060
UP_SEQ_FEATURE	lipid moiety-binding region:S-palmitoyl cysteine	0.0094
SP_PIR_KEYWORDS	lipoprotein	0.0000
BIOCARTA	m_eif2Pathway:Regulation of eIF2	0.0083
BIOCARTA	m_eifPathway:Eukaryotic protein translation	0.0058
SP_PIR_KEYWORDS	magnesium	0.0001
SP_PIR_KEYWORDS	membrane	0.0000
SP_PIR_KEYWORDS	metal-binding	0.0000
SP_PIR_KEYWORDS	Methylation	0.0000
SP_PIR_KEYWORDS	microtubule	0.0000
SP_PIR_KEYWORDS	Mitochondrion	0.0005
KEGG_PATHWAY	mmu00510:N-Glycan biosynthesis	0.0008
KEGG_PATHWAY	mmu00970:Aminoacyl-tRNA biosynthesis	0.0002
KEGG_PATHWAY	mmu01030:Glycan structures - biosynthesis 1	0.0000
KEGG_PATHWAY	mmu04080:Neuroactive ligand-receptor interaction	0.0008
KEGG_PATHWAY	mmu04120:Ubiquitin mediated proteolysis	0.0030
KEGG_PATHWAY	mmu05221:Acute myeloid leukemia	0.0136
SP_PIR_KEYWORDS	motor protein	0.0004
SP_PIR_KEYWORDS	mrna processing	0.0000
SP_PIR_KEYWORDS	mrna splicing	0.0000

Category	Term	p-value
SP_PIR_KEYWORDS	Muscle protein	0.0001
UP_SEQ_FEATURE	mutagenesis site	0.0051
SP_PIR_KEYWORDS	Myosin	0.0000
UP_SEQ_FEATURE	nucleotide phosphate-binding region:ATP	0.0000
UP_SEQ_FEATURE	nucleotide phosphate-binding region:GTP	0.0000
SP_PIR_KEYWORDS	nucleotide-binding	0.0000
SP_PIR_KEYWORDS	nucleus	0.0000
SP_PIR_KEYWORDS	Palmitate	0.0149
SP_PIR_KEYWORDS	phosphoprotein	0.0003
SP_PIR_KEYWORDS	phosphotransferase	0.0002
PIR_SUPERFAMILY	PIRSF000613:RAC serine/threonine-protein kinase	0.0089
PIR_SUPERFAMILY	PIRSF000615:tyrosine-protein kinase, CSF-1/PDGF receptor type	0.0148
PIR_SUPERFAMILY	PIRSF001543:arginine-tRNA ligase	0.0011
PIR_SUPERFAMILY	PIRSF001626:pancreatic secretory trypsin inhibitor	0.0012
PIR_SUPERFAMILY	PIRSF002308:dynein heavy chain, ciliary	0.0049
PIR_SUPERFAMILY	PIRSF002350:calmodulin	0.0000
PIR_SUPERFAMILY	PIRSF002419:CD9 antigen	0.0049
PIR_SUPERFAMILY	PIRSF002437:ionotropic glutamate receptor, AMPA/kainate types	0.0108
PIR_SUPERFAMILY	PIRSF015841:MAX interacting protein	0.0108
PIR_SUPERFAMILY	PIRSF025373:receptor activity-modifying protein	0.0133
PIR_SUPERFAMILY	PIRSF028830:Luc7/Luc7-like proteins	0.0024
PIR_SUPERFAMILY	PIRSF500423:Luc7-like protein	0.0016
SP_PIR_KEYWORDS	Postsynaptic cell membrane	0.0041
SP_PIR_KEYWORDS	potassium	0.0002
SP_PIR_KEYWORDS	potassium transport	0.0001
SP_PIR_KEYWORDS	prenylation	0.0000
SP_PIR_KEYWORDS	protease	0.0000
SP_PIR_KEYWORDS	protease inhibitor	0.0001
SP_PIR_KEYWORDS	protein biosynthesis	0.0000
SP_PIR_KEYWORDS	protein phosphatase	0.0002
SP_PIR_KEYWORDS	protein transport	0.0017
SP_PIR_KEYWORDS	receptor	0.0000
UP_SEQ_FEATURE	region of interest:Glutamate binding	0.0073
UP_SEQ_FEATURE	region of interest:Interaction with microtubules	0.0029
UP_SEQ_FEATURE	repeat:LRR 1	0.0052
UP_SEQ_FEATURE	repeat:LRR 2	0.0052
UP_SEQ_FEATURE	repeat:LRR 3	0.0047
UP_SEQ_FEATURE	repeat:LRR 4	0.0038
UP_SEQ_FEATURE	repeat:TNFR-Cys 3	0.0138
UP_SEQ_FEATURE	repeat:WD 1	0.0000
UP_SEQ_FEATURE	repeat:WD 2	0.0000
UP_SEQ_FEATURE	repeat:WD 3	0.0000
UP_SEQ_FEATURE	repeat:WD 4	0.0000
UP_SEQ_FEATURE	repeat:WD 5	0.0000
UP_SEQ_FEATURE	repeat:WD 6	0.0000
SP_PIR_KEYWORDS	repressor	0.0000
SP_PIR_KEYWORDS	ribonucleoprotein	0.0001
SP_PIR_KEYWORDS	ribosomal protein	0.0000
SP_PIR_KEYWORDS	ribosome biogenesis	0.0095

Category	Term	p-value
SP_PIR_KEYWORDS	rna-binding	0.0000
SP_PIR_KEYWORDS	rrna processing	0.0000
SP_PIR_KEYWORDS	Secreted	0.0000
SP_PIR_KEYWORDS	serine protease	0.0000
SP_PIR_KEYWORDS	Serine protease inhibitor	0.0001
SP_PIR_KEYWORDS	Serine/threonine-protein kinase	0.0000
SP_PIR_KEYWORDS	serine/threonine-specific protein kinase	0.0034
UP_SEQ_FEATURE	short sequence motif:[NKR]KIAxRE	0.0129
UP_SEQ_FEATURE	short sequence motif:Antp-type hexapeptide	0.0000
UP_SEQ_FEATURE	short sequence motif:Effector region	0.0000
UP_SEQ_FEATURE	short sequence motif:Selectivity filter	0.0008
SP_PIR_KEYWORDS	signal	0.0000
UP_SEQ_FEATURE	signal peptide	0.0000
COG_ONTOLOGY	Signal transduction mechanisms / Cytoskeleton / Cell division and chromosome partitioning / General function prediction only	0.0000
SP_PIR_KEYWORDS	signal-anchor	0.0000
UP_SEQ_FEATURE	site:Reactive bond	0.0039
SMART	SM00005:DEATH	0.0101
SMART	SM00020:Tryp_SPc	0.0007
SMART	SM00028:TPR	0.0000
SMART	SM00054:EFh	0.0000
SMART	SM00082:LRRCT	0.0068
SMART	SM00112:CA	0.0000
SMART	SM00129:KISc	0.0095
SMART	SM00133:S_TK_X	0.0000
SMART	SM00174:RHO	0.0001
SMART	SM00179:EGF_CA	0.0000
SMART	SM00181:EGF	0.0000
SMART	SM00184:RING	0.0000
SMART	SM00208:TNFR	0.0101
SMART	SM00212:UBCc	0.0027
SMART	SM00219:TyrKc	0.0000
SMART	SM00220:S_TKc	0.0000
SMART	SM00225:BTB	0.0006
SMART	SM00233:PH	0.0035
SMART	SM00256:FBOX	0.0000
SMART	SM00280:KAZAL	0.0138
SMART	SM00303:GPS	0.0003
SMART	SM00320:WD40	0.0000
SMART	SM00325:RhoGEF	0.0002
SMART	SM00331:PP2C_SIG	0.0084
SMART	SM00332:PP2Cc	0.0084
SMART	SM00343:ZnF_C2HC	0.0097
SMART	SM00355:ZnF_C2H2	0.0006
SMART	SM00360:RRM	0.0000
SMART	SM00389:HOX	0.0000
SMART	SM00408:IGc2	0.0012
SMART	SM00515:eIF5C	0.0023
SMART	SM00653:eIF2B_5	0.0007
SMART	SM00715:LA	0.0039

Category	Term	p-value
SP_PIR_KEYWORDS	sodium	0.0001
SP_PIR_KEYWORDS	sodium transport	0.0000
UP_SEQ_FEATURE	splice variant	0.0077
SP_PIR_KEYWORDS	spliceosome	0.0000
SP_PIR_KEYWORDS	Symport	0.0037
SP_PIR_KEYWORDS	synapse	0.0000
SP_PIR_KEYWORDS	thiol protease	0.0000
UP_SEQ_FEATURE	topological domain:Cytoplasmic	0.0000
UP_SEQ_FEATURE	topological domain:Cytoplasmic	0.0001
UP_SEQ_FEATURE	topological domain:Extracellular	0.0000
UP_SEQ_FEATURE	topological domain:Extracellular	0.0001
UP_SEQ_FEATURE	topological domain:Lumenal	0.0000
UP_SEQ_FEATURE	topological domain:Vesicular	0.0121
SP_PIR_KEYWORDS	TPR repeat	0.0000
SP_PIR_KEYWORDS	Transcription	0.0000
SP_PIR_KEYWORDS	Transcription regulation	0.0000
SP_PIR_KEYWORDS	transferase	0.0000
SP_PIR_KEYWORDS	transit peptide	0.0004
COG_ONTOLOGY	Translation, ribosomal structure and biogenesis	0.0022
SP_PIR_KEYWORDS	transmembrane	0.0000
SP_PIR_KEYWORDS	transmembrane protein	0.0001
UP_SEQ_FEATURE	transmembrane region	0.0000
SP_PIR_KEYWORDS	transport	0.0000
SP_PIR_KEYWORDS	tyrosine-protein kinase	0.0000
SP_PIR_KEYWORDS	tyrosine-specific protein kinase	0.0039
SP_PIR_KEYWORDS	Ubl conjugation pathway	0.0000
SP_PIR_KEYWORDS	voltage-gated channel	0.0000
SP_PIR_KEYWORDS	wd repeat	0.0000
SP_PIR_KEYWORDS	zinc	0.0000
SP_PIR_KEYWORDS	zinc finger	0.0004
UP_SEQ_FEATURE	zinc finger region:C2H2-type; atypical	0.0038
UP_SEQ_FEATURE	zinc finger region:MYND-type	0.0019
UP_SEQ_FEATURE	zinc finger region:RING-type	0.0003
SP_PIR_KEYWORDS	zinc-finger	0.0000
SP_PIR_KEYWORDS	Zymogen	0.0018

**APPENDIX E. ENRICHED ANNOTATION TERMS RELATED TO
INFLAMMATION FROM GENES SIGNIFICANTLY CHANGED IN LA1
KRAS MOUSE LUNGS ONE YEAR AFTER FRACTIONATED 1.0 GY
DOSE OF ⁵⁶FE- PARTICLE IRRADIATION.**

Category	Term	p-value
SP_PIR_KEYWORDS	apoptosis	0.0000
SP_PIR_KEYWORDS	Developmental protein	0.0000
UP_SEQ_FEATURE	domain:Death	0.0058
UP_SEQ_FEATURE	domain:Ig-like C2-type	0.0479
GOTERM_BP_ALL	GO:0000074~regulation of progression through cell cycle	0.0002
GOTERM_BP_ALL	GO:0001501~skeletal development	0.0093
GOTERM_BP_ALL	GO:0001568~blood vessel development	0.0173
GOTERM_BP_ALL	GO:0001655~urogenital system development	0.0485
GOTERM_BP_ALL	GO:0001775~cell activation	0.0000
GOTERM_BP_ALL	GO:0001816~cytokine production	0.0002
GOTERM_BP_ALL	GO:0001822~kidney development	0.0411
GOTERM_BP_ALL	GO:0001944~vasculature development	0.0181
GOTERM_BP_ALL	GO:0001974~blood vessel remodeling	0.0022
GOTERM_BP_ALL	GO:0002200~somatic diversification of immune receptors	0.0098
GOTERM_BP_ALL	GO:0002252~immune effector process	0.0000
GOTERM_BP_ALL	GO:0002376~immune system process	0.0000
GOTERM_BP_ALL	GO:0002377~immunoglobulin production	0.0007
GOTERM_BP_ALL	GO:0002440~production of molecular mediator of immune response	0.0008
GOTERM_BP_ALL	GO:0002520~immune system development	0.0000
GOTERM_BP_ALL	GO:0002521~leukocyte differentiation	0.0005
GOTERM_BP_ALL	GO:0002562~somatic diversification of immune receptors via germline recombination within a single locus	0.0077
GOTERM_BP_ALL	GO:0002682~regulation of immune system process	0.0023
GOTERM_BP_ALL	GO:0002684~positive regulation of immune system process	0.0126
GOTERM_CC_ALL	GO:0005634~nucleus	0.0380
GOTERM_BP_ALL	GO:0006606~protein import into nucleus	0.0342
GOTERM_BP_ALL	GO:0006915~apoptosis	0.0000
GOTERM_BP_ALL	GO:0006916~anti-apoptosis	0.0000
GOTERM_BP_ALL	GO:0006917~induction of apoptosis	0.0000
GOTERM_BP_ALL	GO:0006950~response to stress	0.0010
GOTERM_BP_ALL	GO:0006952~defense response	0.0405
GOTERM_BP_ALL	GO:0006954~inflammatory response	0.0178
GOTERM_BP_ALL	GO:0006955~immune response	0.0000
GOTERM_BP_ALL	GO:0007049~cell cycle	0.0156
GOTERM_BP_ALL	GO:0007242~intracellular signaling cascade	0.0060
GOTERM_BP_ALL	GO:0007243~protein kinase cascade	0.0003
GOTERM_BP_ALL	GO:0007249~I-kappaB kinase/NF-kappaB cascade	0.0035

Category	Term	p-value
GOTERM_BP_ALL	GO:0007275~multicellular organismal development	0.0000
GOTERM_BP_ALL	GO:0007389~pattern specification process	0.0211
GOTERM_BP_ALL	GO:0007507~heart development	0.0001
GOTERM_BP_ALL	GO:0007517~muscle development	0.0482
GOTERM_BP_ALL	GO:0008104~protein localization	0.0255
GOTERM_BP_ALL	GO:0008219~cell death	0.0000
GOTERM_BP_ALL	GO:0008283~cell proliferation	0.0000
GOTERM_BP_ALL	GO:0008284~positive regulation of cell proliferation	0.0000
GOTERM_BP_ALL	GO:0009306~protein secretion	0.0000
GOTERM_BP_ALL	GO:0009605~response to external stimulus	0.0218
GOTERM_BP_ALL	GO:0009611~response to wounding	0.0130
GOTERM_BP_ALL	GO:0009653~anatomical structure morphogenesis	0.0143
GOTERM_BP_ALL	GO:0009790~embryonic development	0.0039
GOTERM_BP_ALL	GO:0009792~embryonic development ending in birth or egg hatching	0.0173
GOTERM_BP_ALL	GO:0009887~organ morphogenesis	0.0085
GOTERM_BP_ALL	GO:0009893~positive regulation of metabolic process	0.0488
GOTERM_BP_ALL	GO:0009967~positive regulation of signal transduction	0.0114
GOTERM_BP_ALL	GO:0012501~programmed cell death	0.0000
GOTERM_BP_ALL	GO:0012502~induction of programmed cell death	0.0000
GOTERM_BP_ALL	GO:0016064~immunoglobulin mediated immune response	0.0432
GOTERM_BP_ALL	GO:0016265~death	0.0000
GOTERM_BP_ALL	GO:0016444~somatic cell DNA recombination	0.0077
GOTERM_BP_ALL	GO:0016445~somatic diversification of immunoglobulins	0.0087
GOTERM_BP_ALL	GO:0016447~somatic recombination of immunoglobulin gene segments	0.0067
GOTERM_BP_ALL	GO:0017038~protein import	0.0485
GOTERM_BP_ALL	GO:0019724~B cell mediated immunity	0.0453
GOTERM_BP_ALL	GO:0022402~cell cycle process	0.0045
GOTERM_BP_ALL	GO:0030097~hemopoiesis	0.0000
GOTERM_BP_ALL	GO:0030098~lymphocyte differentiation	0.0117
GOTERM_BP_ALL	GO:0030099~myeloid cell differentiation	0.0000
GOTERM_BP_ALL	GO:0030154~cell differentiation	0.0000
GOTERM_BP_ALL	GO:0030217~T cell differentiation	0.0371
GOTERM_BP_ALL	GO:0030218~erythrocyte differentiation	0.0000
GOTERM_BP_ALL	GO:0030326~embryonic limb morphogenesis	0.0333
GOTERM_BP_ALL	GO:0030888~regulation of B cell proliferation	0.0042
GOTERM_BP_ALL	GO:0031325~positive regulation of cellular metabolic process	0.0395
GOTERM_CC_ALL	GO:0031967~organelle envelope	0.0228
GOTERM_CC_ALL	GO:0031975~envelope	0.0233
GOTERM_BP_ALL	GO:0032501~multicellular organismal process	0.0000
GOTERM_BP_ALL	GO:0032502~developmental process	0.0000
GOTERM_BP_ALL	GO:0032940~secretion by cell	0.0089
GOTERM_BP_ALL	GO:0032943~mononuclear cell proliferation	0.0000

Category	Term	p-value
GOTERM_BP_ALL	GO:0032944~regulation of mononuclear cell proliferation	0.0001
GOTERM_BP_ALL	GO:0032946~positive regulation of mononuclear cell proliferation	0.0007
GOTERM_BP_ALL	GO:0033036~macromolecule localization	0.0312
GOTERM_BP_ALL	GO:0035107~appendage morphogenesis	0.0432
GOTERM_BP_ALL	GO:0035108~limb morphogenesis	0.0432
GOTERM_BP_ALL	GO:0035113~embryonic appendage morphogenesis	0.0333
GOTERM_BP_ALL	GO:0035136~forelimb morphogenesis	0.0019
GOTERM_BP_ALL	GO:0035295~tube development	0.0019
GOTERM_BP_ALL	GO:0042098~T cell proliferation	0.0305
GOTERM_BP_ALL	GO:0042100~B cell proliferation	0.0000
GOTERM_BP_ALL	GO:0042110~T cell activation	0.0004
GOTERM_BP_ALL	GO:0042113~B cell activation	0.0008
GOTERM_BP_ALL	GO:0042127~regulation of cell proliferation	0.0000
GOTERM_BP_ALL	GO:0042129~regulation of T cell proliferation	0.0182
GOTERM_BP_ALL	GO:0042981~regulation of apoptosis	0.0000
GOTERM_BP_ALL	GO:0043009~chordate embryonic development	0.0166
GOTERM_BP_ALL	GO:0043065~positive regulation of apoptosis	0.0000
GOTERM_BP_ALL	GO:0043066~negative regulation of apoptosis	0.0000
GOTERM_BP_ALL	GO:0043067~regulation of programmed cell death	0.0000
GOTERM_BP_ALL	GO:0043068~positive regulation of programmed cell death	0.0000
GOTERM_BP_ALL	GO:0043069~negative regulation of programmed cell death	0.0000
GOTERM_BP_ALL	GO:0043122~regulation of I-kappaB kinase/NF-kappaB cascade	0.0161
GOTERM_BP_ALL	GO:0043123~positive regulation of I-kappaB kinase/NF-kappaB cascade	0.0134
GOTERM_MF_ALL	GO:0043565~sequence-specific DNA binding	0.0318
GOTERM_BP_ALL	GO:0045184~establishment of protein localization	0.0168
GOTERM_BP_ALL	GO:0045321~leukocyte activation	0.0000
GOTERM_BP_ALL	GO:0045595~regulation of cell differentiation	0.0012
GOTERM_BP_ALL	GO:0045637~regulation of myeloid cell differentiation	0.0147
GOTERM_BP_ALL	GO:0045786~negative regulation of progression through cell cycle	0.0032
GOTERM_BP_ALL	GO:0046649~lymphocyte activation	0.0000
GOTERM_BP_ALL	GO:0046651~lymphocyte proliferation	0.0000
GOTERM_BP_ALL	GO:0046903~secretion	0.0041
GOTERM_BP_ALL	GO:0048305~immunoglobulin secretion	0.0010
GOTERM_BP_ALL	GO:0048468~cell development	0.0000
GOTERM_BP_ALL	GO:0048513~organ development	0.0000
GOTERM_BP_ALL	GO:0048518~positive regulation of biological process	0.0000
GOTERM_BP_ALL	GO:0048519~negative regulation of biological process	0.0000
GOTERM_BP_ALL	GO:0048522~positive regulation of cellular process	0.0000
GOTERM_BP_ALL	GO:0048523~negative regulation of cellular process	0.0000

Category	Term	p-value
GOTERM_BP_ALL	GO:0048534~hemopoietic or lymphoid organ development	0.0000
GOTERM_BP_ALL	GO:0048598~embryonic morphogenesis	0.0107
GOTERM_BP_ALL	GO:0048731~system development	0.0000
GOTERM_BP_ALL	GO:0048732~gland development	0.0044
GOTERM_BP_ALL	GO:0048736~appendage development	0.0464
GOTERM_BP_ALL	GO:0048741~skeletal muscle fiber development	0.0391
GOTERM_BP_ALL	GO:0048747~muscle fiber development	0.0391
GOTERM_BP_ALL	GO:0048771~tissue remodeling	0.0170
GOTERM_BP_ALL	GO:0048856~anatomical structure development	0.0000
GOTERM_BP_ALL	GO:0048869~cellular developmental process	0.0000
GOTERM_BP_ALL	GO:0050670~regulation of lymphocyte proliferation	0.0001
GOTERM_BP_ALL	GO:0050671~positive regulation of lymphocyte proliferation	0.0007
GOTERM_BP_ALL	GO:0050708~regulation of protein secretion	0.0001
GOTERM_BP_ALL	GO:0050776~regulation of immune response	0.0022
GOTERM_BP_ALL	GO:0050778~positive regulation of immune response	0.0120
GOTERM_BP_ALL	GO:0050789~regulation of biological process	0.0000
GOTERM_BP_ALL	GO:0050793~regulation of developmental process	0.0020
GOTERM_BP_ALL	GO:0050794~regulation of cellular process	0.0000
GOTERM_BP_ALL	GO:0050863~regulation of T cell activation	0.0004
GOTERM_BP_ALL	GO:0050864~regulation of B cell activation	0.0008
GOTERM_BP_ALL	GO:0050865~regulation of cell activation	0.0000
GOTERM_BP_ALL	GO:0050870~positive regulation of T cell activation	0.0205
GOTERM_BP_ALL	GO:0050871~positive regulation of B cell activation	0.0072
GOTERM_BP_ALL	GO:0051046~regulation of secretion	0.0029
GOTERM_BP_ALL	GO:0051170~nuclear import	0.0362
GOTERM_BP_ALL	GO:0051239~regulation of multicellular organismal process	0.0000
GOTERM_BP_ALL	GO:0051240~positive regulation of multicellular organismal process	0.0205
GOTERM_BP_ALL	GO:0051249~regulation of lymphocyte activation	0.0000
GOTERM_BP_ALL	GO:0051251~positive regulation of lymphocyte activation	0.0002
GOTERM_BP_ALL	GO:0051641~cellular localization	0.0465
GOTERM_BP_ALL	GO:0051726~regulation of cell cycle	0.0002
GOTERM_BP_ALL	GO:0060173~limb development	0.0464
GOTERM_BP_ALL	GO:0065007~biological regulation	0.0000
INTERPRO	IPR000488:Death	0.0002
INTERPRO	IPR001368:TNFR/CD27/30/40/95 cysteine-rich region	0.0000
INTERPRO	IPR008063:Fas receptor	0.0001
BIOCARTA	m_asbcellPathway:Antigen Dependent B Cell Activation	0.0022
BIOCARTA	m_bbcellPathway:Bystander B Cell Activation	0.0007
BIOCARTA	m_th1th2Pathway:Th1/Th2 Differentiation	0.0072
KEGG_PATHWAY	mmu04060:Cytokine-cytokine receptor interaction	0.0000

Category	Term	<i>p</i>-value
KEGG_PATHWAY	mmu04620:Toll-like receptor signaling pathway	0.0042
UP_SEQ_FEATURE	repeat:TNFR-Cys 1	0.0000
UP_SEQ_FEATURE	repeat:TNFR-Cys 2	0.0000
UP_SEQ_FEATURE	repeat:TNFR-Cys 3	0.0000
UP_SEQ_FEATURE	repeat:TNFR-Cys 4	0.0000
SMART	SM00005:DEATH	0.0005
SMART	SM00208:TNFR	0.0000
SP_PIR_KEYWORDS	transmembrane protein	0.0138

BIBLIOGRAPHY

ACS (2009). What Are the Key Statistics About Lung Cancer? (American Cancer Society).

Adamson, I.Y., and Bowden, D.H. (1974). The type 2 cell as progenitor of alveolar epithelial regeneration. A cytodynamic study in mice after exposure to oxygen. *Lab Invest* 30, 35-42.

Adhikary, S., and Eilers, M. (2005). Transcriptional regulation and transformation by Myc proteins. *Nat Rev Mol Cell Biol* 6, 635-645.

Affolter, M., Bellusci, S., Itoh, N., Shilo, B., Thiery, J.P., and Werb, Z. (2003). Tube or not tube: remodeling epithelial tissues by branching morphogenesis. *Dev Cell* 4, 11-18.

Al-Hajj, M., Wicha, M.S., Benito-Hernandez, A., Morrison, S.J., and Clarke, M.F. (2003). Prospective identification of tumorigenic breast cancer cells. *Proc Natl Acad Sci U S A* 100, 3983-3988.

Alexandrow, M.G., Kawabata, M., Aakre, M., and Moses, H.L. (1995). Overexpression of the c-Myc oncoprotein blocks the growth-inhibitory response but is required for the mitogenic effects of transforming growth factor beta 1. *Proc Natl Acad Sci U S A* 92, 3239-3243.

Alison, M.R., Vig, P., Russo, F., Bigger, B.W., Amofah, E., Themis, M., and Forbes, S. (2004). Hepatic stem cells: from inside and outside the liver? *Cell Prolif* 37, 1-21.

Aso, Y., Yoneda, K., and Kikkawa, Y. (1976). Morphologic and biochemical study of pulmonary changes induced by bleomycin in mice. *Lab Invest* 35, 558-568.

Barth, P.J., and Muller, B. (1999). Effects of nitrogen dioxide exposure on Clara cell proliferation and morphology. *Pathol Res Pract* 195, 487-493.

Bellantuono, I. (2004). Haemopoietic stem cells. *Int J Biochem Cell Biol* 36, 607-620.

Bellusci, S., Furuta, Y., Rush, M.G., Henderson, R., Winnier, G., and Hogan, B.L. (1997a). Involvement of Sonic hedgehog (Shh) in mouse embryonic lung growth and morphogenesis. *Development* 124, 53-63.

Bellusci, S., Grindley, J., Emoto, H., Itoh, N., and Hogan, B.L. (1997b). Fibroblast growth factor 10 (FGF10) and branching morphogenesis in the embryonic mouse lung. *Development* 124, 4867-4878.

Besnard, V., Wert, S.E., Hull, W.M., and Whitsett, J.A. (2004). Immunohistochemical localization of Foxa1 and Foxa2 in mouse embryos and adult tissues. *Gene Expr Patterns* 5, 193-208.

Bodnar, A.G., Ouellette, M., Frolkis, M., Holt, S.E., Chiu, C.P., Morin, G.B., Harley, C.B., Shay, J.W., Lichtsteiner, S., and Wright, W.E. (1998). Extension of life-span by introduction of telomerase into normal human cells. *Science* 279, 349-352.

Bohinski, R.J., Di Lauro, R., and Whitsett, J.A. (1994). The lung-specific surfactant protein B gene promoter is a target for thyroid transcription factor 1 and hepatocyte nuclear factor 3, indicating common factors for organ-specific gene expression along the foregut axis. *Mol Cell Biol* 14, 5671-5681.

Borthwick, D.W., Shahbazian, M., Krantz, Q.T., Dorin, J.R., and Randell, S.H. (2001). Evidence for stem-cell niches in the tracheal epithelium. *Am J Respir Cell Mol Biol* 24, 662-670.

Brooks, A., Bao, S., Rithidech, K., Couch, L.A., and Braby, L.A. (2001). Relative effectiveness of HZE iron-56 particles for the induction of cytogenetic damage in vivo. *Radiat Res* 155, 353-359.

Bruno, M.D., Bohinski, R.J., Huelsman, K.M., Whitsett, J.A., and Korfhagen, T.R. (1995). Lung cell-specific expression of the murine surfactant protein A (SP-A) gene is mediated by interactions between the SP-A promoter and thyroid transcription factor-1. *J Biol Chem* 270, 6531-6536.

Buckpitt, A., Buonarati, M., Avey, L.B., Chang, A.M., Morin, D., and Plopper, C.G. (1992). Relationship of cytochrome P450 activity to Clara cell cytotoxicity. II. Comparison of stereoselectivity of naphthalene epoxidation in lung and nasal mucosa of mouse, hamster, rat and rhesus monkey. *J Pharmacol Exp Ther* 261, 364-372.

- Burri, P.H. (2006). Structural aspects of postnatal lung development - alveolar formation and growth. *Biol Neonate* 89, 313-322.
- Cardoso, W.V., and Lu, J. (2006). Regulation of early lung morphogenesis: questions, facts and controversies. *Development* 133, 1611-1624.
- Chatterjee, A., and Schaefer, H.J. (1976). Microdosimetric structure of heavy ion tracks in tissue. *Radiat Environ Biophys* 13, 215-227.
- Coppens, J.T., Van Winkle, L.S., Pinkerton, K., and Plopper, C.G. (2007). Distribution of Clara cell secretory protein expression in the tracheobronchial airways of rhesus monkeys. *Am J Physiol Lung Cell Mol Physiol* 292, L1155-1162.
- Cordenonsi, M., Montagner, M., Adorno, M., Zacchigna, L., Martello, G., Mamidi, A., Soligo, S., Dupont, S., and Piccolo, S. (2007). Integration of TGF-beta and Ras/MAPK signaling through p53 phosphorylation. *Science* 315, 840-843.
- Crystal, R.G., Randell, S.H., Engelhardt, J.F., Voynow, J., and Sunday, M.E. (2008). Airway epithelial cells: current concepts and challenges. *Proc Am Thorac Soc* 5, 772-777.
- Curtis, S.B., and Letaw, J.R. (1989). Galactic cosmic rays and cell-hit frequencies outside the magnetosphere. *Adv Space Res* 9, 293-298.
- Daniely, Y., Liao, G., Dixon, D., Linnoila, R.I., Lori, A., Randell, S.H., Oren, M., and Jetten, A.M. (2004). Critical role of p63 in the development of a normal esophageal and tracheobronchial epithelium. *Am J Physiol Cell Physiol* 287, C171-181.
- Datto, M.B., Li, Y., Panus, J.F., Howe, D.J., Xiong, Y., and Wang, X.F. (1995). Transforming growth factor beta induces the cyclin-dependent kinase inhibitor p21 through a p53-independent mechanism. *Proc Natl Acad Sci U S A* 92, 5545-5549.
- de Visser, K.E., Eichten, A., and Coussens, L.M. (2006). Paradoxical roles of the immune system during cancer development. *Nat Rev Cancer* 6, 24-37.
- Denman, A.R., Eatough, J.P., Gillmore, G., and Phillips, P.S. (2003). Assessment of health risks to skin and lung of elevated radon levels in abandoned mines. *Health Phys* 85, 733-739.

- Ding, L.H., Xie, Y., Park, S., Xiao, G., and Story, M.D. (2008). Enhanced identification and biological validation of differential gene expression via Illumina whole-genome expression arrays through the use of the model-based background correction methodology. *Nucleic Acids Res* 36, e58.
- Donnelly, G.M., Haack, D.G., and Heird, C.S. (1982). Tracheal epithelium: cell kinetics and differentiation in normal rat tissue. *Cell Tissue Kinet* 15, 119-130.
- Dor, Y., Brown, J., Martinez, O.I., and Melton, D.A. (2004). Adult pancreatic beta-cells are formed by self-duplication rather than stem-cell differentiation. *Nature* 429, 41-46.
- Eramo, A., Lotti, F., Sette, G., Pilozzi, E., Biffoni, M., Di Virgilio, A., Conticello, C., Ruco, L., Peschle, C., and De Maria, R. (2008). Identification and expansion of the tumorigenic lung cancer stem cell population. *Cell Death Differ* 15, 504-514.
- Evans, M.J., Cabral, L.J., Stephens, R.J., and Freeman, G. (1975). Transformation of alveolar type 2 cells to type 1 cells following exposure to NO₂. *Exp Mol Pathol* 22, 142-150.
- Evans, M.J., Cabral-Anderson, L.J., and Freeman, G. (1978). Role of the Clara cell in renewal of the bronchiolar epithelium. *Lab Invest* 38, 648-653.
- Evans, M.J., Johnson, L.V., Stephens, R.J., and Freeman, G. (1976a). Cell renewal in the lungs of rats exposed to low levels of ozone. *Exp Mol Pathol* 24, 70-83.
- Evans, M.J., Johnson, L.V., Stephens, R.J., and Freeman, G. (1976b). Renewal of the terminal bronchiolar epithelium in the rat following exposure to NO₂ or O₃. *Lab Invest* 35, 246-257.
- Evans, M.J., Shami, S.G., Cabral-Anderson, L.J., and Dekker, N.P. (1986). Role of nonciliated cells in renewal of the bronchial epithelium of rats exposed to NO₂. *Am J Pathol* 123, 126-133.
- Fisher, G.H., Wellen, S.L., Klimstra, D., Lenczowski, J.M., Tichelaar, J.W., Lizak, M.J., Whitsett, J.A., Koretsky, A., and Varmus, H.E. (2001). Induction and apoptotic regression of lung adenocarcinomas by regulation of a K-Ras transgene in the presence and absence of tumor suppressor genes. *Genes Dev* 15, 3249-3262.

- Fry, R.J., and Nachtwey, D.S. (1988). Radiation protection guidelines for space missions. *Health Phys* 55, 159-164.
- Fulcher, M.L., Gabriel, S., Burns, K.A., Yankaskas, J.R., and Randell, S.H. (2005). Well-differentiated human airway epithelial cell cultures. *Methods Mol Med* 107, 183-206.
- Geiser, A.G., Kim, S.J., Roberts, A.B., and Sporn, M.B. (1991). Characterization of the mouse transforming growth factor-beta 1 promoter and activation by the Ha-ras oncogene. *Mol Cell Biol* 11, 84-92.
- Giangreco, A., Arwert, E.N., Rosewell, I.R., Snyder, J., Watt, F.M., and Stripp, B.R. (2009). Stem cells are dispensable for lung homeostasis but restore airways after injury. *Proc Natl Acad Sci U S A* 106, 9286-9291.
- Giangreco, A., Reynolds, S.D., and Stripp, B.R. (2002). Terminal bronchioles harbor a unique airway stem cell population that localizes to the bronchoalveolar duct junction. *Am J Pathol* 161, 173-182.
- Granville, C.A., Memmott, R.M., Balogh, A., Mariotti, J., Kawabata, S., Han, W., Lopiccolo, J., Foley, J., Liewehr, D.J., Steinberg, S.M., *et al.* (2009). A central role for Foxp3+ regulatory T cells in K-Ras-driven lung tumorigenesis. *PLoS One* 4, e5061.
- Guengerich, F.P. (2002). Cytochrome P450 enzymes in the generation of commercial products. *Nat Rev Drug Discov* 1, 359-366.
- Guyton, A.C., and Hall, J.E. (2006). *Textbook of medical physiology*, 11th edn (Philadelphia, Elsevier Saunders).
- Hall, E.J., and Giaccia, A.J. (2006). *Radiobiology for the radiologist*, 6th edn (Philadelphia, Lippincott Williams & Wilkins).
- Hong, K.U., Reynolds, S.D., Giangreco, A., Hurley, C.M., and Stripp, B.R. (2001). Clara cell secretory protein-expressing cells of the airway neuroepithelial body microenvironment include a label-retaining subset and are critical for epithelial renewal after progenitor cell depletion. *Am J Respir Cell Mol Biol* 24, 671-681.
- Hong, K.U., Reynolds, S.D., Watkins, S., Fuchs, E., and Stripp, B.R. (2004a). Basal cells are a multipotent progenitor capable of renewing the bronchial epithelium. *Am J Pathol* 164, 577-588.

Hong, K.U., Reynolds, S.D., Watkins, S., Fuchs, E., and Stripp, B.R. (2004b). In vivo differentiation potential of tracheal basal cells: evidence for multipotent and unipotent subpopulations. *Am J Physiol Lung Cell Mol Physiol* 286, L643-649.

Huang da, W., Sherman, B.T., and Lempicki, R.A. (2009). Systematic and integrative analysis of large gene lists using DAVID bioinformatics resources. *Nat Protoc* 4, 44-57.

Huang da, W., Sherman, B.T., Tan, Q., Kir, J., Liu, D., Bryant, D., Guo, Y., Stephens, R., Baseler, M.W., Lane, H.C., *et al.* (2007). DAVID Bioinformatics Resources: expanded annotation database and novel algorithms to better extract biology from large gene lists. *Nucleic Acids Res* 35, W169-175.

Ikeda, K., Clark, J.C., Shaw-White, J.R., Stahlman, M.T., Boutell, C.J., and Whitsett, J.A. (1995). Gene structure and expression of human thyroid transcription factor-1 in respiratory epithelial cells. *J Biol Chem* 270, 8108-8114.

Ikeda, K., Shaw-White, J.R., Wert, S.E., and Whitsett, J.A. (1996). Hepatocyte nuclear factor 3 activates transcription of thyroid transcription factor 1 in respiratory epithelial cells. *Mol Cell Biol* 16, 3626-3636.

Ito, T., Udaka, N., Okudela, K., Yazawa, T., and Kitamura, H. (2003). Mechanisms of neuroendocrine differentiation in pulmonary neuroendocrine cells and small cell carcinoma. *Endocr Pathol* 14, 133-139.

Jackson, E.L., Willis, N., Mercer, K., Bronson, R.T., Crowley, D., Montoya, R., Jacks, T., and Tuveson, D.A. (2001). Analysis of lung tumor initiation and progression using conditional expression of oncogenic K-ras. *Genes Dev* 15, 3243-3248.

Ji, H., Houghton, A.M., Mariani, T.J., Perera, S., Kim, C.B., Padera, R., Tonon, G., McNamara, K., Marconcini, L.A., Hezel, A., *et al.* (2006). K-ras activation generates an inflammatory response in lung tumors. *Oncogene* 25, 2105-2112.

Johnson, L., Mercer, K., Greenbaum, D., Bronson, R.T., Crowley, D., Tuveson, D.A., and Jacks, T. (2001). Somatic activation of the K-ras oncogene causes early onset lung cancer in mice. *Nature* 410, 1111-1116.

Kalina, M., Mason, R.J., and Shannon, J.M. (1992). Surfactant protein C is expressed in alveolar type II cells but not in Clara cells of rat lung. *Am J Respir Cell Mol Biol* 6, 594-600.

- Kaplan, H.S. (1948). Comparative susceptibility of the lymphoid tissues of strain C57 black mice to the induction of lymphoid tumors by irradiation. *J Natl Cancer Inst* 8, 191-197.
- Kelly, S.E., Bachurski, C.J., Burhans, M.S., and Glasser, S.W. (1996). Transcription of the lung-specific surfactant protein C gene is mediated by thyroid transcription factor 1. *J Biol Chem* 271, 6881-6888.
- Kim, C.F., Jackson, E.L., Woolfenden, A.E., Lawrence, S., Babar, I., Vogel, S., Crowley, D., Bronson, R.T., and Jacks, T. (2005). Identification of bronchioalveolar stem cells in normal lung and lung cancer. *Cell* 121, 823-835.
- Kohyama, J., Kojima, T., Takatsuka, E., Yamashita, T., Namiki, J., Hsieh, J., Gage, F.H., Namihira, M., Okano, H., Sawamoto, K., *et al.* (2008). Epigenetic regulation of neural cell differentiation plasticity in the adult mammalian brain. *Proc Natl Acad Sci U S A* 105, 18012-18017.
- Land, C.E., Shimosato, Y., Saccomanno, G., Tokuoka, S., Auerbach, O., Tateishi, R., Greenberg, S.D., Nambu, S., Carter, D., Akiba, S., *et al.* (1993). Radiation-associated lung cancer: a comparison of the histology of lung cancers in uranium miners and survivors of the atomic bombings of Hiroshima and Nagasaki. *Radiat Res* 134, 234-243.
- Lapidot, T., Sirard, C., Vormoor, J., Murdoch, B., Hoang, T., Caceres-Cortes, J., Minden, M., Paterson, B., Caligiuri, M.A., and Dick, J.E. (1994). A cell initiating human acute myeloid leukaemia after transplantation into SCID mice. *Nature* 367, 645-648.
- Lawson, G.W., Van Winkle, L.S., Toskala, E., Senior, R.M., Parks, W.C., and Plopper, C.G. (2002). Mouse strain modulates the role of the ciliated cell in acute tracheobronchial airway injury-distal airways. *Am J Pathol* 160, 315-327.
- Lazzaro, D., Price, M., de Felice, M., and Di Lauro, R. (1991). The transcription factor TTF-1 is expressed at the onset of thyroid and lung morphogenesis and in restricted regions of the foetal brain. *Development* 113, 1093-1104.
- Lee, G.Y., Kenny, P.A., Lee, E.H., and Bissell, M.J. (2007). Three-dimensional culture models of normal and malignant breast epithelial cells. *Nat Methods* 4, 359-365.

- Limoli, C.L., Ponnaiya, B., Corcoran, J.J., Giedzinski, E., Kaplan, M.I., Hartmann, A., and Morgan, W.F. (2000). Genomic instability induced by high and low LET ionizing radiation. *Adv Space Res* 25, 2107-2117.
- Little, M.P. (2009). Cancer and non-cancer effects in Japanese atomic bomb survivors. *J Radiol Prot* 29, A43-59.
- Liu, J.Y., Nettesheim, P., and Randell, S.H. (1994). Growth and differentiation of tracheal epithelial progenitor cells. *Am J Physiol* 266, L296-307.
- Liu, Y., and Hogan, B.L. (2002). Differential gene expression in the distal tip endoderm of the embryonic mouse lung. *Gene Expr Patterns* 2, 229-233.
- Lu, Y., Okubo, T., Rawlins, E., and Hogan, B.L. (2008). Epithelial progenitor cells of the embryonic lung and the role of microRNAs in their proliferation. *Proc Am Thorac Soc* 5, 300-304.
- Lunyak, V.V., and Rosenfeld, M.G. (2008). Epigenetic regulation of stem cell fate. *Hum Mol Genet* 17, R28-36.
- Madsen, J., Kliem, A., Tornøe, I., Skjodt, K., Koch, C., and Holmskov, U. (2000). Localization of lung surfactant protein D on mucosal surfaces in human tissues. *J Immunol* 164, 5866-5870.
- Maeda, Y., Dave, V., and Whitsett, J.A. (2007). Transcriptional control of lung morphogenesis. *Physiol Rev* 87, 219-244.
- Mailleux, A.A., Tefft, D., Ndiaye, D., Itoh, N., Thiery, J.P., Warburton, D., and Bellusci, S. (2001). Evidence that SPROUTY2 functions as an inhibitor of mouse embryonic lung growth and morphogenesis. *Mech Dev* 102, 81-94.
- Mbeunkui, F., and Johann, D.J., Jr. (2009). Cancer and the tumor microenvironment: a review of an essential relationship. *Cancer Chemother Pharmacol* 63, 571-582.
- Meira, L.B., Bugni, J.M., Green, S.L., Lee, C.W., Pang, B., Borenshtein, D., Rickman, B.H., Rogers, A.B., Moroski-Erkul, C.A., McFaline, J.L., *et al.* (2008). DNA damage induced by chronic inflammation contributes to colon carcinogenesis in mice. *J Clin Invest* 118, 2516-2525.
- Metzger, R.J., and Krasnow, M.A. (1999). Genetic control of branching morphogenesis. *Science* 284, 1635-1639.

Min, H., Danilenko, D.M., Scully, S.A., Bolon, B., Ring, B.D., Tarpley, J.E., DeRose, M., and Simonet, W.S. (1998). Fgf-10 is required for both limb and lung development and exhibits striking functional similarity to *Drosophila* branchless. *Genes Dev* 12, 3156-3161.

Morgan, W.F., Hartmann, A., Limoli, C.L., Nagar, S., and Ponnaiya, B. (2002). Bystander effects in radiation-induced genomic instability. *Mutat Res* 504, 91-100.

Nakajima, M., Kawanami, O., Jin, E., Ghazizadeh, M., Honda, M., Asano, G., Horiba, K., and Ferrans, V.J. (1998). Immunohistochemical and ultrastructural studies of basal cells, Clara cells and bronchiolar cuboidal cells in normal human airways. *Pathol Int* 48, 944-953.

National Council on Radiation Protection and Measurements. (2001). Fluence-based and microdosimetric event-based methods for radiation protection in space : recommendations of the National Council on Radiation Protection and Measurements (Bethesda, Md., National Council on Radiation Protection and Measurements).

National Council on Radiation Protection and Measurements. (2006). Information needed to make radiation protection recommendations for space missions beyond low-earth orbit (Bethesda, MD, National Council on Radiation Protection and Measurements).

Netter, F.H. (2006). Atlas of human anatomy, 4th edn (Philadelphia, PA, Saunders/Elsevier).

Park, K.S., Wells, J.M., Zorn, A.M., Wert, S.E., Laubach, V.E., Fernandez, L.G., and Whitsett, J.A. (2006). Transdifferentiation of ciliated cells during repair of the respiratory epithelium. *Am J Respir Cell Mol Biol* 34, 151-157.

Pepicelli, C.V., Lewis, P.M., and McMahon, A.P. (1998). Sonic hedgehog regulates branching morphogenesis in the mammalian lung. *Curr Biol* 8, 1083-1086.

Pierce, D.A., Sharp, G.B., and Mabuchi, K. (2003). Joint effects of radiation and smoking on lung cancer risk among atomic bomb survivors. *Radiat Res* 159, 511-520.

Pitt, B.R., and Ortiz, L.A. (2004). Stem cells in lung biology. *Am J Physiol Lung Cell Mol Physiol* 286, L621-623.

- Politi, K., Zakowski, M.F., Fan, P.D., Schonfeld, E.A., Pao, W., and Varmus, H.E. (2006). Lung adenocarcinomas induced in mice by mutant EGF receptors found in human lung cancers respond to a tyrosine kinase inhibitor or to down-regulation of the receptors. *Genes Dev* 20, 1496-1510.
- Pouget, J.P., Frelon, S., Ravanat, J.L., Testard, I., Odin, F., and Cadet, J. (2002). Formation of modified DNA bases in cells exposed either to gamma radiation or to high-LET particles. *Radiat Res* 157, 589-595.
- Preston, D.L., Ron, E., Tokuoka, S., Funamoto, S., Nishi, N., Soda, M., Mabuchi, K., and Kodama, K. (2007). Solid cancer incidence in atomic bomb survivors: 1958-1998. *Radiat Res* 168, 1-64.
- Prise, K.M., and O'Sullivan, J.M. (2009). Radiation-induced bystander signalling in cancer therapy. *Nat Rev Cancer* 9, 351-360.
- Qutob, S.S., Multani, A.S., Pathak, S., McNamee, J.P., Bellier, P.V., Liu, Q.Y., and Ng, C.E. (2006). Fractionated X-radiation treatment can elicit an inducible-like radioprotective response that is not dependent on the intrinsic cellular X-radiation resistance/sensitivity. *Radiat Res* 166, 590-599.
- Ramirez, R.D., Sheridan, S., Girard, L., Sato, M., Kim, Y., Pollack, J., Peyton, M., Zou, Y., Kurie, J.M., Dimaio, J.M., *et al.* (2004). Immortalization of human bronchial epithelial cells in the absence of viral oncoproteins. *Cancer Res* 64, 9027-9034.
- Randell, S.H. (2006). Airway epithelial stem cells and the pathophysiology of chronic obstructive pulmonary disease. *Proc Am Thorac Soc* 3, 718-725.
- Rawlins, E.L., and Hogan, B.L. (2006). Epithelial stem cells of the lung: privileged few or opportunities for many? *Development* 133, 2455-2465.
- Rawlins, E.L., and Hogan, B.L. (2008). Ciliated epithelial cell lifespan in the mouse trachea and lung. *Am J Physiol Lung Cell Mol Physiol* 295, L231-234.
- Rawlins, E.L., Okubo, T., Xue, Y., Brass, D.M., Auten, R.L., Hasegawa, H., Wang, F., and Hogan, B.L. (2009). The role of Scgb1a1+ Clara cells in the long-term maintenance and repair of lung airway, but not alveolar, epithelium. *Cell Stem Cell* 4, 525-534.
- Rawlins, E.L., Ostrowski, L.E., Randell, S.H., and Hogan, B.L. (2007). Lung development and repair: contribution of the ciliated lineage. *Proc Natl Acad Sci U S A* 104, 410-417.

Ray, M.K., Chen, C.Y., Schwartz, R.J., and DeMayo, F.J. (1996). Transcriptional regulation of a mouse Clara cell-specific protein (mCC10) gene by the NKx transcription factor family members thyroid transcription factor 1 and cardiac muscle-specific homeobox protein (CSX). *Mol Cell Biol* 16, 2056-2064.

Reisman, D., Elkind, N.B., Roy, B., Beamon, J., and Rotter, V. (1993). c-Myc trans-activates the p53 promoter through a required downstream CACGTG motif. *Cell Growth Differ* 4, 57-65.

Reynisdottir, I., Polyak, K., Iavarone, A., and Massague, J. (1995). Kip/Cip and Ink4 Cdk inhibitors cooperate to induce cell cycle arrest in response to TGF-beta. *Genes Dev* 9, 1831-1845.

Reynolds, S.D., Giangreco, A., Power, J.H., and Stripp, B.R. (2000a). Neuroepithelial bodies of pulmonary airways serve as a reservoir of progenitor cells capable of epithelial regeneration. *Am J Pathol* 156, 269-278.

Reynolds, S.D., Hong, K.U., Giangreco, A., Mango, G.W., Guron, C., Morimoto, Y., and Stripp, B.R. (2000b). Conditional clara cell ablation reveals a self-renewing progenitor function of pulmonary neuroendocrine cells. *Am J Physiol Lung Cell Mol Physiol* 278, L1256-1263.

Richardson, G.E., and Johnson, B.E. (1993). The biology of lung cancer. *Semin Oncol* 20, 105-127.

Ringvoll, J., Moen, M.N., Nordstrand, L.M., Meira, L.B., Pang, B., Bekkelund, A., Dedon, P.C., Bjelland, S., Samson, L.D., Falnes, P.O., *et al.* (2008). AlkB homologue 2-mediated repair of ethenoadenine lesions in mammalian DNA. *Cancer Res* 68, 4142-4149.

Rock, J.R., Onaitis, M.W., Rawlins, E.L., Lu, Y., Clark, C.P., Xue, Y., Randell, S.H., and Hogan, B.L. (2009). Basal cells as stem cells of the mouse trachea and human airway epithelium. *Proc Natl Acad Sci U S A* 106, 12771-12775.

Ron, E. (2003). Cancer risks from medical radiation. *Health Phys* 85, 47-59.

Sachs, R.K., Hlatky, L.R., and Trask, B.J. (2000). Radiation-produced chromosome aberrations: colourful clues. *Trends Genet* 16, 143-146.

Saeed, A.I., Sharov, V., White, J., Li, J., Liang, W., Bhagabati, N., Braisted, J., Klapa, M., Currier, T., Thiagarajan, M., *et al.* (2003). TM4: a free, open-source system for microarray data management and analysis. *Biotechniques* 34, 374-378.

Sato, M., Lee, W., Girard, L., Xie, Y., Xie, X-J., Yan, J., Smith, A.L., Shames, D.S., Ramirez, R.D., Gazdar, A.F., Shay, and J.W., Minna, J.D. (2009). The Combination of Five Changes (*Telomerase*, *p16/Rb* Bypass, *p53* Knockdown, *Mutant KRAS^{V12}*, *c-Myc*) Together With Serum-induced Epithelial Mesenchymal Transition Progresses Normal Human Bronchial Epithelial Cells to Full Malignancy. (Dallas, TX, University of Texas Southwestern Medical Center at Dallas).

Sato, M., Shames, D.S., Gazdar, A.F., and Minna, J.D. (2007). A translational view of the molecular pathogenesis of lung cancer. *J Thorac Oncol* 2, 327-343.

Sato, M., Vaughan, M.B., Girard, L., Peyton, M., Lee, W., Shames, D.S., Ramirez, R.D., Sunaga, N., Gazdar, A.F., Shay, J.W., *et al.* (2006). Multiple oncogenic changes (K-RAS(V12), p53 knockdown, mutant EGFRs, p16 bypass, telomerase) are not sufficient to confer a full malignant phenotype on human bronchial epithelial cells. *Cancer Res* 66, 2116-2128.

Schwartz, L.W., Dungworth, D.L., Mustafa, M.G., Tarkington, B.K., and Tyler, W.S. (1976). Pulmonary responses of rats to ambient levels of ozone: effects of 7-day intermittent or continuous exposure. *Lab Invest* 34, 565-578.

Sears, R., Leone, G., DeGregori, J., and Nevins, J.R. (1999). Ras enhances Myc protein stability. *Mol Cell* 3, 169-179.

Sears, R., Nuckolls, F., Haura, E., Taya, Y., Tamai, K., and Nevins, J.R. (2000). Multiple Ras-dependent phosphorylation pathways regulate Myc protein stability. *Genes Dev* 14, 2501-2514.

Sekine, K., Ohuchi, H., Fujiwara, M., Yamasaki, M., Yoshizawa, T., Sato, T., Yagishita, N., Matsui, D., Koga, Y., Itoh, N., *et al.* (1999). Fgf10 is essential for limb and lung formation. *Nat Genet* 21, 138-141.

Serls, A.E., Doherty, S., Parvatiyar, P., Wells, J.M., and Deutsch, G.H. (2005). Different thresholds of fibroblast growth factors pattern the ventral foregut into liver and lung. *Development* 132, 35-47.

Serrano, M., Lin, A.W., McCurrach, M.E., Beach, D., and Lowe, S.W. (1997). Oncogenic ras provokes premature cell senescence associated with accumulation of p53 and p16INK4a. *Cell* 88, 593-602.

- Shikazono, N., Noguchi, M., Fujii, K., Urushibara, A., and Yokoya, A. (2009). The yield, processing, and biological consequences of clustered DNA damage induced by ionizing radiation. *J Radiat Res (Tokyo)* 50, 27-36.
- Singh, S.K., Hawkins, C., Clarke, I.D., Squire, J.A., Bayani, J., Hide, T., Henkelman, R.M., Cusimano, M.D., and Dirks, P.B. (2004). Identification of human brain tumour initiating cells. *Nature* 432, 396-401.
- Snyder, J.C., Teisanu, R.M., and Stripp, B.R. (2009). Endogenous lung stem cells and contribution to disease. *J Pathol* 217, 254-264.
- Stenmark, K.R., and Abman, S.H. (2005). Lung vascular development: implications for the pathogenesis of bronchopulmonary dysplasia. *Annu Rev Physiol* 67, 623-661.
- Stripp, B.R., Maxson, K., Mera, R., and Singh, G. (1995). Plasticity of airway cell proliferation and gene expression after acute naphthalene injury. *Am J Physiol* 269, L791-799.
- Suit, H., Goldberg, S., Niemierko, A., Ancukiewicz, M., Hall, E., Goitein, M., Wong, W., and Paganetti, H. (2007). Secondary carcinogenesis in patients treated with radiation: a review of data on radiation-induced cancers in human, non-human primate, canine and rodent subjects. *Radiat Res* 167, 12-42.
- Tefft, J.D., Lee, M., Smith, S., Leinwand, M., Zhao, J., Bringas, P., Jr., Crowe, D.L., and Warburton, D. (1999). Conserved function of mSpry-2, a murine homolog of *Drosophila* sprouty, which negatively modulates respiratory organogenesis. *Curr Biol* 9, 219-222.
- Tubiana, M. (2009). Can we reduce the incidence of second primary malignancies occurring after radiotherapy? A critical review. *Radiother Oncol* 91, 4-15; discussion 11-13.
- Van Obberghen-Schilling, E., Roche, N.S., Flanders, K.C., Sporn, M.B., and Roberts, A.B. (1988). Transforming growth factor beta 1 positively regulates its own expression in normal and transformed cells. *J Biol Chem* 263, 7741-7746.
- Vaughan, M.B., Ramirez, R.D., Wright, W.E., Minna, J.D., and Shay, J.W. (2006). A three-dimensional model of differentiation of immortalized human bronchial epithelial cells. *Differentiation* 74, 141-148.
- Visvader, J.E., and Lindeman, G.J. (2008). Cancer stem cells in solid tumours: accumulating evidence and unresolved questions. *Nat Rev Cancer* 8, 755-768.

Vogelstein, B., and Kinzler, K.W. (1993). The multistep nature of cancer. *Trends Genet* 9, 138-141.

Wagers, A.J., and Weissman, I.L. (2004). Plasticity of adult stem cells. *Cell* 116, 639-648.

Weaver, M., Batts, L., and Hogan, B.L. (2003). Tissue interactions pattern the mesenchyme of the embryonic mouse lung. *Dev Biol* 258, 169-184.

Weissman, I.L., Anderson, D.J., and Gage, F. (2001). Stem and progenitor cells: origins, phenotypes, lineage commitments, and transdifferentiations. *Annu Rev Cell Dev Biol* 17, 387-403.

Wuenschell, C.W., Sunday, M.E., Singh, G., Minoo, P., Slavkin, H.C., and Warburton, D. (1996). Embryonic mouse lung epithelial progenitor cells co-express immunohistochemical markers of diverse mature cell lineages. *J Histochem Cytochem* 44, 113-123.

Wyman, C., and Kanaar, R. (2006). DNA double-strand break repair: all's well that ends well. *Annu Rev Genet* 40, 363-383.

Yin, T., and Li, L. (2006). The stem cell niches in bone. *J Clin Invest* 116, 1195-1201.

Yue, J., and Mulder, K.M. (2000). Requirement of Ras/MAPK pathway activation by transforming growth factor beta for transforming growth factor beta 1 production in a smad-dependent pathway. *J Biol Chem* 275, 35656.

Zhou, L., Lim, L., Costa, R.H., and Whitsett, J.A. (1996). Thyroid transcription factor-1, hepatocyte nuclear factor-3beta, surfactant protein B, C, and Clara cell secretory protein in developing mouse lung. *J Histochem Cytochem* 44, 1183-1193.